THÈSE

En vue de l'obtention du

DOCTORAT DE L'UNIVERSITÉ DE TOULOUSE

Délivré par :

Institut National Polytechnique de Toulouse (INP Toulouse)

Discipline ou spécialité :

Océan, Atmosphère et surfaces continentales

Présentée et soutenue par :

M. SILIANG LIU

le mercredi 11 juin 2014

Titre :

IMPLEMENTATION OF A SATELLITE-BASED PROGNOSTIC DAILY SURFACE ALBEDO DEPENDING ON SOIL WETNESS: IMPACT STUDY IN SURFEX MODELLING PLATFORM OVER FRANCE

Ecole doctorale :

Sciences de l'Univers de l'Environnement et de l'Espace (SDUEE)

Unité de recherche :

Centre National de Recherches Météorologiques (CNRM)

Directeur(s) de Thèse :

M. JEAN-LOUIS ROUJEAN

Rapporteurs :

Mme CRYSTAL BARKER SCHAAF, UNIVERSITY OF MASSACHUSSETS BOSTON

M. SHUNLIN LIANG, UNIVERSITE DE MARYLAND

Membre(s) du jury :

M. FRANCK ROUX, UNIVERSITE TOULOUSE 3, Président

M. JEAN-LOUIS ROUJEAN, METEO FRANCE TOULOUSE, Membre

Mme DOMINIQUE COURAULT, INRA AVIGNON, Membre

Mme FABIENNE MAIGNAN, UNIVERSITE DE VERSAILLES, Membre

Thèse préparée au sein du Laboratoire de Centre National de Recherches Météorologiques, Météo-France

Résumé

L'albédo de la surface est une variable clé en météorologie car elle assure le contrôle du rayonnement solaire absorbé par la surface, et par là même elle régule le bilan d'énergie en surface. L'albédo est encore généralement prescrit à ce jour comme une grandeur climatologique organisée par classe d'occupation des sols afin de disposer d'atlas globaux spatialement cohérents. Une telle approche a fait son chemin alors que la télédétection propose maintenant des produits albédos fiables et fréquemment réactualisés, notamment réactifs à la chronologie des précipitations. C'est l'objet majeur de cette étude en cherchant à calibrer l'albédo de sol nu avec l'humidité superficielle et à mesurer l'impact sur les flux d'énergie.

La première étape de l'étude consiste à réaliser un état de l'art de la climatologie d'albédo de surface fondée sur les produits satellitaires, parmi quoi figure la base de données duale ECOCLIMAP qui comprend une carte d'occupation des sols et des paramètres de surface associés. Une originalité de l'étude repose sur le développement d'une méthode pour obtenir un albédo MODIS journalier à 500m à partir du produit standard BRDF/Albédo à 8 jours et de la réflectivité mesurée lors du passage d'orbite de MODIS, ensuite renormalisé donc en albédo quotidien MODIS. Ce dernier est ensuite validé avec l'albédo similaire de l'instrument SEVIRI à bord du satellitaire géostationnaire MSG. Les 2 produits albédos montrent un bon accord général avec toutefois des différences en hiver, ce qui semble lié à la géométrie d'illumination, différente dans les 2 cas. Mais ces écarts restent faibles comparé à la climatologie actuelle de l'albédo considérée dans le schéma de surface ISBA-A-gs.

Dans les schémas de surface tel ISBA-A-gs, la séparation entre les albédos du sol nu et de la végétation permet de mieux prendre en compte des processus qui sont spatialement et temporellement indépendants. Alors que l'albédo de la végétation évolue plutôt sur une base saisonnière, celui du sol nu varie sur de courtes échelles de temps comme étant impacté par les événements de pluie générant une humidité superficielle. L'accumulation de séries pluri-annuelles de données MODIS a permis tout d'abord d'établir des albédos de sol nu et de végétation sur une base climatologique, pour être ensuite comparés, favorablement, avec leurs équivalents dans le modèle JULES du Met Office.

Un albédo de surface pronostique est ensuite mis en place pour les besoins du schéma de surface ISBA-A-gs en prenant en compte notamment l'humidité des sols et la chlorophylle des feuilles. Le volet humidité est cependant mieux consolidé grâce notamment à une calibration entre les albédos satellitaires de sol nu et l'humidité du sol mesurée en routine sur les 12 stations

SMOSMANIA du sud-ouest de la France. Le résultat est la prescription d'un albédo évolutif avec l'humidité bien corrélé avec les albédos satellitaires à l'échelle du paysage. Pour la composante végétation de l'albédo, l'étude repose sur des simulations du modèle détaillé de transfert radiatif PROSAIL. On en déduit des relations simplifiées entre l'albédo de la feuille et la chlorophylle, puis une nécessaire prise en compte de l'indice foliaire LAI lors du passage à l'échelle de la canopée végétale. L'albédo de la végétation ainsi obtenu combiné avec celui du sol nu permet de prescrire un albédo total, ce qui se vérifie bien avec les données de la station de Majadas (Espagne) situé dans l'écosystème naturel de grande échelle 'dehesa' et pour lequel humidité, chlorophylle et LAI sont continûment mesurés. Une fois consolidé la paramétrisation d'un albédo de surface pronostique, il est regardé les études d'impact de celui-ci par rapport à la climatologie. Pour cela, on considère le modèle SURFEX du bilan d'énergie sur la France et le forçage SAFRAN. Des simulations offline montrent des effets non négligeables sur la température et l'humidité à 2m ainsi que sur les flux (rayonnement net, chaleurs sensibles et latentes) pendant plusieurs jours en raison de la prise en compte d'un albédo réaliste qui soit moins sec. Dans une dernière étape, on a développé un schéma d'assimilation de l'albédo de type Simple Ensemble Kalman Filter (SEKF), ce qui a un effet sur le LAI simulé par ISBA-A-gs pour des végétations de densité faible à moyenne.

Abstract

Surface albedo is a key parameter in meteorology as it controls the absorbed solar radiation and besides regulates the surface energy balance. It is generally established as a climatologic value staged in land cover units to get trusting atlas. Such approach yields obviously some limits whereas today remote sensing observations offer a frequent update of surface albedo fields to be the echo of rainfall chronology. Owing to this, the surface albedo could be predicted from soil wetness.

The first step of this study consists to review state-of-art satellite-based climatology of surface albedo, amongst which ECOCLIMAP-II, as it still popular for meteorology. The novelty relies on method development to get a a 500m daily surface albedo from LEO (low elevation orbit) MODIS 8 day BRDF/Albedo standard product renormalized to orbital pass reflectance. Daily MODIS surface albedo is further validated against LSA SAF product issued from geostationary (GEO) sensor SEVIRI data. LEO and GEO surface albedo show discrepancies over SMOSMANIA stations in winter and early spring periods in relation to the geometry of illumination. But more significant bias are conspicuous between satellite-based surface albedo products and the actual climatology used in ISBA-A-gs model. In land surface models, the partitioning of the surface albedo into soil and vegetation distinct albedo components allows to address different processes that are time-scale dependent. Vegetation albedo primarily varies along with the growing season while soil albedo shows day-to-day variations caused by rainfall events. Multi-years MODIS accumulated observations are harnessed to firt stress a static unravelling between soil and vegetation serving for climatology. Resulting visible and near infrared albedos present assets in terms of completion and spatial consistency compared to equivalence in JULES model.

A prognostic surface albedo is further implemented for the purpose of ISBA-A-gs land surface model in accounting for (1) soil moisture and more preliminary on (2) leaf chlorophyll. Tests are carried on over the 12 SMOSMANIA anchor stations designed to measure routinely the soil moisture (SM) in south-western France for the cal/val SMOS. Using a physically-based parameterization between soil albedo and SM, forecast surface albedo matches well in time with LEO and GEO products. Besides, numerical simulations of vegetation canopies with PROSAIL radiative transfer model serve to derive a generic relationship between visible vegetation albedo and chlorophyll content (Cab), that is however constrained by the leaf area index (LAI). This relationship yields an update of vegetation albedo further combined with soil albedo to get a completion of the prognostic surface albedo. The approach is validated with in-situ measurements from ICOS station of Majadas (Spain) representative of the dehesa ecosystem.

Impact of changing surface albedo is accomplished using ISBA-A-gs over France running offline with SAFRAN as forcing. Through incorporating an 'albedo-soil moisture' dependence in ISBA-A-gs, improvements are demonstrated for its modeling ability for energy balance. The energy fluxes (net radiation, sensible heat, latent heat) and surface temperature are revealing distinct seasonal and daily variations after introducing this soil wetness dependence of prognostic albedo.

Table des figures

Liste des tableaux

Table des matières

Introduction Générale

Le changement climatique global est devenu l'un des plus importants centres d'intérêt scientifique et politique en matière de débat. Il existe plusieurs signes avant-coureurs à l'origine de la causalité du changement climatique, tel l'augmentation de la concentration des gaz à effet de serre, les aléas extrêmes, l'augmentation de la température, l'accroissement des précipitations, l'acidification des océans, la hausse du niveau des mers, le retrait des glaces, etc (Stocker et al., 2013). Ces constats avérés ont gagné la reconnaissance du public et influencé les décisions politiques quelque peu, mais ont avant tout renforcé une collaboration internationale afin de dynamiser les études en science environnementales axées sur le système Terre.

Le système Terre comprend plusieurs composantes ayant des frontières ténues : l'atmosphère, l'hydrosphère, la cryosphère, la biosphère et la géosphère. L'état de l'art des modèles représentant le fonctionnement du système Terre montre que ceux-ci peuvent représenter les processus pour chacune des composantes et simuler le stockage et les échanges de flux d'eau, d'énergie, et de matière biochimique entre les différents composants. En outre, les activités humaines, qui est l'un des facteurs les plus actifs et contrôlables, a de plus en plus d'influence sur le système climatique depuis l'ère industrielle. Comme montré en Fig.4, les différentes composantes du système Terre-atmosphère interagissent entre elles.

Les modèles de climat sont des outils puissants pour simuler la variabilité climatique constatée et pour faire des projections sur ce que pourrait être son état futur sous plusieurs scénarios de l'impact humain (Stocker et al., 2013). Les représentations des processus du système Terre se sont améliorées avec le temps en raison des ressources de calcul croissantes qui permettent de considérer des modèles ayant des résolutions de grille affinées. Ceci est particulièrement évident pour les composantes radiatives et les aérosols en liaison avec les interactions avec les nuages, aussi pour le traitement de la cryosphère. La représentation du cycle du carbone a été incorporée de façon extensive dans un grand nombre de modèles avec un effort significatif soutenu en matière de représentation depuis les conclusions du 4ième rapport d'évaluation de l'IPCC.

Le bilan d'énergie est l'une des composantes les plus importantes représentée dans les modèles de climat étant donnée que le système climatique est piloté par le rayonnement solaire. Une carte schématique montre la contribution du rayonnement incident distribué entre les différentes composantes (fig.5). La réflectance de la planète Terre est approximativement 0.30, ce qui signifie qu'à peu près 30% de l'énergie rayonnée est rétro réfléchie vers l'espace. Le reste représente le rayonnement solaire incident rétro réfléchi vers l'atmosphère, les nuages, la surface, alors que la

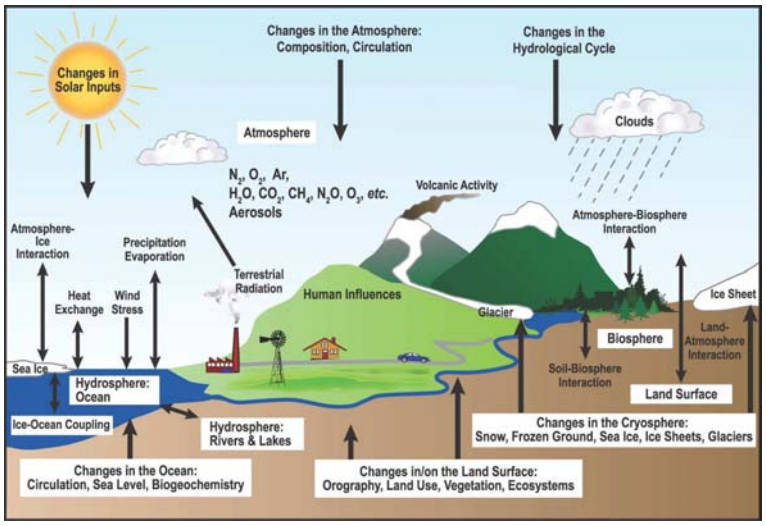

FIGURE 1 – Vue schématique des composantes du système climatique, de leurs processus et interactions. (Source from IPCC, 2007)

part restante est absorbée par la surface ou l'atmosphère. Cette quantité représente approximativement 240 W/m^2. Généralement, le rayonnement réchauffe la surface et refroidit l'atmosphère. L'énergie absorbée par la surface est retournée vers l'atmosphère sous forme de flux d'énergie sensible et latente. Pour équilibrer l'énergie incidente, la Terre elle-même émet du rayonnement infra-rouge, en moyenne d'une quantité équivalente à l'énergie dirigée en direction de l'espace.

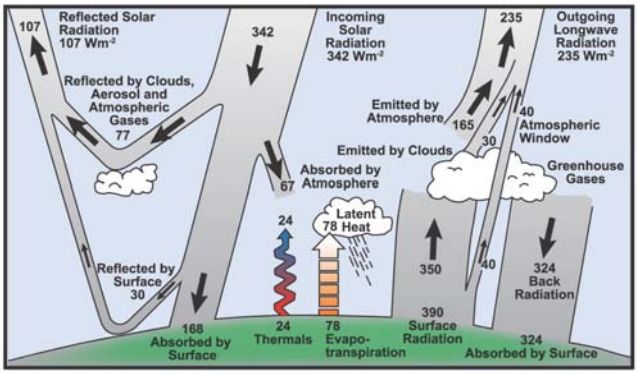

FIGURE 2 – Estimation du bilan d'énergie annuel et global de la Terre.(Source from Kiehl and Trenberth, 1997)

Le flux d'énergie entre le soleil, la terre et l'espace relatif à l'équilibre radiatif Top of Atmosphere (TOA) peut être mesuré à partir du bilan radiatif réalisé par des missions tel CERES (Clouds and the Earth's Radiant Energy System) (Wielicki et al., 1998) et Solar Radiation and

TABLE 1 – Albédo de surface : résolution, précision et stabilité.

Variable parameter	Horizontal Resolution	Temporal Resolution	Accuracy	Stability
BSA	1KM	Daily to Weekly	max(5%,0.0025)	max(1%,0.0001)
WSA	1KM	Daily to Weekly	max(5%,0.0025)	max(1%,0.0001)

Climate Experiment (SORCE) (Kopp et al., 2005), respectivement. Les composantes du bilan radiatif à la surface sont plus difficiles à estimer de par le fait qu'elles ne peuvent être mesurées directement par satellite alors que les mesures en surface à partir de réseaux sol sont trop dispersées pour être régionalement ou globalement représentatives. Des études récentes révèlent en global une atténuation et un éclaircissement, partant d'observations à long terme de photomètres solaires. Plusieurs études (Wild et al., 2008, 2004) ont indiqué un déclin dans le rayonnement net terrestre de l'ordre de $2W/m^2$ par décade entre 1960s et 1980s, et une augmentation du même taux entre 1980s et 2000. Ces constats sont fondés sur les échanges estimés des composantes radiatives individuelles qui constituent le rayonnement net à la surface :

$$Rn = (1-\alpha)F_d^s + \varepsilon F_d^l - \sigma\varepsilon T_s^4 = H + \lambda E + G \quad (1)$$

où apparaît le rayonnement descendant ondes-courtes F_d^s et thermique F_d^l. L'albédo (α) et l'émissivité (ε) sont également 2 variables critiques déterminantes pour le rayonnement net, en optique et en thermique, respectivement, en considérant la constante de Planck σ et la température de peau T pour la seconde quantité. Le rayonnement net est équilibré par le flux de chaleur sensible (H), de chaleur latente (λE) et le terme de transport dans le sol (G).

Un suivi interprétable du climat de la Terre requiert des observations en routine de plusieurs paramètres atmosphériques, océaniques et terrestres. De fait, cela doit répondre à des technologies combinées, depuis des instruments basés au sol à des bateaux, bouées, profileurs océaniques, ballons, avions, instruments embarqués, etc.. Global Climate Observing System (GCOS, 2009) a défini une liste de 50 Variables Climatiques Essentielles (ECV en anglais), qui sont techniquement et économiquement possiblement observables, afin de supporter le travail des United Nations Framework Convention on Climate Change(UNFCCC) et de l'IPCC. Parmi les ECV terrestres, l'albédo de surface en est une de particulièrement critique pour le bilan d'énergie dans le spectre solaire. Les résolutions temporelles et spatiales de l'albédo de surface et ses précision et stabilité attendues sont listées dans la Table 2.

Les changements dans l'atmosphère, la surface émergée, l'océan, la biosphère et la cryosphère – à la fois naturels et anthropiques - peuvent perturber le bilan radiatif de la Terre, et produire un forçage radiatif (RF) qui affecte le climat. RF est une mesure du changement net du bilan d'énergie en réponse à une perturbation externe. Tous ces forçages radiatifs issus d'un ou de plusieurs facteurs affectant le climat et comme étant associés avec l'activité humaine ou les processus naturels sont discutés ici. L'albédo de surface est listé comme étant une variable ECV en lien avec le changement climatique qui soit possiblement encore quelque peu erronée et qui doit définitivement gagner en précision. Fig.6 montre les rangs de variation du forçage

radiatif moyen et leur incertitude pour les différents termes, parmi lesquels l'albédo indique un effet double. Selon les estimations faites entre 1750 et 2005 par le Intergovernmental Panel on Climate (IPCC), le changement sur l'albédo de surface causé par l'occupation des sols est estimé avoir un forçage négatif (refroidissement), de l'ordre de -0.2±0.2W/m^2 ; et un forçage positif (réchauffement) causé par le dépôt de carbone suie sur la neige, de l'ordre de 0.1±0.1W/m^2.

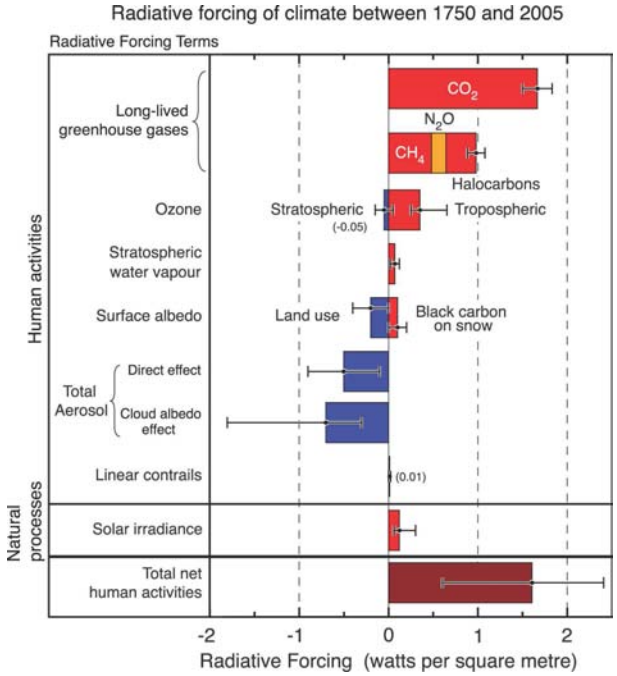

FIGURE 3 – Résumé des principales composantes du forçage radiatif en lien avec le changement climatique. La ligne horizontale rattachée à chaque couleur représente le rang d'incertitude pour la valeur respective. (Source from IPCC, 2007)

Les rétroactions de l'albédo de surface sur le climat et le cycle du carbone ont fait l'objet de nombreuses études. A ce propos, la région du Sahel a été un premier exemple mis en exergue durant la sécheresse sévissant dans la période 1970s-1980s (Charney et al., 1977). Un autre exemple de rétroaction positive typique existe avec l'albédo de la neige sur le système climatique pour les régions les plus septentrionales (Fletcher et al., 2009). En outre, la forêt Amazonienne a aussi été le centre d'intérêt de nombreuses études. De manière générale, il est maintenant largement reconnu que les mécanismes dus à un accroissement des valeurs d' albédo soit dues à la désertification ou la déforestation résultent en une réduction des précipitations et de l'évapotranspiration (Dirmeyer and Shukla, 1994; Lofgren, 1995; Xue, 1996; Xue and Shukla, 1993). La déforestation boréale due à une baisse de l'albédo de surface a montré un biais pour les puits de carbone potentiels (Betts, 2000). Cependant, l'effet de refroidissement inhérent à un bond de l' albédo de surface est possiblement compensé par un scénario de réchauffement résultant d'une évapotranspiration significativement réduite. Le manque d'accord entre les résultants de modèle est en partie du à des différences entre les formulations des schémas de surface et de leurs champs de

paramètres, en dehors du fait que les mécanismes d'interaction surface-atmosphère ne sont pas entièrement maîtrisés.

La surface terrestre est une composante en soit du système Terre et aussi une composante interactive avec l'atmosphère et l'océan. Les modèles de surface (LSM en anglais) ont été originellement développés pour simuler grossièrement les échanges d'énergie, de matière et de moments vers l'atmosphère. De nos jours, le degré de sophistication des LSM a considérablement évolué pour répondre aux besoins des simulations climatiques. Dans la revue qui en a été faite de ces modèles par (Sellers et al., 1997), les LSM ont suivi 3 stades de développement :
(1) Le premier, opéré entre 1960 et 1970, était basé simplement sur les formules de transfert aérodynamique pour un bloc avec le plus souvent une prescription uniforme de paramètres de surface (albédo, rugosité aérodynamique, et disponibilité en humidité du sol).
(2) Dans les années 1980s, une seconde génération de modèles ont explicitement reconnu les effets de la végétation dans le calcul du bilan d'énergie à la surface. Les paramètres des propriétés de la surface furent assemblés selon des considérations écologiques et géographiques disponibles dans la littérature scientifique.
(3) La troisième génération de modèles utilise des théories modernes sur la photosynthèse et sa relation avec l'eau des plantes afin de fournir une description consistante du transfert d'énergie, de l'évapotranspiration, et des échanges de carbone par les plantes. Une série d'expériences de grand échelle ont pu être réalisées pour valider les processus des modèles et les hypothèses de changement d'échelle induites dans les schémas surface-atmosphère. Ces expériences ont aussi accéléré le développement de méthodes pour assurer le transfert de données satellitaires dans des jeux de données globales de paramètres de surface au bénéfice des modèles.

Les processus de surface ont été pris en compte dans les modèles de climat via des paramétrisations qui vont de schémas simples à des représentations complexes. Les paramètres clé des modèles incluent notamment l'albédo, la fraction de végétation et la couverture de neige, la longueur de rugosité, la température de peau, et les propriétés du couvert végétal. Cependant, ces variables ont été représentées de façon crue avec le temps en raison des capacités limitées d'observation. Mais la génération actuelle des satellites peut maintenant fournir le degré souhaitable d'information en terme d'échantillonnage spatial global à des intervalles de temps réguliers. Ainsi, la télédétection a clairement atteint un niveau de capacité suffisant pour estimer avec précision maintenant les paramètres de surface de façon systématique, comme requis. D'un autre côté, la disponibilité des données d'observation des satellites a motivé les modélisateurs avides d'améliorer leur représentation des interactions entre le sol, la végétation, et l'atmosphère avec quelques différences sensibles mises en lumière dans le cadre de l'initiative PILPS (the Intercomparison of Land-surface Parameterization Schemes).

Dans la droite ligne de PILPS, comme étant un 'open-access' et une activité pérenne, RAdiation transfer Model Intercomparison (RAMI) a opéré des phases successives. Chacune de ces phases cherche à redéfinir la capacité, la performance et l'accord de la dernière génération de modèles de transfert radiatif (RT). Ceci peut conduire à des perfectionnements de modèle et plus loin à des développements au bénéfice de la communauté modélisatrice en charge du transfert radiatif. Les modèles sont comparés à différents scénarios avec des densités de végétation diffé-

rentes, ce qui vaut aussi pour le LAI, le sol, etc. Depuis la première phase de RAMI I en 1999, 4 phases ont été réalisées. La dernière, RAMI IV, constitue une comparaison prenant en compte un modèle 3D de Monte Carlo comme référence. Le détail d'information peut être retrouvé sous `http://rami-benchmark.jrc.ec.europa.eu/HTML/`. Cependant, RAMI est axé sur des couverts thématiquement homogènes avec pour objectif de guider le développement de modèles de transfert radiatif. Cela ne peut servir pour valider les modèles de TR à la résolution de grille lâche du pixel d'un instrument satellitaire où des attributs complexes de la surface se trouvent être mélangés.

Avec la nouvelle génération de satellites d'observation de la Terre durant les 2 dernières décades, des jeux variés d'albédos de surface à l'échelle globale et continentale ont été constitués. Cela concerne les instruments à orbite polaire tel MODIS (Moderate Resolution Imaging Spectroradiometer), POLDER (Polarization and Directionality of Earth Reflectance) et VEGETATION embarqué sur SPOT, aussi les systèmes géostationnaires d'observation tel SEVIRI (Spinning Enhanced Visible and InfraRed Imager) sur METEOSAT Second Generation (MSG). Ces données enregistrées sont dérivées de réflectance bien calibrées grâce à l'utilisation de chaînes de traitement élaborées et à des algorithmes physiques mieux consolidés. Les communautés climat et aussi prévision du temps sensible avancent régulièrement qu'une précision de l'ordre de 2-5% est requise pour un albédo de surface observé utilisable dans la modélisation de la surface. (selon le GCOS) Plusieurs exercices de validation (exemple du LPV/CEOS) ont confirmé la bonne précision obtenue avec les produits satellitaires récents, i.e. MODIS (Jin, 2003). Cela suppose davantage d'efforts pour raffiner la description de l'albédo de surface dans les modèles d'interface (Oleson, 2003). L'accumulation de jeux d' observations consistants sur le long terme, typiquement sur une base pluriannuelle, est jugée prometteuse pour servir à établir une climatologie des albédos du sol et de la végétation. Récemment une carte statique globale de l'albédo du sol nu a été proposée par (Houldcroft et al., 2009) en exploitant des séries pluriannuelles de données MODIS. Mais les variations à court terme de l'albédo du sol nu, principalement pilotées par l'humidité de surface (SSM en anglais) ne furent pas explorées. En fait, un examen quotidien de l'albédo de surface est au minimum requis afin d'évaluer l'humidité superficielle du sol. Il s'agit là véritablement d'un challenge pour les instruments à orbite polaire tel MODIS étant donné qu'avec une simple revisite quotidienne, toute information potentiellement réactualisable peut être sévèrement occultée par une haute fréquence d'ennuagement pour certaines régions. D'un autre côté, une analyse soignée des variations à court-terme de l'albédo de surface est réalisable avec les satellites géostationnaires mais pour des zones limitées du globe. Cependant les systèmes d'observation LEO (low elevation orbit) peuvent toujours offrir des résolutions spatiales et spectrales améliorées comparées aux satellites GEO (geostationnary). De fait, une combinaison entre LEO et GEO paraît opportune, ce qui passe nécessairement par des études séparées pour commencer. En sus d'un produit humidité du sol SSM, les aléas climatiques (inondations, orages, vents violents) peuvent être à la base de variations à court terme de l'albédo de surface du fait qu'ils alimentent et modulent la chronologie des épisodes de chute de pluie, de neige et des périodes alternées de croissance et de sénescence pour la végétation.

Dans les modèles de type SVAT, on considère une séparation entre la végétation et le sol nu car ces 2 entités font référence à différentes propriétés prises en compte dans différents processus

relativement au rayonnement solaire, à la chaleur, et au transfert hydrique. L'albédo de la végétation peut varier à des échelles de temps journalières et semainales en phase avec la variation de croissance des feuilles, du déplacement du contenu en chlorophylle, des pigments bruns ou même du contenu en eau des feuilles, tout cela dépendant plus ou moins de la longueur d'onde. D'un autre côté, l'albédo d'un sol nu va plutôt varier sur une base horaire car le champ principal de perturbation est l'humidité SSM liée aux précipitations. La modélisation des variations saisonnières de l'albédo de la végétation est primordiale pour réaliser des estimations quantitatives du changement de l'écosystème. Au lieu de cela, de rapides variations causées sur l'albédo du sol nu seront connectées avec la chronologie de la pluie, ce qui doit forcément être pris en compte dans la recherche de fermeture du bilan d'énergie.

Bien que plusieurs objectifs soient balayés dans ce travail de thèse, on peut résumer l'étude en se focalisant simplement sur les points suivants : (1) en premier lieu la mise en oeuvre d'un albédo de surface pronostique dans ISBA fondée sur un étalonnage des données de satellites LEO et GEO avec des données d'humidité SSM mesurées in-situ, et pour un cas pilote avec la chlorophylle ; (2) ensuite il est évalué l'impact d'un changement de l'albédo de surface du à l'humidité dans le bilan d'énergie de la plate-forme de développement SURFEX sur la France ; (3) en dernier lieu, on montre pour la première fois une assimilation de l'albédo de surface conjointement avec l'indice folaire LAI et l'humidité pour une station pilote de référence.

General Introduction

Global climate change has becoming one of the most important scientific and political topics. Many indicators have implied climate change, as green house gas concentration augmentation, extreme events, surface temperature rising, precipitation change, ocean acidification, sea level rise, glacial retreat, etc (Stocker et al., 2013). These findings gained the public recognition, influenced political decision, enhanced the international cooperation, and boosted the study of earth system science.

Earth system has various components : atmosphere, hydrosphere, cryosphere, biosphere and geosphere. State-of-the-art Earth System Models (ESMs) can represent the processes within each components and simulate the storage and exchange fluxes of water, energy, and biochemistry matter between different components. Further, the human activities, which is one of the most active and controllable factor, has more and more influence to the climate system since industry era. As shown in Fig.4, various components in the Earth-atmosphere system interact with each other.

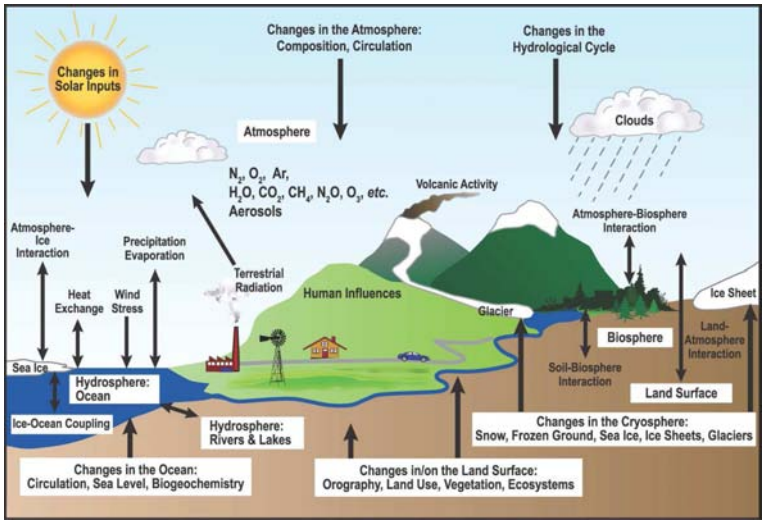

FIGURE 4 – Skematic view of the components of the climate system, their processes and interactions. (Source from IPCC, 2007)

Climate models are used to simulate climate variability and to project the future status under various scenarios of human impact (Stocker et al., 2013). The horizontal and vertical resolution is augmenting. Representations of Earth system processes are much more extensive and improved, particularly for the radiation and the aerosol cloud interactions and for the treatment of the cryosphere. The representation of the carbon cycle was added to a larger number of models and has been improved since IPCC 4th Assessment Report.

Energy balance is one of the most important components represented by climate models since the climate system is driven by solar radiation. A sketch map shows the participation of incoming radiation distributed between different components (fig.5). The Earth's planet reflectance is approximate 0.30, meaning that nearly 30% energy is reflected back to the space. Incoming solar radiation is reflected back by atmosphere, cloud, and surface, while the remaining part is absorbed by surface or atmosphere. The energy that is not reflected back to space is absorbed by the Earth's surface and atmosphere. This amount is approximately 240 Watts per squaremetre (W/m^2). Generally, the radiation warms the surface and cools the atmosphere. The absorbed energy of surface is returning back through atmosphere as sensible and latent heat fluxes. To balance the incoming energy, the Earth itself radiate through longwave radiation, on average, the same amount of energy back to space.

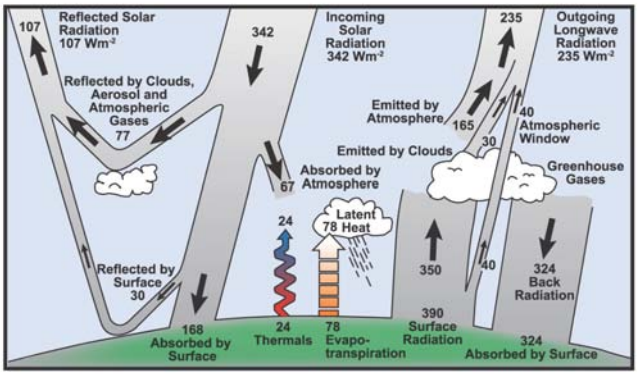

FIGURE 5 – Estimate of the Earth's annual and global mean energy balance. (Source from Kiehl and Trenberth, 1997)

The energy flux between Sun, Earth, and Space relative to Top of Atmosphere (TOA) radiation balance can be measured from CERES (Clouds and the Earth's Radiant Energy System) (Wielicki et al., 1998) and the Solar Radiation and Climate Experiment (SORCE), (Kopp et al., 2005), respectively. While the components of the radiation budget at the surface are more difficult to estimate since they can not be measured by satellite directly and the surface measurements are not regionally or globally representative. Recent studies reveal the global 'dimming' and 'brightening' from long-term sun-photometer observations. Wild et al. (2008, 2004) inferred a decline in land surface net radiation on the order of $2W/m^2$ per decade from

TABLE 2 – Alb de surface : rlution, prsion et stabilit

Variable parameter	Horizontal Resolution	Temporal Resolution	Accuracy	Stability
BSA	1KM	Daily to Weekly	max(5%,0.0025)	max(1%,0.0001)
WSA	1KM	Daily to Weekly	max(5%,0.0025)	max(1%,0.0001)

the 1960s to the 1980s, and an increase at a similar rate from the 1980s to 2000, based on estimated changes of the individual radiative components that constitute the surface net radiation.

$$Rn = (1-\alpha)F_d^s + \varepsilon F_d^l - \sigma\varepsilon T_s^4 = H + \lambda E + G \tag{2}$$

Surface net radiation can be expressed as the combination of downward shortwave radiation F_d^s and longwave radiation F_d^l . Albedo and emissivity are two critical variables determining the net radiation, in shortwave and thermal range, respectively. This net radiation is balanced by sensible heat (H), latent heat (λE) and ground transportation (G).

Improved understanding and systematic monitoring of Earth's climate requires observations of various atmospheric, oceanic and terrestrial parameters and therefore has to reply on various technologies (ranging from ground-based instruments to ships, buoys, ocean profilers, ballons, aircraft, satellite-borne sensors, etc.). The Global Climate Observing System (GCOS, 2009) defined a list of 50 so-called Essential Climate Variables (ECVs), that are technically and economically feasible to observe, to support the work of the United Nations Framework Convention on Climate Change(UNFCCC) and the IPCC. Among the terrestrial ECVs, albedo is a critical one for energy balance in solar range. The temporal and spatial resolution of surface albedo and its precision are listed in talbe 2.

Changes in the atmosphere, land, ocean, biosphere and cryosphere-both natural and anthropogenic-can perturb the Earth's radiation budget, producing a radiative forcing (RF) that affects climate. RF is a measure of the net change in the energy balance in response to an external perturbation. All these radiative forcings result from one or more factors that affect climate and are associated with human activities or natural processes as discussed in the text. Surface albedo is listed as one of the uncertain variables for climate change. Fig.6 shows the radiative forcing mean range and uncertainty for different terms, among which albedo shows a two-side effect. According to the estimation between 1750 and 2005 from Intergovernmental Panel on Climate (GIEC), the surface albedo change caused by land use is estimated to have a negative forcing (cooling effect), as -0.2±0.2W/m^2 ; and a positive forcing (warming effect) caused by black carbon deposition on snow, ranging from 0.1±0.1W/m^2.

A number of studies carried out have explored the effects of land cover change on regional climate since late 1970s (Lofgren, 1995). The effect of surface albedo feedback to climate and carbon cycle has been investigated by bulks of studies. Among them, Sahel is a hot region cha-

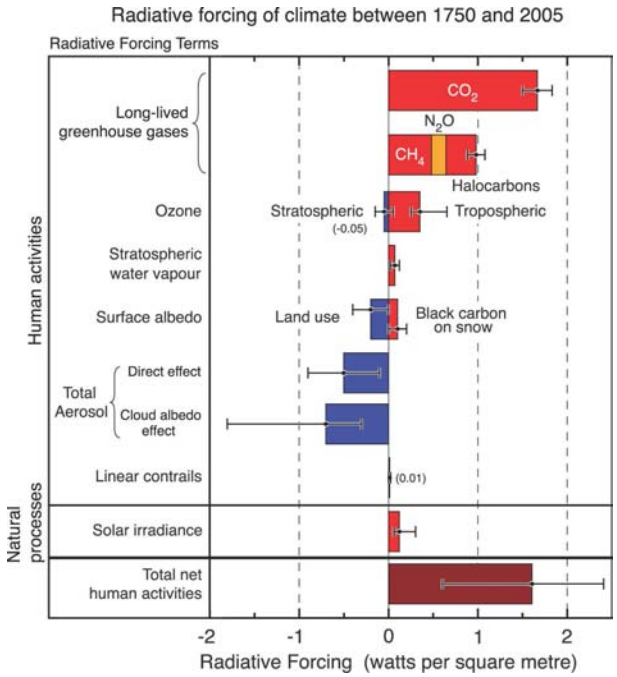

FIGURE 6 – Summary of the principal components of the radiative forcing of climate change. The think black line attached to each color bar represents the range of uncertainty for the respective value. (Source from IPCC, 2007)

racterized by the drought from 1970s-1980s (Charney et al., 1977). A positive snow/ice-albedo feedback within the global climate system has been recognized (Fletcher et al., 2009). It is widely recognized that higher albedo due to desertification and deforestation result in a reduction of precipitation and evapotranspiration (Dirmeyer and Shukla, 1994; Lofgren, 1995; Xue, 1996; Xue and Shukla, 1993). Boreal deforest by decrease in surface albedo has shown a offset for potential carbon sink (Betts, 2000). The cooling effect of the surface albedo increase however is possibly balanced by warming resulting from significantly reduced evapotraspiration. The lack of agreement between model results is partly caused by the differences between the formulations of the land-surface schemes and their parameter fields, besides the fact that the mechanisms of the land-atmopshere interaction are not completely understood.

Snow deposition on vegetation has the effect to alter the albedo due to the complex interaction between vegetation and snow. It is found that the forecast of temperature and humidity in ECMWF at high-latitude is always biased. Primary measurements has bee done under the framework of BOREAS field campaign (Betts and Ball, 1997). After reducing the albedo of snow surfaces from 0.8 to 0.2 for boreal forests in the European Centre for Medium-Range Weather Forecasts (ECMWF) model, it is showed that model's systematic cold bias is largely eliminated over boreal forests in the spring (Viterbo and Betts, 1999). Snow impact the albedo of vegetated land surfaces is illustrated through analyzing MODIS albedo/BRDF dataset along with IGBP cover. Forests have the lowest albedo as expected from their high canopy density and the shading effects, while albedos of nonforested surfaces become much larger with snow but remain less than

that of Greenland, presumed to have albedos of pure snow (Jin et al., 2002). Snowy backgrounds is shown to enhance the absorption of visible light in forest canopies through analysis of Fpar derived from MODIS albedo products (Pinty et al., 2011c). Recent field campaign as SNORTEX (Snow Reflectance Transition Experiment) conducted during 2008-2010 is devoted to study the snow-melt pattern in boreal region at different scale (Roujean et al., 2009). Key variables (albedo, BRDF, fraction, water equivalent) are measured at site level and through helicopters for the validation of satellite products and improve the characterization of snow-forest interaction.

Terrestrial surface is an important component of Earth system, interacting with atmosphere and ocean. Land surface models are developed to simulate the energy, matter and momentum exchange of land surface and atmosphere. They can be served as the surface component for weather forecast models and climate models. In the review of Sellers et al. (1997), land surface models have experienced three generations of development :

(1) The first, developed in the late 1960s and 1970s, was based on simple aerodynamic bulk transfer formulas and often uniform prescriptions of surface parameters (albedo, aerodynamic roughness, and soil moisture availability).

(2) In the early 1980s, a second generation of models explicitly recognized the effects of vegetation in the calculation of the surface energy balance. The parameters of land surface properties were assembled from ecological and geographical surveys published in the scientific literature.

(3) The third generation models use modern theories relating photosynthesiss and plant water relations to provide a consistent description of energy exchange, evapotranspiration, and carbon exchange by plants. A series of large scale field experiments have been executed to validate the process models and scaling assumptions involved in land-atmosphere schemes. These experiments have also accelerated the development of methods for translating satellite data into global surface parameter sets for the models.

Land surface processes have been characterized in climate models by parameterizations that range from rather simple schemes to complex representations. Key model parameters include albedo, fractional vegetation and snow cover, roughness length, surface skin temperature, and canopy properties. However, these variables have been only crudely represented due to limited observations. Satellites provide information of global spatial sampling at regular temporal intervals and thus have the capability to estimate accurately model parameters globally. The availability of satellite observations has motivated many modelers to improve the representation of interactions between soil, vegetation, and the atmosphere.

PILPS (the Intercomparison of Land-surface Parameterization Schemes) is a part of Global Land Atmosphere System Study (GLASS) program aiming to off-line evaluate land surface schemes. It was initialized in 1992, and experienced four phases. The philosophy is outlined by (Henderson-Sellers et al., 1995, 1993a). 23 participating models are inter-compared and compared with observations referring fluxes and state variables. The goal is to improve the parameterization of the land-surface schemes for the use in weather forecast and climate models.

As an open-access, on-going activity, RAdiation transfer Model Intercomparison (RAMI) operates in successive phases each one aiming at re-assessing the capability, performance and agreement of the latest generation of radiation transfer (RT) models. This might lead to model enhancements and further developments that benefit the RT modeling community. Models are compared at several scenarios with different density of vegetation, LAI, soil, etc. Since the first phase of RAMI I in 1999, it has experienced four phases. The latest RAMI IV compared taking the 3D Monte Carlo model as reference. Detailed information can be found in `http://rami-benchmark.jrc.ec.europa.eu/HTML/`.

In virtue of the advent of new generation of Earth observing satellites during the last two decades, various global and continental scale albedo data records were generated , from polar orbiting instruments like MODIS (Moderate Resolution Imaging Spectroradiometer), POLDER (Polarization and Directionality of Earth Reflectance) and VEGETATION onboard SPOT, and also from geostationary observing systems like SEVIRI (Spinning Enhanced Visible and InfraRed Imager) onboard METEOSAT Second Generation (MSG). These data records are derived from well-calibrated reflectance by using well-suited pre-processing chains and consolidated physical algorithms. Climate and also weather forecast communities commonly argue that a 2-5% accuracy range is required for an observed surface albedo to be used in surface modelling. Various validation exercises showed the accuracy of the recent satellite-based albedo products, e.g. MODIS (Jin, 2003), thereby justifying the efforts for refining the description of the surface albedo in land surface models (Oleson, 2003). The accumulation of observations over long time series, typically pluriannual, can be judged useful in order to establish a climatology of soil and vegetation albedos. Recently a global soil background field for climate modelling using multi-annual time series of MODIS observations was produced by (Houldcroft et al., 2009) but the dynamic effects due to SSM were not thoroughly investigated so far. In the case of polar orbiting sensors such as MODIS, a daily revisit may be severely hampered by the high frequency of cloudiness for certain regions. On the other part, a short-term diagnose analysis can be realised by geostationary satellites, while it is geographical limited to reach global coverage. Moreover, Low Elevation Orbit (LEO) observation system normally has higher spatial and spectral resolution comparing with GEO (GEOstationary) satellites. A trimmed analysis of time variations of surface albedo is now possible with the combination of polar and geostationary sensor systems. Apart from hazardous events (flood, storms, strong winds), short-term variations in surface albedo are driven by snow, by SSM, and by the vegetation growth and senescence periods. In this regard, the accumulation of observations over long time series, typically pluriannual, is needed to establish climatology of soil and vegetation albedos.

In SVAT models, vegetation and soil are parameterized separately since they are different properties and involved in different processes relative to solar radiation, heat, and water transfer. Vegetation albedo may vary at daily-weekly time scales corresponding to leaf amount variation, chlorophyll content shift, and brown pigment or even water leaf content, as wavelength dependence. On the other hand, soil albedo would more likely vary on an hourly-daily basis, as its main perturbing field is surface soil moisture (SSM). Modeling the seasonal variation of vegetation albedo is paramount for quantitative assessment of the ecosystem change. Instead, amenable short-term variations of soil albedo would connect to rainfall events, which must be accounted for in the energy budget closure.

The objectives of the thesis are as follows : (1) to construct a prognostic surface albedo in ISBA based on the calibration of LEO and GEO satellite data with in-situ measured SSM and chlorophylle ; (2) to evaluate the impact on energy balance of surface albedo change with moisture within the SURFEX modelling famwork over France ; (3) to perform a joint assimilation of surface albedo with LAI and soil moisture at a reference station.

Organisation of the Paper

The thesis is organized as follows :

Albedo intercomparison is presented in Chapter 2. The objective is to check the spatial and temporal consistency of model albedo with satellite products at daily basis. Firstly, a novel method is proposed to generate daily albedo using MODIS daily directional reflectance and BRDF/Albedo products. Then, the derived daily MODIS albedo is compared with SEVIRI counterparts over France during a 4 year period from 2007 to 2010. Finally, these two daily products are both used to assess the albedo database in ISBA-A-gs model.

Chapter 3 focuses on the separation of total albedo into vegetation and soil components. The motivation and ration is introduced in Section 3.1 towards a modeling perspective. In Section 3.2, a 2-stream radiative transfer scheme is proposed for simulate albedo from vegetation structure, optical property parameters and background information. Stationary and dynamic methods are both applied to MODIS albedo products to generate soil background albedo and vegetation albedo datasets. In Section 3.3, two stationary soil background albedos using different methods : Centre National de Recherches Morologiques (CNRM) and SWANSEA are compared at global scale. In Section 3.4, a dynamic retrieval is performed over France to yield soil background albedo and vegetation leaf reflectance based on 2-stream radiative transfer proposed in Section 3.2. The retrieved soil background albedo and leaf single reflectance are statistically analyzed within main PFT types and soil units.

In Chapter 4, a prognostic total albedo is proposed depending on surface soil moisture and leaf chlorophyll content. The semi-empirical exponential relationship of surface soil albedo and surface soil moisture is calibrated with SEVIRI albedo product and in-situ moisture measurement. Vegetation albedo is parameterized as the function of LAI and leaf chlorophyll content, which is established from simulations using PROSAIL model. Sensitivity test is performed to found the most sensible spectral range with input parameters. MERIS albedo at 560nm is treated as a proxy for chlorophyll content, which would be applied as an observation to constrain the model status.

After integrating the new soil albedo parameterization (depending on surface soil moisture) into the surface model ISBA-A-gs. It is expected that the components of surface energy balance, as net radiation, sensible and latent heat, would be altered. This impact of these improvements of surface albedo on energy budget is evaluated under the framework of SURFEX in Chapter 5.

Conclusions and perspectives are summarized in Chapter 6. The subjects as the accuracy and precision of the satellite albedo products, representation of albedo parameterization in surface model, and assimilation of albedo products into land surface model are discussed.

Chapitre 1

Scientific Context

Contents

1.1 Physical Principle

Surface albedo, defined as the ratio of the reflected solar radiation at the land surface to the total incoming solar radiation, is a primary controlling factor for the surface energy balance. The definition of reflectance and albedo are clarified by (Schaepman-Strub et al., 2006), with different configurations of incoming and outgoing radiance (fig. 1.1). Here, we are focusing on the notations of DHR and BHR, since the two are mostly used in remote sensing products. These albedo are depending a description of directional function BRDF (Bidirectional Reflectance Distribution Function). Symbols and subscripts used in the equations are listed in table 1.1.

$$BRDF = f_r(\Theta_i, \phi_i; \Theta_r, \phi_r) = \frac{dL_r(\Theta_i, \phi_i; \Theta_r, \phi_r)}{dE_i(\Theta_i, \phi_i)}[sr^{-1}] \tag{1.1}$$

Directional-Hemispherical Reflectance (DHR), this is equivalent to Black Sky Albedo (BSA). It is the ratio of the radiant flux for light reflected by a unit surface area into the view hemisphere to the illuminated with a parallel beam of light from a single direction.

$$DHR = \rho(\theta_i, \phi_i, 2\pi) = \frac{d\Phi_r(\theta_i, \phi_i, 2\pi)}{d\Phi_r(\theta_i, \phi_i)} = \int_0^{2\pi} \int_0^{\frac{2}{\pi}} f_r(\theta_i, \phi_i, \theta_r, \phi_r) cos\theta_r sin\theta_r d\theta_r d\phi_r \tag{1.2}$$

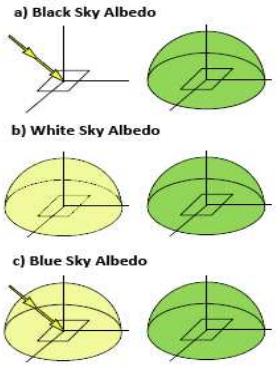

Figure 1.1 – Sketch figure on the definitions of Black Sky Albedo, White Sky Albedo and Blue Sky albedo.

Table 1.1 – Symbols and subscripts for albedo definition.

Symbols	
ϕ	Radiant flux
L	Radiance
ρ	Reflectance
Θ	Zenith angle
φ	Azimuth angle
λ	Wavelength
Subscripts	
i	Incident
r	Reflected

Bi-Hemispherical Reflectance (BHR), this is the ratio of the radiant flux reflected from a unit surface area into the whole hemisphere to the incident radiant flux of hemispherical angular extent. It is equivalent to Blue Sky Albedo.

$$BHR = \rho(2\pi, 2\pi) = \frac{1}{\pi}\int_0^{2\pi}\int_0^{\frac{2}{\pi}} \rho(\theta_i, \phi_i, 2\pi) cos\theta_i sin\theta_i d\theta_i d\theta_i d\phi_i \tag{1.3}$$

If the incoming radiation is pure diffuse, then BHR is the so-called White Sky Albedo (WSA) :

$$BHR = \rho(2\pi, 2\pi) = \frac{1}{\pi}\int_0^{2\pi}\int_0^{\frac{\pi}{2}} \rho(\theta_i, \phi_i, 2\phi cos\theta_i sin\theta_i d\theta_i d\phi_i \tag{1.4}$$

$$\alpha(\theta_i; \Lambda) = \frac{F_u(\theta_i; \Lambda)}{F_d(\theta_i; \Lambda)} = \frac{\int_1^{\lambda_2} F_u(\theta_i; \lambda) d}{\int_1^{\lambda_2} F_d(\theta_i; \lambda) d} \tag{1.5}$$

In clear days, normally incoming radiation is the combination of direct and diffuse, the blue sky albedo.

Where, Λ denote the spectral band ranging from wavelength λ_1 to λ_2. The spectral integration is conducted both to upwelling flux (F_u) and downward flux (F_d) respective to wavelength λ. The spectral albedo is the division of these two integrated fluxes. For narrow to brand band conversion, details can be referred from (Liang, 2001).

1.2 Environment Factors Driving Albedo Variation

Shifts in land cover tend to cause persistent changes in surface albedo. However, similar effects can be also generated by factors that are more temporally dynamic. A local study on the albedo variation conducted by (Samain et al., 2008) reveals the time scale and range of albedo variation caused by various factors : surface moisture, PAR/SW spectral composition, storm, vegetation growth and decay, precipitation inter-annual anomalies. The study used MODIS data, local daily albedo measurements, and aucilliary dataset.

After that, we are focusing on the impact on albedo of fire, surface soil moisture and vegetation growth and decay.

(1) Fire. Fire is a factor of surface change, either natural or anthropogenic, and occurs in most vegetation zones over the world. It destroys vegetation and deposits charcoal and ash, which generally reduces reflectance, especially at infrared wavelengths, whose impact can be detected from satellite fire burn area products (Roy et al., 2008). Fire has two effects on radiative forcing, through surface albedo changes and emission of greenhouse gases and aerosols emitted from biomass burning. The effect of fire on albedo is complex and depends on the pre-fire vegetation structure and underlying soil reflectance ; the combustion completeness of the fire ; unburned leaf drop ; and vegetation regrowth and recovery after the fire (Govaerts, 2002; Roy et al., 2005) analyzed a Meteosat temporal surface albedo data set over Northern Hemisphere Africa and estimated that fires cause a relative albedo decrease of up to 25%. The radiative forcing due to surface albedo relative to fire is estimated in northern Australia (Jin, 2005) and boreal North America (Jin et al., 2012) from MODIS albedo products.

(2) Surface Soil Moisture.

A theory explains the darkening of the soil due to wetness by a reduction of the inner material reflection in presence of films of water coating soil particles (Ångström, 1925). Somewhat as a paradox, the multiple bouncing between a light ray and soil attributes leads to an increase probability of light absorption by water component. According to (Twomey et al., 1986), such phenomenon could be even enhanced by having a weaker relative index of refraction between soil and water (compared to air), thereby having a less deviated light ray to the advantage of increased soil absorption. Above elements of physics seems to support a better coherent response

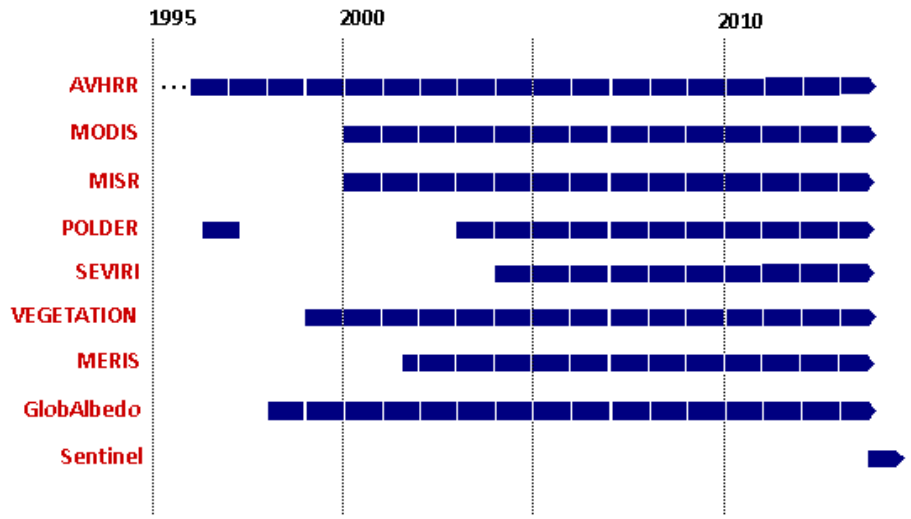

Figure 1.2 – Schematic representation of amplitude and duration of the sources of albedo variations inferred from 7 years of MODIS and in situ data. (Sources from Samain et al., 2008)

to water content for visible wavelengths compared to infrared range. In fact, water absorption is more significant in the near infrared, which could create noise on the results when its characteristics cannot be thoroughly prescribed at coarse scale. Being treated as pure extinction feature of light trapping by any medium, the modeling by an exponential formula seems to find here some justification. The influence of the texture is expected to be significant in theory since the composition in pebbles, stones and relative proportion of sand and clay will shape the dependence of wetness on soil albedo. In this respect, it connects to the degree of porosity while it remains that apparent soil color changes lightly when soils darken. Despite a panorama of different textures between stations, it could not make clear its influence on the calibration between soil moisture and reflectance at the satellite moderate resolution. Even it is not certain that the collection of ground-based measurements would support a transposition to satellite applications due to the complexity of soil landscape in general. Another key issue that cannot be ignored is the chemistry composition of the water, which encompasses air particles deposition and soil organic matter composition. Knowing how dissolved organic material plays on the deviation from an absorption

spectrum of pure water is certainly matter of concern and the role of microbial activity is also probably worth to know. Considering all these sources of uncertainties, it is likely that there exists a physical frontier in terms of appropriate information such like explaining 30% of the variance of the soil reflectance by wetness may be perceived as a reasonable targeted objective. The mixing of different soils at the scale of a satellite pixel justifies the effort for performing directly a calibration at a resolution to be consistent with foremost studies such like meteorological purpose.

After the pioneering work on the relationship between bare soil albedo and soil moisture by (Idso et al., 1975), numerous studies have been devoted to investigate a relationship between bare soil albedo and soil moisture (Duke and Guérif, 1998; Lobell and Asner, 2002). Linear or exponential empirical function is found to well approximate the dependence of this dependence, which is confirmed by numerous field and laboratory measurements (Guan et al., 2009; Roxy et al., 2010). A new finding of (Liu et al., 2002) shows that after a critical water content value, soil reflectance increases with soil moisture. Recently, surface soil albedo dependence on soil moisture is investigated using in-situ data from the moraine of an Andean glacier (Bolivia), and a good approximation to the exponential function is achieved (Gascoin et al., 2009b). This parameterization is incorporated into ORCHIDEE model, and it is found that an increase in the net radiation and a change of turbulent fluxes at annual and monthly time scales (Gascoin et al., 2009a).

(3) Vegetation growth and decay

Phenology, which represents the annual cycles and temporal patterns of plant growth and development, has a seasonal impact on vegetation albedo. Results from regional leaf color survey, local webcam monitoring and satellite observations has show intra-annual variation of phenological metrics (Zhang and Goldberg, 2011). Leaf chlorophyll and water contents are the two important factors controlling leaf optical and short-wave infrared characteristics such as reflectance and transmittance. Further the available wetness condition control the vegetation status, for example, stress or drought would have rapid impact on soil moisture, but also relative slow effect on leaf water and leaf carbon assimilation, this finally influence albedo at canopy level.

Albedo variability for major global vegetation types is examined using MODIS standard Climate Modeling Grid (CMG) albedo and BRDF products (Gao, 2005). The seasonal variation of albedo is strongly dependent on the vegetation types and their location, especially in the near-infrared waveband. The feedback effects of canopy albedo and nitrogen content are recently revealed and confirmed by site-level statistics, which implies the benefits to incorporate such relationship in LSMs (Fisher, 2009; Hollinger et al., 2010; Ollinger et al., 2008).

In SVAT models, vegetation and soil are parameterized separately since they are different properties and involved in different processes relative to solar radiation, heat, and water transfer. Vegetation albedo may vary at daily-weekly time scales corresponding to leaf amount variation, chlorophyll content shift, and brown pigment or even water leaf content, as wavelength dependence. On the other hand, soil albedo would more likely vary on an hourly-daily basis, as its main perturbing field is surface soil moisture (SSM). Modeling the seasonal variation of vegeta-

Table 1.2 – Albedo variation scale and driven factors for vegetation and soil

	Vegetation albedo	Soil albedo
Time scale of variations	Weekly-Monthly	Hourly-Daily
Dependence of properties	Brown pigment Chlorophyll content Leaf water content	Moisture Texture Soil color
Time evolving factors	Stress Mortality	Rain Run-off Drainage

tion albedo is paramount for quantitative assessment of the ecosystem change. Instead, amenable short-term variations of soil albedo would connect to rainfall events, which must be accounted for in the energy budget closure. The time scale of variation and the corresponding driven factors are listed in table 1.2.

1.3 State-of-the-art albedo modeling in surface models

Terrestrial surface is an important component of earth system, interacting with atmosphere and ocean. Land surface models are developed to simulate the energy, matter and momentum exchange of land surface and atmosphere. They can be served as the surface component for weather forecast models and climate models. In the review of (Sellers et al., 1997), land surface models have experienced three generations of development :

(1) The first, developed in the late 1960s and 1970s, was based on simple aerodynamic bulk transfer formulas and often uniform prescriptions of surface parameters (albedo, aerodynamic roughness, and soil moisture availability).

(2) In the early 1980s, a second generation of models explicitly recognized the effects of vegetation in the calculation of the surface energy balance. The parameters of land surface properties were assembled from ecological and geographical surveys published in the scientific literature.

(3) The third generation models use modern theories relating photosynthesiss and plant water relations to provide a consistent description of energy exchange, evapotranspiration, and carbon exchange by plants. A series of large scale field experiments have been executed to validate the process models and scaling assumptions involved in land-atmosphere schemes. These experiments have also accelerated the development of methods for translating satellite data into global surface parameter sets for the models. Land surface processes have been characterized in climate models by parameterizations that range from rather simple schemes to complex representations. Key model parameters include albedo, fractional vegetation and snow cover, roughness length, surface skin temperature, and canopy properties. However, these variables have been only crudely represented due to limited observations. Satellites provide information of global spatial sampling

at regular temporal intervals and thus have the capability to estimate accurately model parameters globally. The availability of satellite observations has motivated many modelers to improve the representation of interactions between soil, vegetation, and the atmosphere.

Common Land Model - Snow-free albedo can be formulated as the weighted sum of the components of soil and vegetation. Bare soil albedo is the function of soil color and soil moisture. Vegetation albedo is calculated by a simplified two-stream scheme depicting the albedo transfer in homogenous canopy interacting with surface ground. Direct and diffuse albedo can be formulated separately. NCAR Community Land Model - Community Land Model-Original albedo construction is similar to Common Land Model. While recently, several improvements have been conducted using remote sensing products to enhance surface parameterization.

Spatial and temporal comparison with MODIS albedo products reveals that snow causes the largest temporal and spatial variations, particularly in VIS band. CLM and MODIS albedo differ considerably in soil albedo over desert and semi-desert regions, especially in the near-infrared band (0.7-5.0 μm), with the largest high bias in the Sahara (Zhou, 2003). Consequently, presenting albedo in CLM using highest quality reprocessed MODIS products of leaf area index (LAI), plant functional type (PFT), and fraction of bare soil, largely reduced the bias (Tian, 2004). Such kind of improvements has been integrated in CLM3.0 simulations. It shows that new parameters significantly improve the climate simulated coupled with Community Climate System Model Version 3.0 (CCSM3.0) (Lawrence and Chase, 2007).

ISBA - In Interaction Sol-Biosph-Atmosph (ISBA) model, land surface physiographic field is parameterized using a 'tile' approach. Snow-free land surface is the combination of vegetation and bare soil weighted by the vegetation fraction. In the version 1 surface physiological database (so called ECOCLIMAP I), bare soil albedo is parameterized as soil mineral composition and organic deposition, which is presented by sand fraction, and woody/herbaceous vegetation types, respectively (Masson et al., 2003). Vegetation albedo is attributed based on land cover type, derived from literatures. The weighted albedo is comparing well with AVHRR datasets (Strugnell et al., 2001).

ECOCLIMAP - In updated version 2 (ECOCLIMAP II), bare soil and vegetation albedo is derived from multi-year MODIS datasets, mainly albedo and LAI (Faroux et al., 2013; Kaptué Tchuenté et al., 2010). Stationary soil and vegetation albedo are derived from total MODIS products with vegetation fraction cover (fveg) using a regression method. fveg is parameterized as an exponential function of LAI. The reconstructed albedo datasets using this parameterization is comparing well with original MODIS products as well as MSG.

EALCO - Ecological Assimilation of Land and Climate Observations (EALCO) is a model developed in CCRS (Canada Centre for Remote Sensing) for ecosystem modeling. A mathematic model based on gap probability is developed, which yields a separation of the canopy into vertical layers for ray tracing (Wang et al., 2002). The parameterization is based on optical parameters ofecosystem elements instead of using albedo parameters of the canopy. The albedo model was applied to a boreal deciduous forest and compared well with field measurements (Wang et al., 2007).

ORCHIDEE - In ancient version, soil and vegetation albedoes are parameterized as the reference values of PFTs, and dynamic variation is only driven by LAI. In the updated version, JRC-2 stream scheme is complemented with explicit parameterization of optical leafy elements, effective LAI, etc. Stratified vertical canopy is modeled in this strategy.

JULES - Vegetation and soil albedo in Joint UK Land Environment Simulator (JULES) are parameterized as reference values of PFTs or soil atlas. These values are attributed based on field measurements or literatures. (Houldcroft et al., 2009) has improved the parameterization using MODIS albedo products. Vegetation albedo for each PFT is derived through 2% of histogram of 'NDVI', which is calculated from broadband albedo. Soil albedo is obtained through regression of broadband albedo against log('NDVI') assuming that these two are linked through a exponential function.

1.4 Albedo Observations

To generate long-term consistent data records for large scales (continental, global), satellite datasets are very useful. SCOPE-CM (Sustained and coordinated processing of Environmental Satellite data for Climate Monitoring) is a network of agencies and operators of environmental satellite systems and interfaces with World Meteorological Organization (WMO), World Climate Research Programme (WCRP), Global Climate Observing System (GCOS), Coordination Group for Meteorological Satellites (CGMS), Committee on Earth Observation Satellites (CEOS) and Global Environment Organization (GEO). It offers its support to coordinate and facilitate international activities to generate Climate Data Records (CDRs) from multi-agency satellite data.

GEWEX is the core project in WRCP (World Climate Research Programme) concerned with studying the dynamics and thermal dynamics of the atmosphere and interactions with the Earth's surface. It is an integrated program of research, observations, and science activitiesthat focuses on the atmospheric, terestrial, radiative, hydrological, coupled processes, and interactions that determine the global and regional hydrological cycle, radiation and energy transitions, and their involvement in climate change. TheInternational GEWEX Project Office (IGPO) is the focal point for the planning and implementation of all GEWEX activities.

1.4.1 Site Measurements

Long-term regular site level albedo measurements are also available from ground based networks as BSRN, SURFRAD, FLUXNET. BSRN-The Baseline Surface Radiation Network (BSRN) is apart of GEWEX, which conceived and implemented in the late 1980s by the World Climate Research Program (WCRP) with the collected data intended to be used for climate research applications, in particular ; satellite product validation, climate model comparisons, and establishment of regional radiation climatologies, all in support of Earth radiation budget studies. Many of these stations began operation in 1992 and each year more stations are added to the network. About 40 stations in contrasting climatic zones, covering a latitude range from 80°N to

90°S (see station maps) are providing data to the BSRN archive located at the Alfred Wegener Institute (AWI) in Bremerhaven, Germany. These stations provide data for the calibration of the GEWEX Surface Radiation Budget (SRB) Project and other satellite-based measurements of radiative fluxes. Detailed information can be found in `http://www.bsrn.awi.de/`.

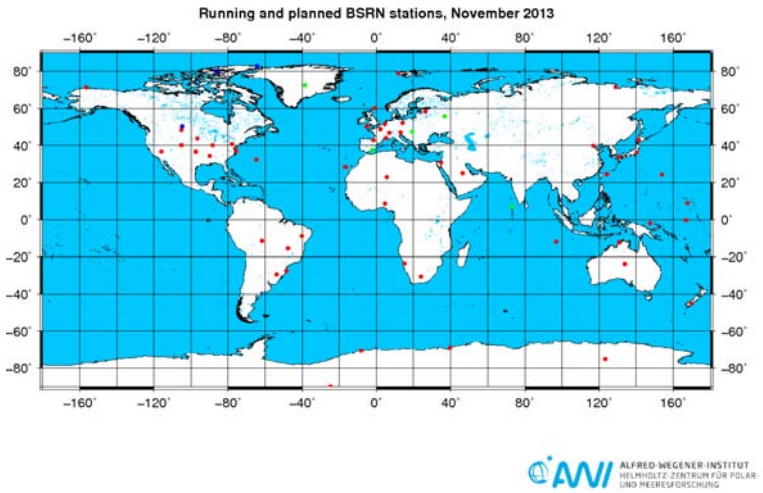

FIGURE 1.3 – Global distribution of BSRN stations. Red dots denote BSRN stations which have already submitted data offered in the WRMC. Green dots represent accepted BSRN stations which plan to submit data in future. BSRN stations which are closed are marked in blue. (Source from BSRN website `http://www.bsrn.awi.de/`.)

SURFRAD-(SURFace RADiation Budget Network) is a network established by National Oceanic And Atmospheric Administration (NOAA) for the objective to support climate research with accurate, continuous, long-term measurements of the surface radiation budget over the United States. Currently seven SURFRAD stations are operating in climatologically diverse regions : Montana, Colorado, Illinois, Mississippi, Pennsylvania, Nevada and South Dakota. Independent measures of upwelling and downwelling, solar and infrared are the primary measurements ; ancillary observations include direct and diffuse solar, photosynthetically active radiation, UVB, spectral solar, and meteorological parameters. It should be noted that SURFRAD contributes to BSRN, they can be identified from fig. 1.3. More descriptions can be referred to `http://www.esrl.noaa.gov/gmd/grad/surfrad/`.

FLUXNET- FLUXNET is a global network of micrometeorological flux measurement sites that measure the exchanges of carbon dioxide, water vapor, and energy between the biosphere and atmosphere (Baldocchi et al., 2001). At present over 140 sites are operating on a long-term and continuous basis (fig.1.4). Vegetation under study includes temperate conifer and broadleaved (deciduous and evergreen) forests, tropical and boreal forests, crops, grasslands, chaparral, wetlands, and tundra. Sites exist on five continents and their latitudinal distribution ranges from 70°N to 30°S. FLUXNET stations are providing tower measurements of energy flux as well as other meteorological variables (Baldocchi et al., 2001). They encompass different vegetation function types : crops, shrub, evergreen broadleaf trees, deciduous broadleaf trees and evergreen

needleleaf trees. These stations are constructed at different period, while the longest data record can be dated from the year of 2000. In the present study, we are using the datasets from 2007-2010. These records are distributed freely in the website : `http://fluxnet.ornl.gov/` since December 2007.

Figure 1.4 – Global distribution of the FLUXNET stations. (Source from website `http://bwc.berkeley.edu/Fluxnet-LaThuile/map/`)

1.4.2 Satellite albedo products

In 1990s, global albedo products were first derived from sensors as AVHRR (Csiszar and Gutman, 1999; Strugnell et al., 2001), Earth Radiation Budget Experiment (ERBE), CERES (Rutan et al., 2009), offer the large-scale consistent observations for characterizing the surface. Early generation of surface models benefit from this kind of information, and digest albedo by different scheme as climatology. In the end of 20th century, with the new generation of platforms and Earth observation sensors, with more spectral bands and well-calibration, more accurate albedo products are derived from MODIS, MISR, VEGETATION, POLarization and Directionality of the Earth's Reflectances (POLDER), Spinning Enhanced Visible and Infrared Imager (SEVIRI), MERIS, etc. These products are derived by using the semi-empirical BRDF model, and taking use of different properties of the sensors, like multi-angle, high re-visit frequency, etc. Recently, ESA has completed a project to generate and distribute global albedo data records by merging data from various European sensors.

For climate modeling, it is generally recongnized that an absolute accuracy of 0.02-0.05, or a relative accuracy of 5% is required (Henderson-Sellers and Wilson, 1983; Henderson-Sellers et al., 1993b). Early stage observations, as AVHRR, are suffered from limitations (incomplete spectral range, directional effects, orbital drifts, incomplete atmospheric corrections, difficulties of sensor intercalibration) which may bring precise characteristics of inter-annual variability and trends close to the noise level. Recent data sets and new generation sensors are greatly improved in these respects. The available global or continential datasets are demonstrated in fig. 1.5.

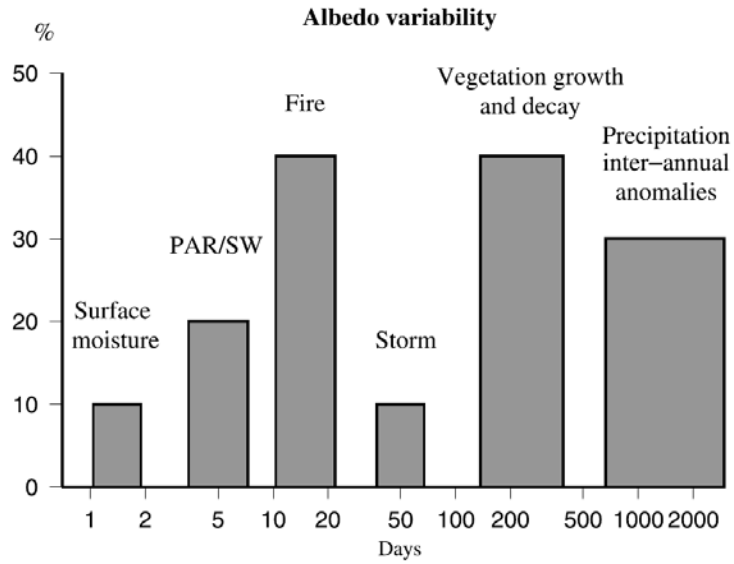

FIGURE 1.5 – Duration period of long-term available continental and global satellite albedo products.

MODIS - The Moderate Resolution Imaging Spectroradiometer (MODIS) is a NASA's instrument for remote sensing of the Earth atmosphere, oceans and land surface. MODIS instrument is flown by the TERRA platform since December 18, 1999 and by the AQUA platform since May 4, 2002. We obtained MODIS products for the period 2007-2008 from REVERB (`http://reverb.echo.nasa.gov/reverb/`) server hosted by NASA. The downloaded products were at a spatial resolution of 500m on Integerized Sinusoidal Grid (ISG) projection. They were tiled and resampled at the resolution of $1/224^{\circ}$ and re-projected on a UTM (Universal Transverse Mercator) grid with the geoid World Geodetic System (WGS) 84. In the latest Collection 5, merged TERRA and AQUA MODIS albedo/BRDF products are distributed on 8-day synthesis period issued from an initial 16-day composite period of clear sky data accumulation. Various solar/observation geometries are combined to adjust a BRDF kernel-driven model further serving to albedo estimate citeSchaaf2002.

Failure to invert the BRDF model is due to missing data - arbitrarily 7 observations are at least necessary - a back-up algorithm is activated. For the case of interest here, 3 MODIS broadband albedo are distributed : VIS (0.3-0.7μm), NIR (0.7-5.0μm), and SW (0.3-5.0μm) along with Quality Assessment (QA) including notably a snow mask. MODIS programme generates in fact directional-hemispherical reflectance or black sky albedo (BSA) and bi-hemispherical reflectance or white sky albedo (WSA). The accuracy of these product was assessed within 5% for main algorithm (Jin, 2003).

POLDER-POLarizationand Directionality of the Earth's Reflectances) is an instrument providing directional and polarization signals designed for atmosphere and land surface studies. It is launched onboard 3 satellites during a period discontinuously : ADEOS-1(Nov, 1996-Jun,

1997), ADEOS-2(Apr, 2003-Oct, 2003), Polarisation et Anisotropie des Rectances au sommet de l'Atmosph, coupl avec un Satellite d'Observation emportant un Lidar (PARASOL) (2005-). It has the advantage of angular sampling with a wide track and around 6km spatial resolution. Albedo and BRDF database is accessible via POSTEL (`http://postel.mediasfrance.org/`). The retrieval algorithm use GLC2000 land cover map, with a modified semi-empirical BRDF model considering hot-spot effect (Maignan et al., 2004). For Polder-2, validation is conducted through comparison with similar existing satellite products and model climatology (Hautecoeur and Roujean, 2007).

SEVIRI-SEVIRI (Spinning Enhanced Visible and Infrared Imager) instrument onboard MSG offers a sub-track resolution of 3 km in the shortwave channels VIS0.6, VIS0.8 and SWIR1.6 centred on 0.6μm, 0.8μm and 1.6μm, respectively. The pixel resolution falls within the range 4-5km over France. Using the three SEVIRI spectral bands, Land Surface Analysis Satellite Applications Facility (LSA-SAF) project (e.g. (Trigo et al., 2011)) generates directional-hemispherical reflectance (DHR) at solar noon as well as bi-hemispherical reflectance (BHR) over Europe, Africa, and eastern part of South America. Compiling slots on same day leads to a daily derivation of BRDF coefficients using the kernel-driven model of (Roujean et al., 1992). The disseminated products are broadband DHR and BHR in the visible (0.3-0.7μm), near infrared (0.7-4.0μm), and solar (0.3-4.0μm) spectral domains (e.g. Geiger et al. 2008). Their quality was judged in valuable adequacy with broadband MODIS albedo products and also albedo issued from ground measurements (Carrer et al., 2010). At the opposite to MODIS, a ground target is viewed by SEVIRI with quasi-similar inclination but various directional illuminations corresponding to the diurnal course of the sun at the frequency of 15 minutes. The algorithm uses a kernel-driven model (Roujean et al., 1992). Observations are accumulated during one day from each 30 min slots. Snow and cloud are masked although the occurrence of residual effects is still a possibility. Quality Assessment (QA) for each observation includes information on cloud, snow, and algorithm inversion status. The required specification for LSA SAF albedo has been fixed to 0.03 for albedo less than 0.15, and 20% for albedo greater than 0.15. Results of comparison show a slight overestimate of SEVIRI visible albedo compared to MODIS and SEVIRI. This discrepancy is thought to be due to the use of different kernels or various angular sampling but more likely aerosol load handled in performing correction.

MERIS-MEdium Resolution Imaging Spectrometer (MERIS) is one of the main instruments on board the European Space Agency (ESA)'s Envisat platform. The 16-day and monthly MERIS albedo products are provided at 0.05 degree resolution. Due to the limitation of its low repeat frequency and relatively less swath width, BRDF inversion is applied using the magnitude algorithm based on the BRDF of MODIS 0.05 degree climate product (MOD43C2) (Gao, 2003). A gapless monthly aerosol dataset is serving as input. 15 spectral as well as VIS, NIR, SW broadband BRDF and albedos are produced. Narrow to broadband conversion is conducted by using similar conversion coefficients as MISR bands. The spectral albedo products of this ALBEDOMAP have been compared with MODIS 16-day and MISR monthly albedo products. Good agreements between MERIS and MODIS while some disagreement features indicate that the atmospheric correction and the cloud detection need to be improved.

MISR-Multi-angle Imaging SpectroRadiometer DHR and BHR products are generated for 4 spectral bands and 3 boardbands : VIS, NIR, SW at 1.1km scale each 16 day. It can be downloaded from : `https://eosweb.larc.nasa.gov/PRODOCS/misr/level3/product.html`. The standard algorithm inverts the Modified-Rahman-Pinty-Verstaete (MRPV) empirical model to fit the BRFs observed at 9 different angles within 4 spectral bands (Martonchik et al., 1998). The albedo products have been compared well with MODIS (Taberner et al., 2010) and ground measurements (Chen et al., 2008).

Table 1.3 – Comparison of existing albedo products from satellites.

Sensors	Time	Pixel	Band	Coverage	Ref
AVHRR	30d	1km	3BB	Global	NOAA
MODIS	8d	0.5-1km	7NB+3BB	Global	NASA/BU
MISR	16d	1km	4NB+3BB	Global	JPL/BU
SEVIRI	1d	3-7km	3BB	MSG Disk	EUMESAT/LSA SAF
POLDER	10d	6km	6NB+3BB	Global	CNES
VEGETATION	10d	1km	4NB+3BB	Global	GEOLAND2
MERIS	16d	0.05d	4NB+3BB	Global	ESA
GlobalAlbedo	16d	1km	3BB	Global	ESA

VEGETATION-Albedo has been derived from VEGETATION onbard Satellite Pour l'Observation de la Terre (SPOT4/5) under the project CYCLOPES and recently GEOLAND2 globally (Geiger et al., 2008). It consists of the broadband ([0.4, 0.7μm], [0.7, 4μm], [0.3-4μm]) black-sky and the white-sky albedo. These products cover the period from 1999 to the present and the production is continuing in near real time with a new product available every 10 days.The SPOT/VEGETATION Surface Albedo products can be ordered through the link : `http://www.geoland2.eu/core-mapping-services/biopar.html`.

GlobAlbedo-ESA has completed the project GlobAlbedo at 2012 aiming to produce global albedo database using merely the European assets (sensors : VEGETATION/SPOT-4/5, MERIS, AASTR/ENVISAT), which can be extended to future operational requirements (`http://www.globalbedo.org`). Products are provided as DHR and BHR as well as the uncertainty at two temporal and spatial composing : 1km and 16 days, 0.05 degree and monthly. The fusion of observations from various sensors improves the sampling of directional reflectance in clear days. A temporal constrain is applied to the BRDF model inversion (Muller et al., 2011). This product is assessed for 11 validation tiles, 53 FLUXNET sites and compared with SEVIRI, MISR and MODIS products (Muller et al., 2011).

ESA is currently pushing forward a satellite mission named 'Sentinel' for the operational needs of the Copernicus program (previously known as Global Monitoring for Environment and Security). It consists of five satellites, both polar-orbiting and geostationary to fulfill revisit and coverage requirements (Donlon et al., 2012). This next generation satellite observations would benefit the studies for atmosphere, terrestrial and ocean. Albedo products generated from this framework is expected to continue the medium resolution data records with higher quality.

Due to the cloud, aerosol and snow, satellite derived terrestrial biophysical products are not spatial and temporal continuously available. For example, tropical regions are masked by cloud frequently. Another limiting factor is the retrieval process. Owning to the representative capability of physical model and retrieval methods, poor quality output might be achieved when there is not enough sampling of observations. However, the climate modeling applications require gapless high-quality input. There are two ways to generate spatial and temporal continuous datasets :

1) Preprocessing and 2) Post-processing. Preprocessing is to reconstruct continuous radiance or reflectance. Then retrieval is performed using the interpolated radiance or reflectance. Alternative way is to fill and smooth time series of products using statistical methods as filtering (spline-cubic, S-G, wavelet etc) (Chen and Deng, 2006; Lu et al., 2007) or considering the QA information (Yuan et al., 2011) or from the kernel temporal constrain (Quaife and Lewis, 2010). Software like TIMESAT is well-known to deal with such problem and seasonality extraction (`http://www.nateko.lu.se/TIMESAT/timesat.asp`) (Jonsson and Eklundh, 2002; Jönsson and Eklundh, 2004). A spatially complete global snow-free land surface albedo dataset is generated by filling in missing data from the official MOD43B3 dataset based on phenology information (Xiao and Moody, 2005).

The consistency of observations can be checked through satellite product intercomparison. Since the global datasets are generated using different sensors onboard different platform, and employing different algorithm, the products are different. Efforts have been done to intercompare these products at global or continental scale, which would offer information for the users and feedback for product developers. A list of publications relative to this objective can be found in `http://lpvs.gsfc.nasa.gov/srad\_background.html`. For instance, MODIS and MISR albedo products are compared over the African continent, presenting a good agreement, while MISR shortwave albedo is a little higher than MODIS counterpart over the study region (Taberner et al., 2010). MODIS and SEVIRI albedo products are compared at Europe and Africa, showing a statistical good consistency, while retrieval from SEVIRI is generally a little bit higher than MODIS (Carrer et al., 2010). POLDER albedo product is validated through comparing with products from MODIS, MISR, Action de Recherche Petite Echelle Grande Echelle (ARPEGE) climatology, Meteosat-7 at 0.5 degree and showing a good consistency (Hautecoeur and Roujean, 2007).

With the encouragement of good consistency of the albedo products, fusion is conducted. A global albedo dataset is generated from geostationary satellites (METEOSAT-5/7, GOES-8/10, GMS-5) (Govaerts et al., 2008; Pinty et al., 2007) retrieved the surface parameters from MODIS and MISR albedo datasets. MODIS BRDF information is used to add information to MERIS (Gao, 2003) and Landsat observations for albedo retrieval (Shuai et al., 2011). A spectral and temporal fusion approach is proposed for medium resolution sensors, as MERIS, MODIS, VEGETATION (Samain et al., 2008).

With advanced albedo parameterization, it is expected to represent better temporal variation and spatial heteorogenity. The assimilation technique would offer a more objective way to gap fill the observations. Moreover, it has the ability to real-time analysis of surface parameters. (Qin et al., 2006) used the KF principle and a-priori BRDF coefficients and associated covariance to inverse noisy measurements. MODIS albedo is assimilated by using Kalman Filter in the study of (Samain et al., 2008) as state variables, temporal evolution is constrained through the time series profiles of BRDF coefficients extracted within different ECOCLIMAP cover types. Compared to presently available products from VEGETATION and MODIS instruments, this new approach allows to fill the gaps and improves the retrieved parameters time consistency.

However, the evolution of the above mentioned studies are not driven by the complex model. To realize the albedo assimilation, parameterization of land surface model should be improved. When digesting the information from satellites, most land surface models are presenting relatively better the spatial heterogeneity, while the temporal evolutions are not so well presented. In the first generation of land surface models, albedo is commonly parameterized in a relative simple formulation, as fixed values depending on vegetation type, soil atlas, etc. This type of attribute values is derived from sparse measurements limited in time and space. With the advent of satellite derived large-scale high precision albedo, improvements are performed in various aspects. In nowadays land surface models, albedo is modeled as the canopy structural parameter, while the dynamic of optical properties are not well presented or treated as reference values. Moreover, with the trend of adding dynamic vegetation into the land surface models, it is required to have a more precise representation of albedo dependence on vegetation structure parameters. Bare soil albedo is normally parameterized as a temporal constant value in land surface models. The spatial heterogeneity is represented by a reference to soil maps, or linked with properties as soil color, textures. Soil moisture effects are rarely incorporated in these models. With incorporation of such surface albedo and surface soil moisture dependence, it is expected to change the simulation capability of surface energy components.

Chapitre 2

Observed and modeled surface albedo for NWP

Contents

2.1 Introduction

Surface albedo is a critical parameter in land surface models (LSMs) and can be observed through satellite remote sensing. In the first and second generation of LSMs, surface albedo is commonly derived from field measurements or fixed as empirical values, which are parameterized as reference value of surface type (Pitman, 2003; Sellers et al., 1997). With the advent of albedo datasets from moderate resolution satellites, as AVHRR, albedo climatology is derived (Csiszar and Gutman, 1999; Strugnell et al., 2001) and integrated in LSMs in 1990s. Nowadays, better-calibrated albedo data records are available, which would benefit the parameterization of albedo in new generation LSMs. To assess the prediction ability of surface models, the first step is to compare model simulated albedo with satellite observations.

Daily observations have the capability to track hazardous events (fire, flooding, snow fall). For instance, firefighters now use daily MODIS products to help allocate resources to fight for wildfires. Timely detection of burned area extent contributes to estimates of forest loss, charcoal and ash deposits, and vegetation removal. The snow physical characteristics, areal coverage, and duration of snow cover have a direct impact on the environmental system. Snow albedo varies as a function of environmental conditions, land cover, and snow metamorphism. It is also useful to capture rapid vegetation change (onset, green-up, senescence, harvest, clear chopping). The phenology metrics can be derived from vegetation index as NDVI, and mapped at global or continental scale, which shows well correlation with ground records. The distribution of phenology quantities are linked with climate factors as temperature, precipitation, etc.

Daily Albedo is found to be benefit for NWP models. (Cedilnik et al., 2012) assessed the impact of using an analysed surface albedo based on daily satellite observations in NWP model ALADIN in substitution to the climatology. Forecasts over a 1-yr period reveal the capacity of satellite information to reduce model biases and RMSE in screen-level temperature. An unexpected behavior produced in summer by the satellite-derived albedo on surface temperature is also explained.

Through comparison with satellite observations, it is benefit to validate and improve model parameterizations. Wei et al. (2001) compared albedos of two land surface models (LSMs), the biosphere-atmosphere transfer scheme (BATS), and the NCAR LSM, with those derived from remote-sensed data. Both BATS and LSM demonstrated a large bias over snow covered, desert and semidesert regions. Oleson (2003) compared land surface albedo from the Community Land Model with white-sky (diffuse) and black-sky albedo (direct at local solar noon) from MODIS. It is found that in regions with extensive snow cover, the model overestimates white- and black-sky albedo by up to 20% absolute. The snow-free visible and near-infrared black-sky albedo is simulated quite well with biases within 5% over most of the land surface. However, a large negative model bias was found for the Sahara Desert and Arabian Peninsula, particularly in the near-infrared. Zhou (2003) analysed the spaial and temporal variation of CLM and MODIS albedo. It indicates that adjustments of the prescribed albedos in CLM based on MODIS observations could reduce such biases.

At the end of this chapter and as a targeted objective, ISBA land surface model is running off-line with forcing Syst d'Analyse Fournissant des Reseignements Atmosphque a la Neige (SAFRAN) to output albedo. This simulated albedo is compared with three types of satellite products previously presented, namely MODIS standard 8D albedo (MODIS 8D), enhanced daily MODIS albedo (MODIS 1D), and SEVIRI albedo (SEVIRI 1D). The method of construction of a daily MODIS albedo in Section 2.3. Validation at FLUXNET sites follows in Section 2.2. Then, a comparison of 1D MODIS albedo products is conducted with aspect to MODIS 8D standard product and daily SEVIRI albedo are presented in Section 2.4. The albedo parameterization of ECOCLIMAP is reviewed in Section in preamble of a further comparison of this latter with MODIS 1D, MODIS 8D, SEVIRI 1D albedo products (Section 2.6). Conclusions are summerized in Section 2.7

2.2 Presentation of SEVIRI albedo product

Spinning Enhanced Visible and InfraRed Imager (SEVIRI) onboard METEOSAT Second Generation (MSG) offers a sub-track resolution of 3 km in the shortwave channels VIS0.6, VIS0.8 and SWIR1.6 centred on 0.6μm, 0.8μm and 1.6μm, respectively. The pixel resolution falls within the range 4-5km over France. Using the three SEVIRI spectral bands, the LSA-SAF service (e.g. (Trigo et al., 2011) generates directional-hemispherical reflectance (DHR) at solar noon as well as bi-hemispherical reflectance (BHR) over Europe, Africa, and eastern part of South America. Compiling slots on same day leads to a daily derivation of BRDF (Bidirectional Reflectance Distribution Function) coefficients using the kernel-driven model of (Roujean et al., 1992). The disseminated products are broadband DHR and BHR in the visible (0.3-0.7μm), near infrared (0.7-4.0μm), and solar (0.3-4.0μm) spectral domains (e.g. (Geiger et al., 2008)). Their quality was assessed through the comparison with the broadband MODIS albedo products and with albedo in situ observations (Carrer et al., 2010). At opposed to MODIS, a ground target is viewed by SEVIRI under quasi-similar inclinations but for various directional illuminations corresponding to the diurnal course of the sun at the frequency of 15 minutes. Observations from 30 min slots are accumulated during one day, from sunrise to sunset, for illumination angles lower than 85°. Snow and clouds are masked although the occurrence of residual effects is still possible. Quality Assessment (QA) for each observation includes information on cloud, snow, and algorithm inversion status. The pixels contaminated by clouds or snow is not considered. The required specification for LSA-SAF albedo has been fixed to 0.03 for albedo less than 0.15, and 20% for albedo greater than 0.15. Results of comparison show that the SEVIRI visible albedo is slightly overestimated compared to MODIS. This discrepancy is thought to be due to the selection of kernels or angular sampling handled to perform the directional correction.

2.3 Construction of a Daily MODIS Albedo product

Daily observations have the capability to capture the track hazardous events (fire, flooding, snow fall) and to better sample the seasonal trends of vegetation attributes (leaf germinate, senescence, harvest, clear chopping). The seasonality of surface albedo is physically linked to vegetation phenology, while short-term variations might depend on incident composition, precipitation, soil moisture (Samain et al., 2008). A daily observation is required to depict the wetness of the surface.

MODIS standard product is 8 day synthesis from given weights to different days during a 16 day composite period. It is derived from inverting a linear kernel model yielding three parameters describing the BRDF shape and angle-integrated albedos. To achieve the temporal enhancement, both original 8D BRDF parameters and albedo products are used in the present study. Daily MODIS directional reflectances are harnessed to generate the daily MODIS albedo.

2.3.1 Input data sets

2.3.1.1 Geographic Domain and Input MODIS files

The study area falls in a geographic domain formed by a lat-lon box of [40.01°N, 5.5°W, 51.50°N, 9.91°E] over the France country. Within the frame of global MODIS ISIN (Intergerized SINusoidal) projection, six tiles 'H17V03', 'H17V04', 'H17V05', 'H18V03', 'H18V04', 'H18V05' are downloaded to cover the study area (red frame in fig. 2.1). Reprojection and mosaic are conducted with the aid of MRT (MODIS Reprojection Tool).

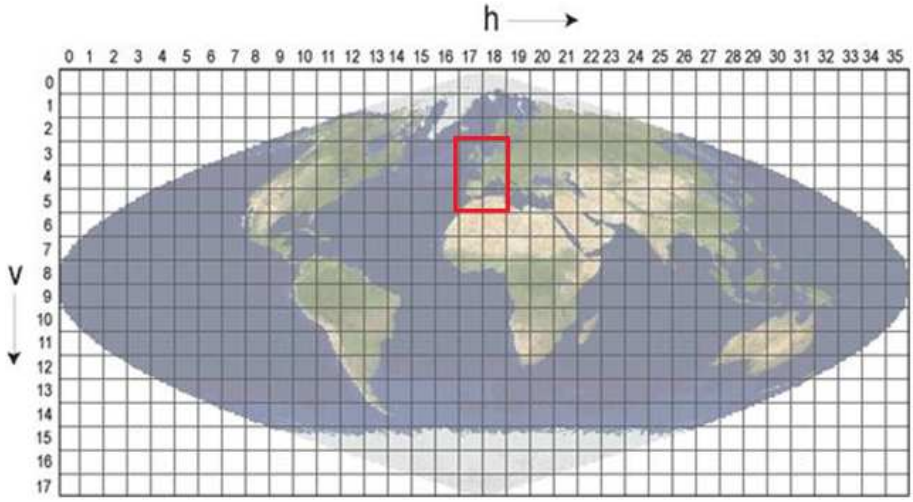

Figure 2.1 – Tiles covering the study area in MODIS ISIN projection (red frame).

MODIS Level 2 products MOD09GA MYD09GA are daily composited surface reflectance with MODIS Band 1-7 observed by TERRA and AQUA satellites respectively. They are distributed in a 'tile' approach at 500m spatial resolution with ISIN (Integerized SINusoidal) projection. Atmosphere effects are corrected from upstream processing chain (Vermote et al., 2002). Quality Control (QC) indicates the quality of reflectance as well as the adjacency and atmospheric correction performance (Vermote and Kotchenova, 2008).

Albedo/BRDF-MCD43A1 is 8 day products of 500m resolution which includes BRDF parameters from combined MODIS sensors onboard TERRA and AQUA satellites (Román et al., 2010). It is generated through inverting a linear kernel-driven BRDF model using directional reflectance accumulated in a temporal window of 16 days. A backup magnitude method is used when there are no enough clear observations for regressing the linear kernel-driven model (Schaaf et al., 2002).

MCD43B3 is 1km albedo from combined MODIS sensors onboard TERRA and AQUA satellites. It comprises seven narrow bands as well as three broad bands : visible (VIS), near-infra-red (NIR), shortwave (SW). The narrow-to broad band conversion is conducted through the linear combination with coefficients indicated in table 2.1 (Liang, 2001). Manyfold field experiments led to the product validation of 0.05.

MCD43A2 provides Albedo/BRDF quality. It is distributed as a companion product of MCD43A1 along with the same spatial resolution of 500m and temporal interval of 8 day. The information on QC is contained in MCD43A2 by flagging the method used : main or backup, and the retrieval quality : good or poor.

2.3.1.2 Ancillary files

ECMWF (European Center for Medium range Weather Forecasting) provides aerosol reanalysis data records in the framework of MACC (Monitoring Atmospheric Composition Climate). They are accessible from interface : `http://data-portal.ecmwf.int/data/d/macc\_reanalysis/`. An aerosol forecasting method was developed (See (Morcrette et al., 2009)) and also an assimilation model (Benedetti et al., 2009).

In this study, daily re-analysed MACC Aerosol Optical Depth (AOD) is downloaded at the wavelength 550nm during the period 2007-2010. It ensures a global coverage with spatial resolution of 0.25 degree. Different time step can be chosen, as 00 :00, 03 :00, 06 :00, 12 :00 from the distribution interface. Daily averaged value is derived as a combination of different hours.

2.3.2 Presentation of the Method

2.3.2.1 Underlying physical assumptions and general description

A key underlying assumption behind the method is that the BRDF shape must remain invariant during the 16-days period of composition. In reality, apart hazards, intense storms or winds, the structure of any surface target is slightly modified day after day, or at least hard to detect from remote sensing scans. Hence, one should wait for a certain number of days, approximately 20 days, which is more or less arbitrarily determined. As for ma crop for instance, which shows rapid growth, in fact the height is increased and thus density is enlarged at a rate less than the pattern of individual plant stand. On the other hand, the day-to-day evolution of the magnitude of the reflectance remains the main driver because the effects of environmental stress factors (light, water, chemical components) are primarily affecting the leafy material. In order to adjust the magnitude, MODIS directional reflectance is used comparing with 8 day average directional reflectance simulated by BRDF model and parameters from MCD43B3 products.

The processing chain is shown in fig. 2.2. It comprises two stages :

(1) The generation of BSA and WSA.

(2) The combination of BSA and WSA to produce TSA (Total Sky Albedo) for validation with FLUXNET.

Input datasets are MODIS 1D directional reflectance MOD09GA, MYD09GA, and 8D surface BRDF parameters MCD43A1, as described in Section 2.3.1.1. Three steps are taken to generate

broadband 1D BSA and WSA, namely :

(1) Scale BRDF shape ;

(2) Angle Integration ;

(3) Narrow to Broad Band Conversion.

In order to combine WSA and BSA to generate TSA, the diffuse fraction is required. Herein, we are using AOD (Aerosol Optical Depth) to estimate this quantity. A relationship of AOD and diffuse fraction is established from 6S code with solar and view zenith angle in consideration. It is applied to MACC re-analysed aerosol products (**??**).

2.3.2.2 Scaling BRDF shape

Hereafter, it is listed the equations used in the scaling processing, first the scaling factor k is calculated in the following equation :

$$k = \frac{\rho(\theta_s, \theta_v, \phi)}{\rho^{'}(\theta_s, \theta_v, \phi)} \tag{2.1}$$

with $\rho(\theta_s, \theta_v, \phi)$: MODIS observed directional reflectance (MOD09GA for TERRA and MYD09GA for Aqua)
$\rho^{'}(\theta_s, \theta_v, \phi)$: MODIS reconstructed directional reflectance from the linear kernel-driven model. This latter reflectance can be expressed as follows :

$$\rho(\theta_s, \theta_v, \phi) = a_0 + a_1 f_1(\theta_s, \theta_v, \phi) + a_2 f_2(\theta_s, \theta_v, \phi) \tag{2.2}$$

Where a_0, a_1, a_2 are three BRDF parameters from MCD43A1 product, f_1, f_2 are kernels as function of observation geometry. The kernel expressions read :

$$f_1 = [(\pi/2 - \xi)cos\xi + sin\xi]/[cos\theta_s + cos\theta_v] - \pi/4 \tag{2.3}$$

where

$$cos\xi = cos\theta_s cos\theta_v + sin\theta_s sin\theta_v cos\phi \tag{2.4}$$

$$f_2 = O(\theta_s, \theta_v, \phi) - sec\theta_s{}' - sec\theta_v^{'} + \frac{(1 + cos\xi^{'})sec\theta_s^{'} sec\theta_v^{'}}{2} \tag{2.5}$$

$$O = \frac{1}{\pi}(t - sintcost)(sec\theta_s^{'} + sec\theta_v^{'}) \tag{2.6}$$

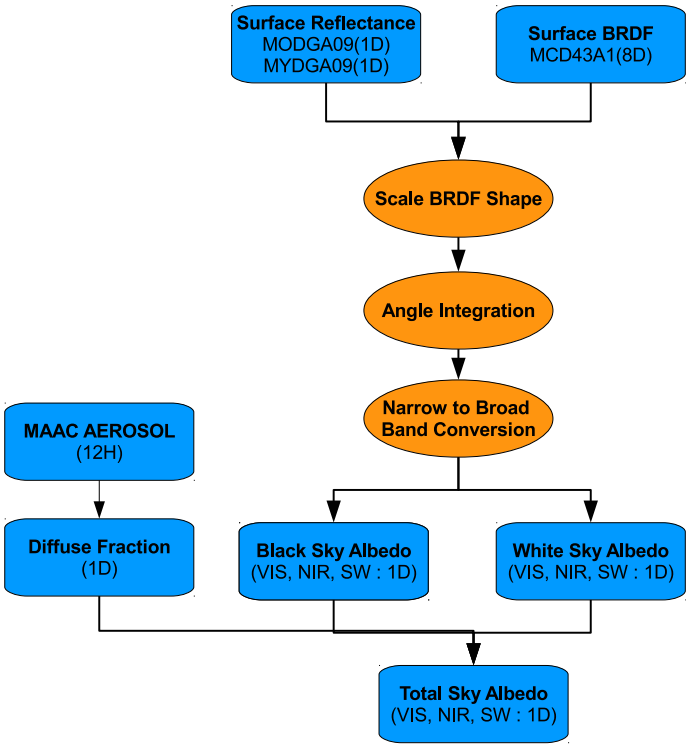

FIGURE 2.2 – Processing chain of daily MODIS albedo.

A scaling factor is used to derive 1-d spectral MODIS albedo from 8-d equivalent, which can be expressed :

$$A'_\lambda = k\bar{A}_\lambda \tag{2.7}$$

Having :
A'_λ : the 1-d spectral albedo at wavelength,
A_λ : the 8-d product from MCD43B3,
k : the scaling factor.

Table 2.1 – Spectral-to-Broadband Conversion coefifcients for MODIS (adopted from MOD09 ATBD)

Band	Wavelength	VIS-BB	NIR-BB	SW-BB
Blue	0.459-0.479	0.4364	0.0000	0.3489
Green	0.545-0.565	0.2366	0.0000	0.2655
Red	0.620-0.670	0.3265	0.0000	0.3489
NIR	0.841-0.876	0.0000	0.5447	0.2382
1.2	1.230-1.250	0.2366	0.0000	0.1604
1.6	1.628-1.652	0.3265	0.0000	0.0138
2.1	2.105-2.155	0.0000	0.2536	0.0682
Intercept		0.0019	0.0068	0.0036

Here, A_λ can be either BSA or WSA.

2.3.2.3 Narrow to Broad Band conversion

Spectral to broadband conversion is performed using the equations in the MOD09 ATBD (Algorithm Theoretical Basis Documents) using the method proposed by (Liang, 2001).

2.3.3 Calculate Sky Diffuse Fraction and Total Sky Albedo

Total Sky Albedo (TSA) can be calculated from White Sky Albedo (WSA) and Black Sky Albedo (BSA) weighted by the sky diffuse fraction (Lewis and Barnsley, 1994; Román et al., 2010). The formula writes as follows :

$$A_{blue-sky} = A_{white-sky} \cdot F_{diff} + A_{balck-sky} \cdot (1 - F_{diff}) \tag{2.8}$$

where, F_{diff} is the sky diffuse fraction. In our study, aerosol optical depth product is used to calculate F_{diff}. The relationship is derived from an approximation of 6S simulation :

$$F_{diff} = \frac{1 - e^{-\tau}}{1 - (1 - \mu)e^{-\tau}} \tag{2.9}$$

Where,
τ is the aerosol optical depth (AOD),
μ is the cosine of solar zenith angle.

This relationship is a general function, and not limited for specific aerosol type. Herein, aerosol information is taken from MACC-II project previously introduced (see Section). The solar zenith angle information comes from ancillary dataset of MOD09/MYD09 HDF file, which is the geometry information accompanying the directional reflectance values.

2.3.4 Results

2.3.4.1 Examination of the input data

The input datasets (reflectance, observation geometry) are examined along with the QC flags, AOD and LAI. The QC comprises : cloud Shadow, Inside Snow, BRDF, Adjacent Cloud, MCD35 Snow, Fire, Inside Cloud, Cirrus, Cloud, Aerosol. Results show that QC flags can efficiently filter the observations contaminated by cloud, aerosol, snow etc.

Daily MODIS albedo is not gap filled mostly due to several elements : cloud, snow, bad BRDF quality. Four periods are chosen representing different seasons from Jan and Jul. Seasonal variation is prominent over the plotting region. After masking all the pixels influenced by these effects, the day by day evolution of albedo can be noticed from scenes during successive days (Fig. 2.4).

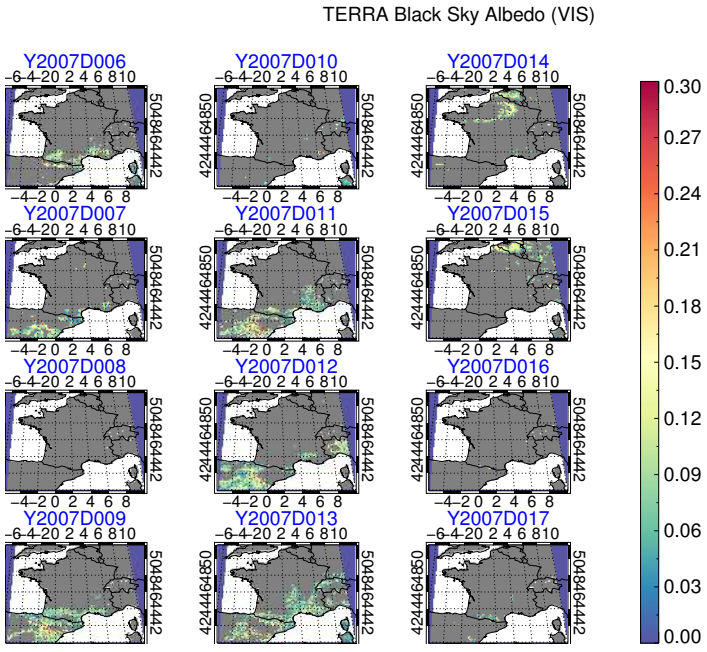

– (a)

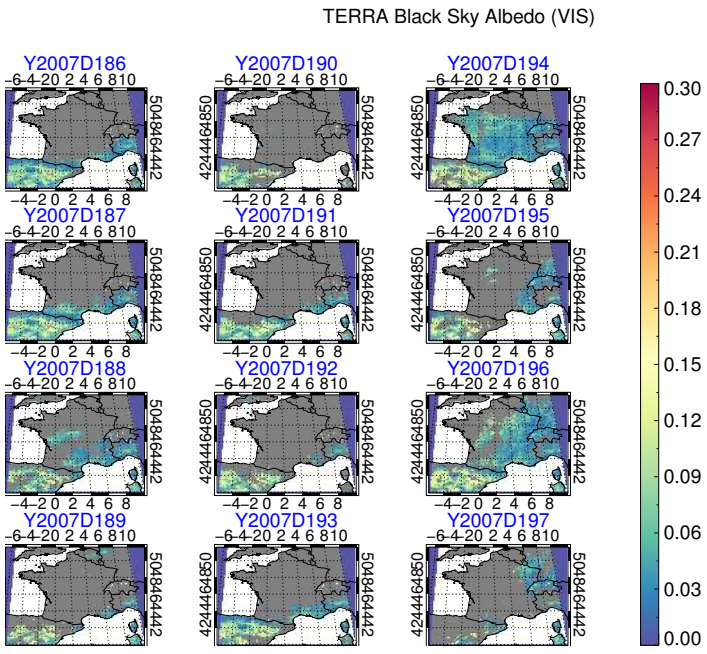

– (b)

Figure 2.3 – Seasonal evolution of selected daily shortwave WSA over France in 2007 : (a)Julian Day 006-017, (b)Julian Day 186-197. Pixels influenced by cloud, snow, and indicated with poor BRDF quality are rendered in grey color.

2.3.4.2 Extracting time series over SMOSMANIA sites

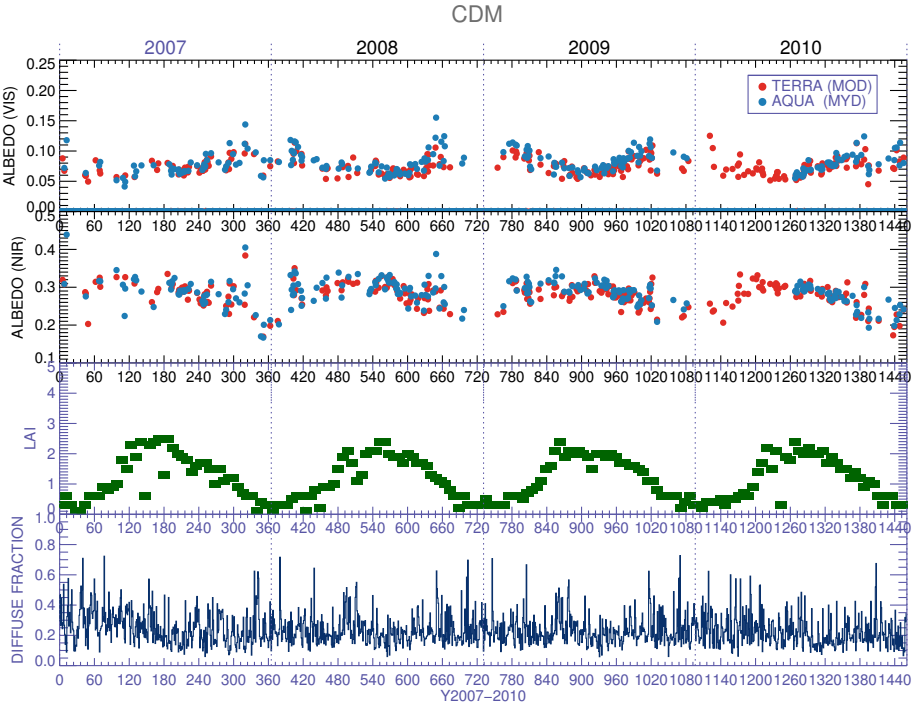

FIGURE 2.4 – Time series of daily (a) MODIS WSA (VIS), (b) WSA (NIR), (c) LAI and (d) Diffuse Fraction during 2007-2010. Daily LAI is a linear interpolation from 8D MCD15A1 product.

A 4-year time series of daily MODIS albedo is extracted for 12 SMOSMANIA stations during 2007-2010 at 500m pixel resolution. Daily MODIS albedo is not available when snow, cloud are indicated or bad BRDF quality, high solar zenith angle are indicated. It is encouraging to note that TERRA and AQUA retrievals are consistent and presenting the same variations and tendency, although the available days do not always overlap (Fig. 2.4).

Seasonal cycles can be identified for pixels around the station with different vegetation cover. Generally, a peak of NIR albedo is present with a depletion of VIS albedo in summer time (Fig. 2.4). LAI and diffuse fraction were superimposed to illustrate the possible causes which are at the root of the seasonal and daily albedo variations. It can be observed that those albedo seasonal cycles are closely related to LAI (Fig. 2.4). High diffuse fraction explains a part of the low abrupt decrease of albedo (Fig. 2.4).

2.3.4.3 Validation with FLUXNET stations

FLUXNET stations are providing tower measurements of energy flux as well as other meteorological variables (Baldocchi et al., 2001). Over France, 13 stations are located spatially evenly (Fig. 2.5). They encompass different vegetation function types : crops, shrub, evergreen broadleaf trees, deciduous broadleaf trees and evergreen needleleaf trees (table 2.2). These stations are constructed at different period, while the longest data record can be dated from the year of 2000. In the present study, we are using the datasets from 2007-2010. These records are distributed freely in the website : `http://fluxnet.ornl.gov/` since December 2007.

Upward and downward energy fluxes are directly measured from sunrise to sunset at each 30 minutes interval along the year in virtue of pyranometers (e.g. Kipp and Zonen) installed at the flux towers. All sky short-wave surface albedo are calculated, being defined as the ratio of upward and downward flux ranging from 280-2800nm. Fill-values are given if the flux measurement is negative or the upward flux is larger than the downward one. At night, without natural illumination, the flux measurement is around zero.

Theoretically, the pyranometers can observe all directions of hemi-sphere. However, due to the uneven response, less signals is coming from off-nadir directions. The representative area of the FLUXNET measurement is depending on the height of the tower, and indicated as within 10-20m centred from the station (after (Cescatti et al., 2012)).

The precision of the stations measurements is estimated as 4-7% in clear sky and 1-4% in overcast condition (Pirazzini, 2004; Pirazzini et al., 2006). The uncertainties can come from the pyranometers itself, assessed to around 5%.

To compare with daily retrieval of albedo datasets, continuous tower measurements is required to be integrated. The 30 min upward and downward fluxes collected from sunrise to sunset are further converted into daily measurements through averaging all the available records. Unrealistic records, such as negative values, are removed before averaging. Finally, daily albedo is calculated as division of daily upward and downward fluxes.

To examine the representation of 13 FLUXNET stations over France, high resolution maps are extracted from GOOGLE MAP^{TM}. The area of 1km^2 centred at the coordinate of the FLUXNET station is extracted to show in Fig.2.6. Sites with high homogeneity are : Bilos, Fontainbleu, Hesse, Laqueuille, Peuchabon and Le Bray. The evaluation method of scores derived from semivariance histogram (Román et al., 2010) is not applied in this study.

Fig.2.7 shows the comparison of TERRA and AQUA Daily MODIS albedo with FLUXNET in-situ measurements during one year long period in 2007. The former is temporally sparse due to the filtering of days contaminated by cloud, snow, poor quality of BRDF parameters, etc. The albedo from TERRA and AQUA are consistent at the both-existing days. Generally, they are comparing well with FLUXNET measurements, reflecting the seasonal variation.

Fig.2.9 shows for the 20th-30rd April 2007 period a comparison between the daily MODIS albedo generated by the scaling method and the in situ measurements for the FLUXNET forest sites. It can be observed that FLUXNET albedo represents a typical U shape for diurnal va-

TABLE 2.2 – Site information of FLUXNET stations. Avalability during 2007-2010 is reported as '*'.

Site	Abbr	PFT	IGBP LC	2007	2008	2009	2010
Aurade	Aur	Cereal Crops	Croplands	*	*	*	*
Avignon	Avi	Cereal Crops	Croplands	*			
Bilos	Bil	Shrub	Woody Savannas				
Couhins	Gou	Cereal Crops	Woody Savannas				
Fontainbleu	Fon	Deciduous Broadleaf Trees	Deciduous Broadleaf Trees	*	*		
Grignon	Gri	Cereal Crops	Cereal Crop	*	*		
Hesse	Hes	Deciduous Broadleaf Trees	Deciduous Broadleaf Forest	*	*	*	*
Lamasquere	Lam	Cereal Crops	Croplands	*	*	*	*
Laqueuille	Lq1	Cereal Crops	Croplands	*	*	*	*
Lamasquere extensive	Lq2	Cereal Crops	Croplands	*	*	*	*
Le Bray	LBr	Shrub	Croplands Natural Vegetation Mosaic	*	*		
Lusignan	Lus	Cereal Crops	Croplands				
Puechabon	Pue	Evergreen Needleleaf Trees	Mixed Forests	*	*	*	*

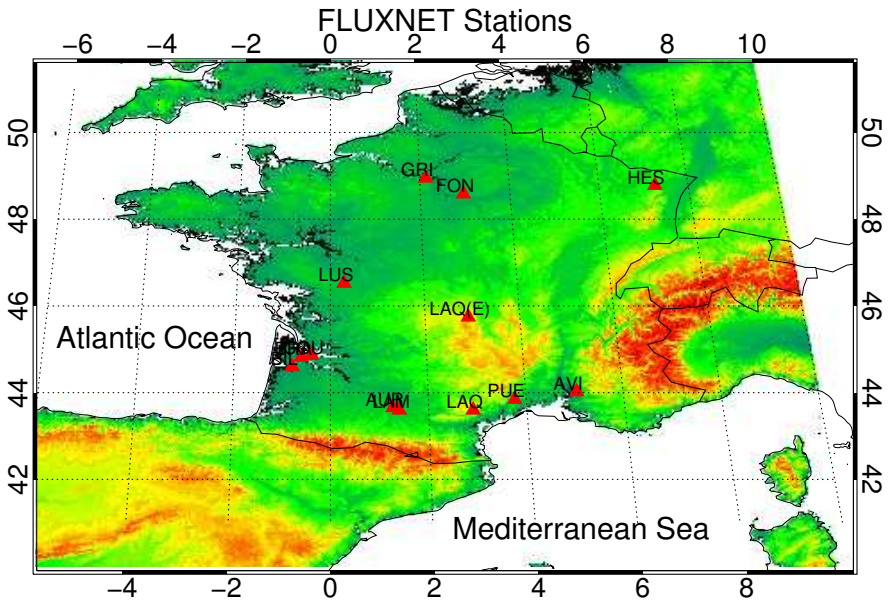

Figure 2.5 – Spatial distribution of 13 FLUXNET stations over France. (Noted : Lq1 and Lq2 are located in the same site, while the records begin at different time.)

riation and there is not always symmetric around noon time. In spite of the uncertainty due to the footprint size, hourly estimation from TERRA and AQUA are able to catch the variation of albedo in relatively good agreement with the records from pyranometers.

The comparison between MODIS daily TERRA/AQUA albedo and FLUXNET measurements are reported in Fig. 2.9. It can be noticed that short-wave albedo are clustering at range 0.1-0.2 for these stations. Linear regressions are conducted separately for TERRA and AQUA daily albedo against FLUXNET albedo for available days. For example, the goodness of the linear fit for station Fontainebleau is 0.22 for TERRA and 0.42 for AQUA ; and for station Le Bray 0.048 for TERRA and 0.19 for AQUA (Fig. 2.9).

– (a) – (b) – (c)

– (d) – (e) – (f)

– (g) – (h) – (i)

– (j) – (k) – (l)

FIGURE 2.6 – High resolution of GOOGLE MAP^{TM} used to check the homogenity. Image covers an area of 1km^2 centre at the coordinate of the FLUXNET station.(a)Aurade, (b)Avignon, (c)Bilos, (d)Couhins, (e)Fontainbleu, (f)Grignon, (g)Hesse, (h)Lamsquerre, (i)Laqueuille, (j)LeBray, (k)Lusignan, (l)Peuchabon.

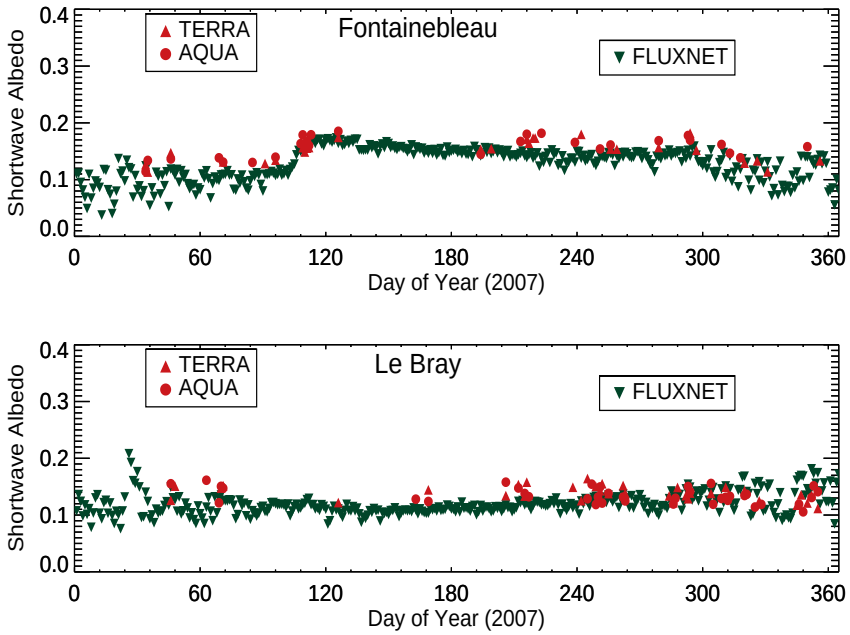

Figure 2.7 – Time series comparison of TERRA/AQUA daily MODIS albedo with FLUXNET in 2007.

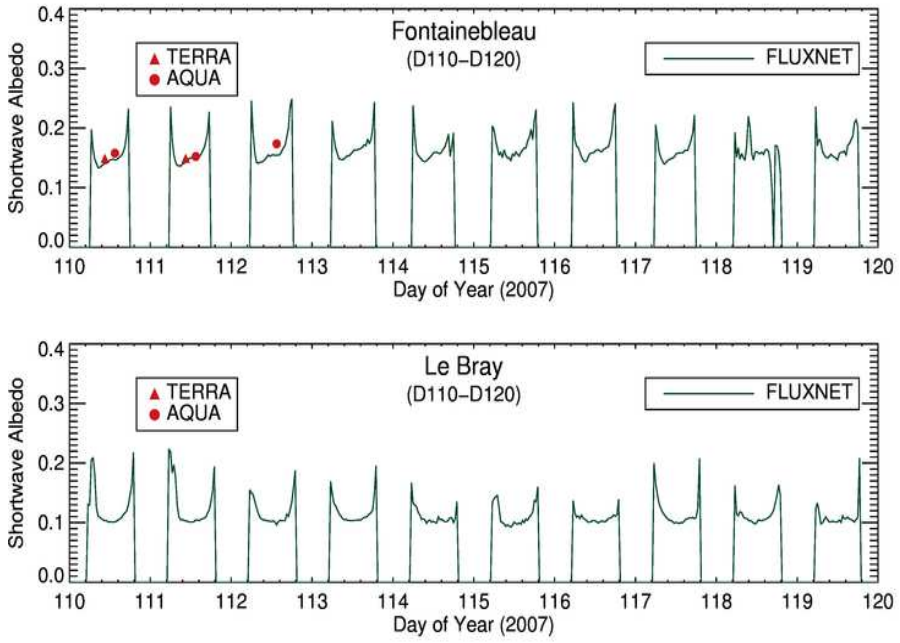

FIGURE 2.8 – Diurnal variation of in-situ measured albedo at two FLUXNET stations : (a) Fontainebleau, (b) Le Bray comparing with daily MODIS albedo during Julian Day 110-120, 2007.

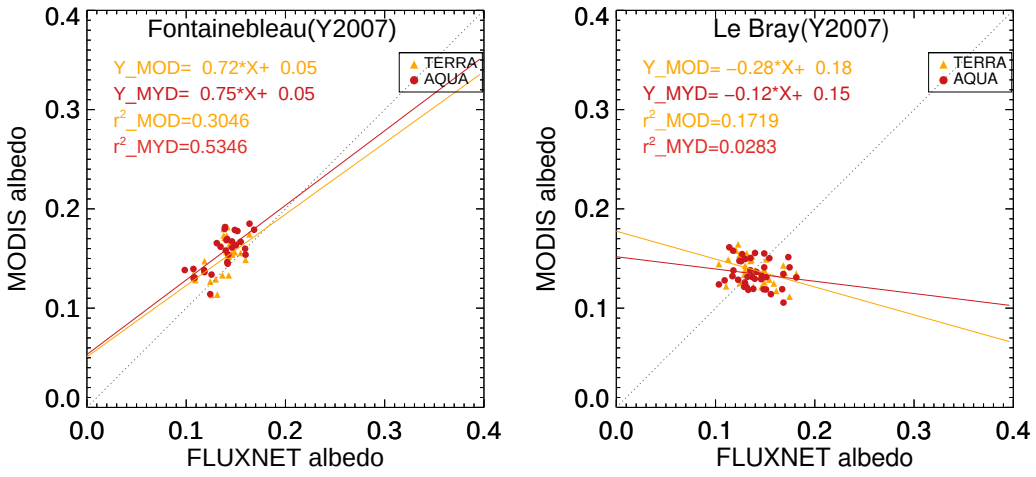

– (a) – (b)

FIGURE 2.9 – Scatter Plot of daily MODIS TERRA/AQUA albedo compared with FLUXNET measurements. Albedo retrievals from TERRA and AQUA are indicated in two different colors : orange and red, respectively.

2.4 Intercomparison and validation of daily MODIS and SEVIRI albedo

2.4.1 Method of Intercomparison

SAF-LAND albedo products derived from SEVIRI observations is distributed at the grid of MSG. The coverage is a fixed round disk range on the earth surface, containing Europe, African and south American. This is a irregular grid specific for geostationary satellite, which is 3km at sub-satellite pixel, and 6-7km at the edge of MSG disk.

MODIS albedo products (MCD43A3) are distributed at 'tile' approach and ISIN projection. With the help of MRT, it is mosaiced and reprojected to a box ranging [40.01°N, 5.5°W, 51.5°N, 9.91°E] and lat-lon projection at 500m.

A comparison of albedo products from these two sensors is listed in table 2.4 . Since these two products are distinct at spatial resolution and projection, comparison should be conducted after resample and reprojection. MODIS albedo is resampled and reprojected to SEVIRI grid to favor the comparison at pixel by pixel level.

2.4.2 Comparison results

Comparison is conducted between TERRA MODIS (MOD 1D), AQUA MODIS (MYD 1D), TERRA+AQUA MODIS (MCD 8D), SEVIRI (SAF 1D). One example of Black Sky Albedo (BSA) is referred in Fig.2.10 . Two days, Julian Day 20 and 200 during 2007, are chosen to represent the winter and summer period.

It can be observed that MCD 8D and SAF 1D albedo are comparable while MOD 1D and MYD 1D albedo are slightly higher than MCD 1D and SAF 1D albedo on Julian Day 20, 2007 (Fig. 2.12). The statistics are shown in Fig. 2.12.

Time Series of MOD, MYD, MCD and SAF are compared within 12 stations of SMOSMANIA. Fig. 2.12 displays the seasonal evolution in 2007 of MODIS and SEVIRI albedo products over four SMOSMANIA stations. The SEVIRI albedo product includes a gap-filling process. In the case of failure of the algorithm, either due to technical issues or persistent cloud coverage, the latest albedo value is prescribed with the associated uncertainty. The magnitude of this uncertainty increases with the time elapsed from the date of acquisition of the last albedo estimate. In Fig. 2.12, error bars represent this uncertainty. A characteristic time scale was fixed to 5

Table 2.4 – Information of MODIS and SEVIRI albedo products

Sensors	Time	Pixel	Band	Coverage	Ref
MODIS	8D	0.5-1.0KM	7NB+3BB	Global	NASA/BU
SEVIRI	1D	3.0-7.0KM	3BB	MSG Disk	EUMESAT/LSA-SAF

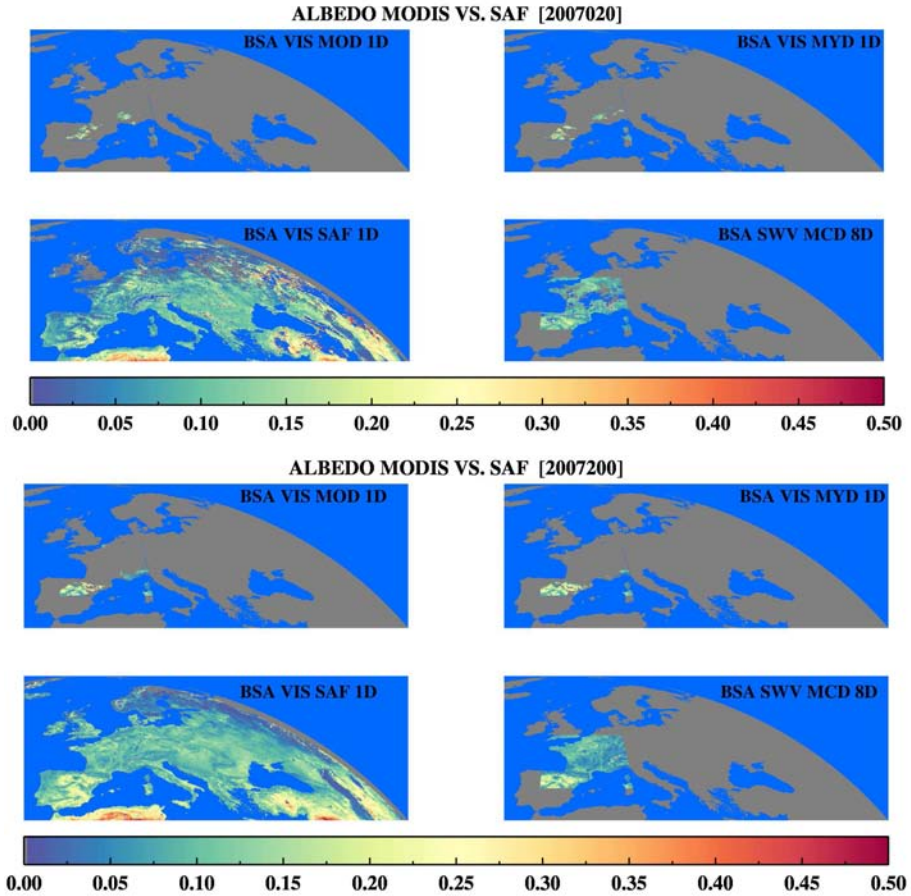

FIGURE 2.10 – Comparison of Black Sky Albedo (BSA) between TERRA MODIS (MOD 1D), AQUA MODIS (MYD 1D), TERRA+AQUA MODIS (MCD 8D), SEVIRI (SAF 1D) on Julian Day 20 and 200 during 2007.

days, which explains the loss of confidence on the product rapidly after a few days. In particular, this occurs during snowfall episodes materialized by high albedo values. SEVIRI albedo shows more seasonality than MODIS albedo with a marked depletion in winter. During that period of time, discrepancies exist with MODIS. In other seasons, conspicuous agreement is observed, in particular during summer and fall periods.

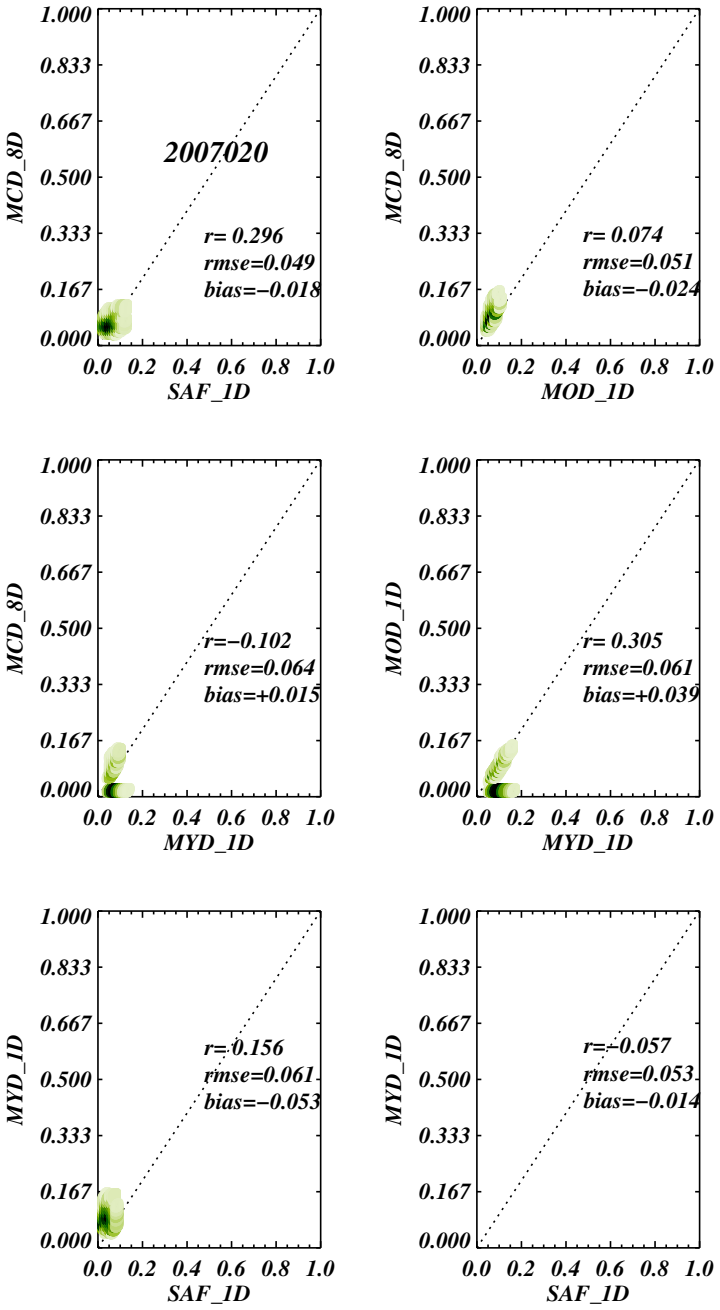

– (a)

Figure 2.11 – Density scatter plot of Black Sky Albedo (BSA) comparing MOD 1D, MYD 1D, MCD 8D, SAF 1D on (a) Julian Day 20 and (b) Julian Day 200 during 2007.

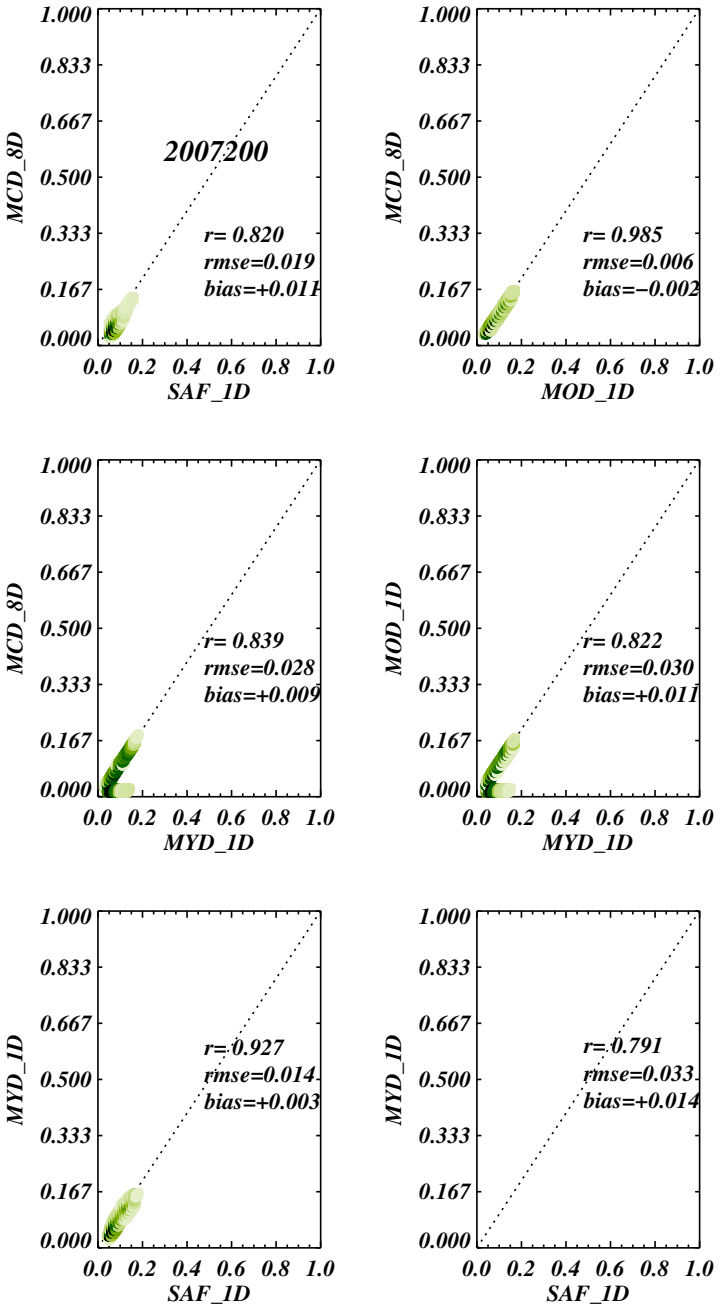

– (b)

Density scatter plot of Black Sky Albedo (BSA) comparing MOD 1D, MYD 1D, MCD 8D, SAF 1D on (a) Julian Day 20 and (b) Julian Day 200 during 2007.

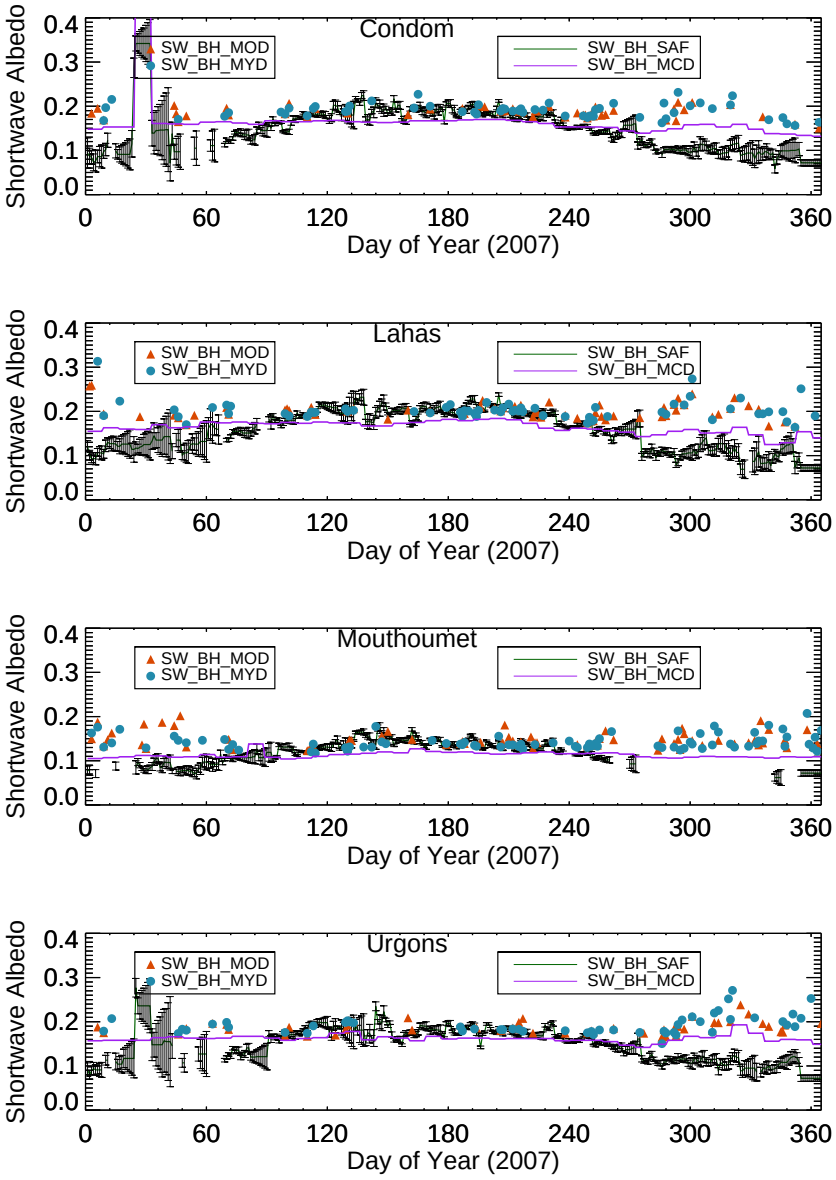

Figure 2.12 – Seasonal evolution of MODIS and SEVIRI albedo products over four SMOSMANIA stations in 2007.

2.5 ISBA albedo simulation state-of-art

2.5.1 Patch Strategy

ECOCLIMAP is a dual database comprising a classification map and biophysical parameters. It was primarily implemented with the aim to initialize surface models devoted to meteorological

TABLE 2.5 – ISBA vegetation patches used in ECOCLIMAP

ISBA veg type	Abbr
Bare soil	NO
Bare rock	ROCK
Permanent snow	SNOW
Deciduous broadleaved	TREE
Needleleaved	CONI
Evergreen broadleaved	EVER
C3 crops	C3
C4 crops	C4
Irrigated crops	IRR
Temperate grassland	GRAS
Tropical grassland	TROG
Wetland,parks and gardens	PARK

and climate applications. Fig.2.13 shows the structure of ECOCLIMAP, 12 patches (PFTs) for classification and sets of associated parameters.

ECOCLIMAP applies a so-called 'tile' approach. Each grid can be splitted into four tiles : nature (NAT), urban areas (TWN), sea or ocean (SEA) and lake (WAT). For NAT surface, it can be further splitted into 12 ISBA patches, which are listed in table 2.5.

Parameters are attributed for sub-pixel types, which can be aggregated from a weighted approach from type fractions (Fig.2.13). These parameters are used for initialize SVAT models. They are keeping as type-dependent, and the models are running for each type, which the outputs are average results of each type.

There exists two versions of ECOCLIMAP : one was developed in 2003 for global coverage (Masson et al., 2003), and the latest was developed more recently for Europe (Faroux et al., 2013) and Africa (Kaptué Tchuenté et al., 2010). ECOCLIMAP I produces 225 ecosystems from land cover, climate maps in addition to one year AVHRR satellite observations (Champeaux et al., 2005). The surface parameters are derived each ecosystem as reference values to LAI constrained by AVHRR. ECOCLIMAP II are produced using an automatic cluster classification method from more recent land cover and climate maps, as well as the SPOT/VEGETATION observations, which is more precise and better calibrated than AVHRR. Surface parameters are derived for each ecosystem as reference values to LAI, which is the smoothed products of MODIS.

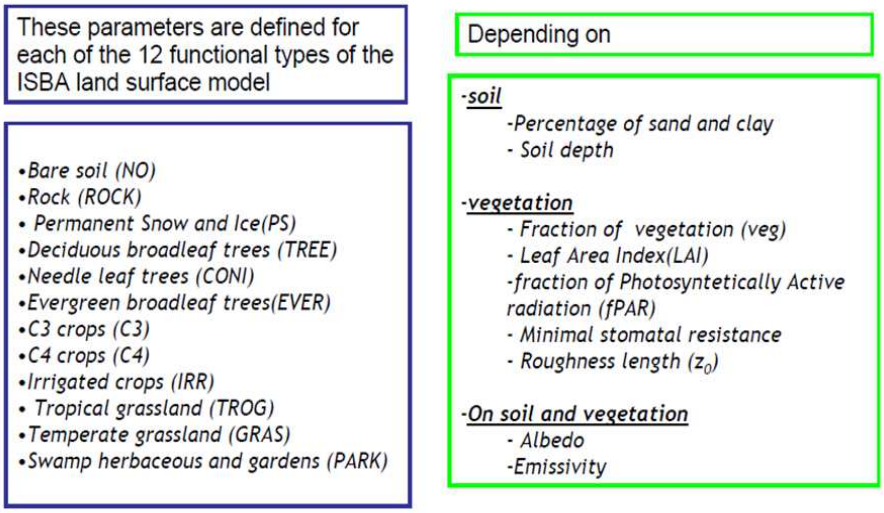

Figure 2.13 – Composition of ECOCLIMAP database.

2.5.2 Two versions of ECOCLIMAP database

2.5.2.1 ECOCLIMAP I

ECOCLIMAP I is a 1-km database developed as surface parameterization for meteorology and climate application in Meteo-France. It is built using the following :
(1) land cover map at 1km resolution from UMD, IGBP/DIS, CORINE, and PELCOM
(2) climate map (FIRS over Europe)
(3) 1km NDVI product from AVHRR
(4) FAO database for soil properties

Global classification is derived from two global land surface maps, UMD and IGBP/DIS. Since the two are noticablely different, a combination is adopted in ECOCLIMAP I. The designation of the cover types is essentially derived from the UMD global land cover map. However, the permanent snow occupation and wetland bodies are based on the IGBP/DIS database. Over Europe, more detailed databases are available (Masson et al., 2003). 250m Coordination of Information on the Environment (CORINE) database covers large parts of Europe while PELCOM is preferred over Scandinavia, which translates into 44 categories over Europe. Climate maps are considered to derive 215 ecosystem classifications finally.

Parameter database are derived from various resources. One year AVHRR/NOAA global 1km dataset from April,1992-March,1993 is used for vegetation proxy. LAI is calculated as the weighted scaling of maximum and minimum LAI using NDVI. Soil texture is generated from FAO soil database.

LAI dataset is validated with in-situ measurement and compared with ISLSCP2 and POLDER map. Climate simulations are conducted to indirectly validation the surface parameteriza-

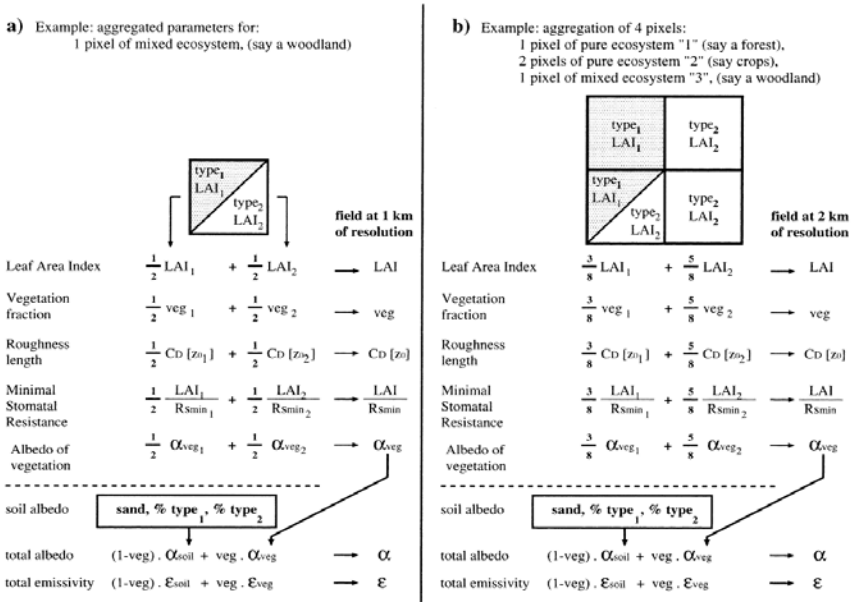

FIGURE 2.14 – Scheme for aggregating parameters for mixed vegetation or soil types.

tion.

2.5.2.2 ECOCLIMAP II

ECOCLIMAP II is an update of the previous version ECOCLIMAP I, developed to use more recent land cover, climate map, remote sensing products, and additional datasets to improve the initialization datasets for surface, meteorology and climate model. It comprises 273 classes for Europe (Fig. 2.15). The classification process combines both an automatic k-means algorithm on NDVI seven year time series from SPOT/VEGETATION, in addition to initial land cover and climate maps.

The ration for the updating can be concluded as follows : with the advent of GLC2000, CLC, it is expected to provide more accurate information for producing ecosystem covers. Beside, ECOCLIMAP I is using AVHRR data, which is 1km nadir to 6km off-nadir ; MODIS and VEGETATION/SPOT are better calibrated and precise with a true 1km resolution.

2.5.2.3 Albedo parameterization in ECOCLIMAP I

In ECOCLIMAP, total albedo α_{total} can be formulated as soil albedo α_{soil} and vegetation albedo α_{veg} weighted by the fraction of vegetation f_{veg}, as shown in Eq. 2.10.

$$\alpha_{total} = \alpha_{soil} \cdot (1 - f_{veg}) + \alpha_{veg} \cdot f_{veg} \tag{2.10}$$

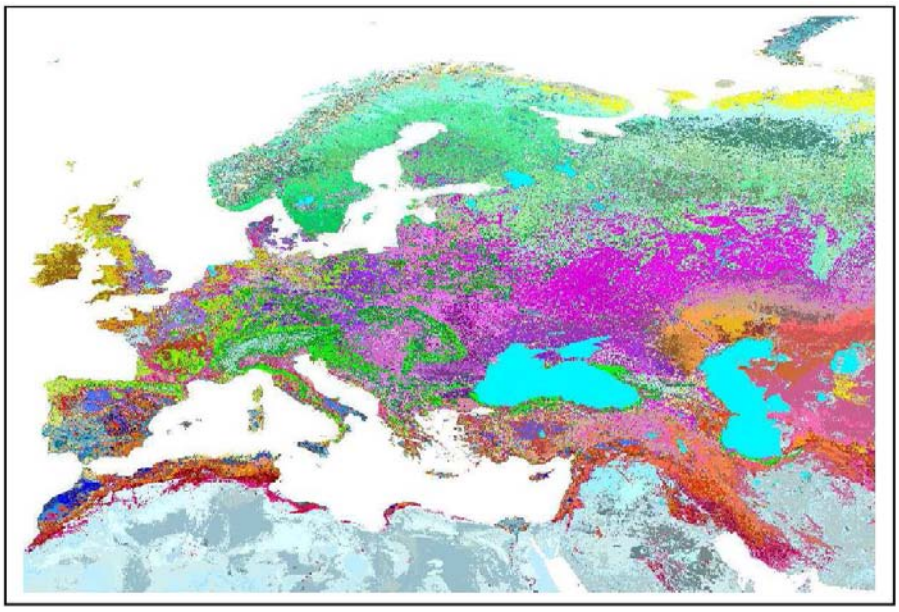

Figure 2.15 – ECOCLIMAP II 273 ecosystem covers in Europe ((Faroux et al., 2013))

Where, vegetation fraction f_{veg} is parameterized as exponential function of LAI :

$$f_{veg} = 1 - e^{-0.6LAI} \tag{2.11}$$

In the version 1 surface physiological database (so called ECOCLIMAP I), bare soil albedo is parameterized as soil mineral composition and organic deposition, which is presented by sand fraction, and woody/herbaceous vegetation types, respectively (Masson et al., 2003).

$$\alpha_{soil} = 0.10 + (0.05 + 0.30 f_{sand}) \cdot [1 - 0.9(f_{woody} + f_{herbaceous})^2] \tag{2.12}$$

Where, f_{sand} is the sand fraction, which is derived from FAO90 soil database. f_{woody} and $f_{herbaceous}$ are woody and herbaceous vegetation fraction, respectively.

Vegetation albedo α_{veg} is attributed as look up table values depending on vegetation types. This is illustrated in table 2.6 .

The weighted total albedo is comparing well with AVHRR datasets (Strugnell et al., 2001).

2.5.2.4 Albedo parameterization in ECOCLIMAP II

In updated version 2 (ECOCLIMAP II), a static vegetation albedo and soil albedo map are derived at pixel level from multi-year MODIS observation from 2000 to 2007. It is designed to im-

TABLE 2.6 – Vegetation albedo parameterization in ECOCLIMAP I

Vegetation type	Vegetation albedo	Total vegetation fraction
Bare soil		0
Bare rock		0
Permanent snow		0
C3 crops	0.20	1-$e^{0.6LAI}$
C4 and irrigated crops	0.20	1-$e^{0.6LAI}$
Other herbaceous	0.20	0.95
Needleleaf trees	0.10	0.95
Evergreen broadleaf trees	0.13	0.95
Deciduous broadleaf trees	0.15	0.95

prove the albedo parameterization in SVAT model as ISBA. The databases have been generated initially for western Africa (Kaptué Tchuenté et al., 2010) and recently expanded to continental Africa and Europe at 1km resolution.

Fraction of vegetation, which is derived from MODIS LAI products, is serving to split vegetation and soil albedo from total MODIS albedo products. Eq. 2.10 and Eq. 2.11 are involved in this splitting processing using a regression method. Detailed descriptions can be found in (Kaptué Tchuenté et al., 2010). Since both the wet and dry soil scenario are included in the generation process, bare soil albedo products represents the average situation.

The reconstructed total albedo datasets using this parameterization is comparing well with original MODIS albedo products as well as MSG albedo products.

2.5.2.5 Differences between ECOCLIMAP I and ECOCLIMAP II vegetation and soil albedo parameterization

The difference between ECOCLIMAP I and ECOCLIMAP II vegetation and soil albedo can be summarized as follows :

(1) ECOCLIMAP I soil albedo is parameterized as function of sand fraction, woody/herbaceous vegetation fraction ; while ECOCLIMAP II soil albedo is parameterized in a pixel-based level. The former is a dry bare soil albedo map, while the later includes the scenario of dry and wet situation, thus is more representative of an averaged value.

(2) ECOCLIMAP I vegetation albedo is parameterized as reference value of vegetation type ; while ECOCLIMAP II vegetation albedo is parameterized in a pixel-based level at 1km resolution.

(3) ECOCLIMAP I soil and vegetation parameterization are derived from literatures and in-situ measurements ; while ECOCLIMAP II vegetation and soil albedo are derived from MODIS satellite products.

2.6 Comparison of ISBA simulation and daily MODIS/SEVIRI albedo

Assessment of model simulations with satellite observation would reveal the difference and direct future improvement. ISBA-A-gs albedo model simulations are compared with MODIS and SEVIRI observations over France during 2007-2010. SAFRAN forcing is used at 8km scale.

Model simulated albedo is assessed here with satellite observations, which have high precision and extensively validated. The benefit from this comparison might indicate the deficit of model and orient the direction for further improvement. In this study, spatial and temporal variations of ISBA albedo are compared with MODIS and SAF albedo products at daily basis during 2007-2010.

Model albedo is generated using off-line ISBA model (integrated in the platform SURFEX V7.3) through A-gs option, driven by French SAFRAN forcing. The output is albedo each 3 hours at SAFRAN 8km grid, which yield 8602 points over France. These albedos are further integrated from 3h to daily basis representing the mean situation during 24 hours.

MODIS albedo is taken from MCD43B3 product, which is distributed each 8 day. SAF albedo is taken from level 2 daily products. In order to perform grid-to-grid comparison, these two albedo products are re-projected from their own projection into model grid. The noon time (12 :00H) albedo is selected to compare with the other products.

Two days 2008/02/03 and 2008/08/03, are selected to represent results during the winter and summer period. It can be found that generally the three types of albedo are consistent in spatial patterns and albedo level (Fig. 2.16). It is worth to mention the effect of snow coverage. On 2008/02/03, surface albedo is influenced by the snow cover, which can be simulated by the model and presented by the two albedo products. MOD43B3 is a synthesis product during a period of 16 days, thus the snow cover is more distinct than the other two.

In order to examine the bias of the model comparing to two observations, the difference are calculated and shown in Fig. 2.17 . Generally, on 2008/02/03, albedo of MODIS is lower than MODEL, while SAF is higher than the MODEL. On 2008/08/03, the bias is quite lower than 2008/02/03.

This is further confirmed by the correlation coefficients. Which are higher in summer period than winter period, i.e. 0.727 and 0.797 for MODIS and SAF on 2008/08/03 comparing to 0.528 and 0.690 for MODIS and SAF on 2008/02/03. The bias is much lower also, 0.001 and 0.003 for MODIS and SAF on 2008/08/03 comparing to 0.027 and 0.051 for MODIS and SAF on 2008/02/03 (2.18).

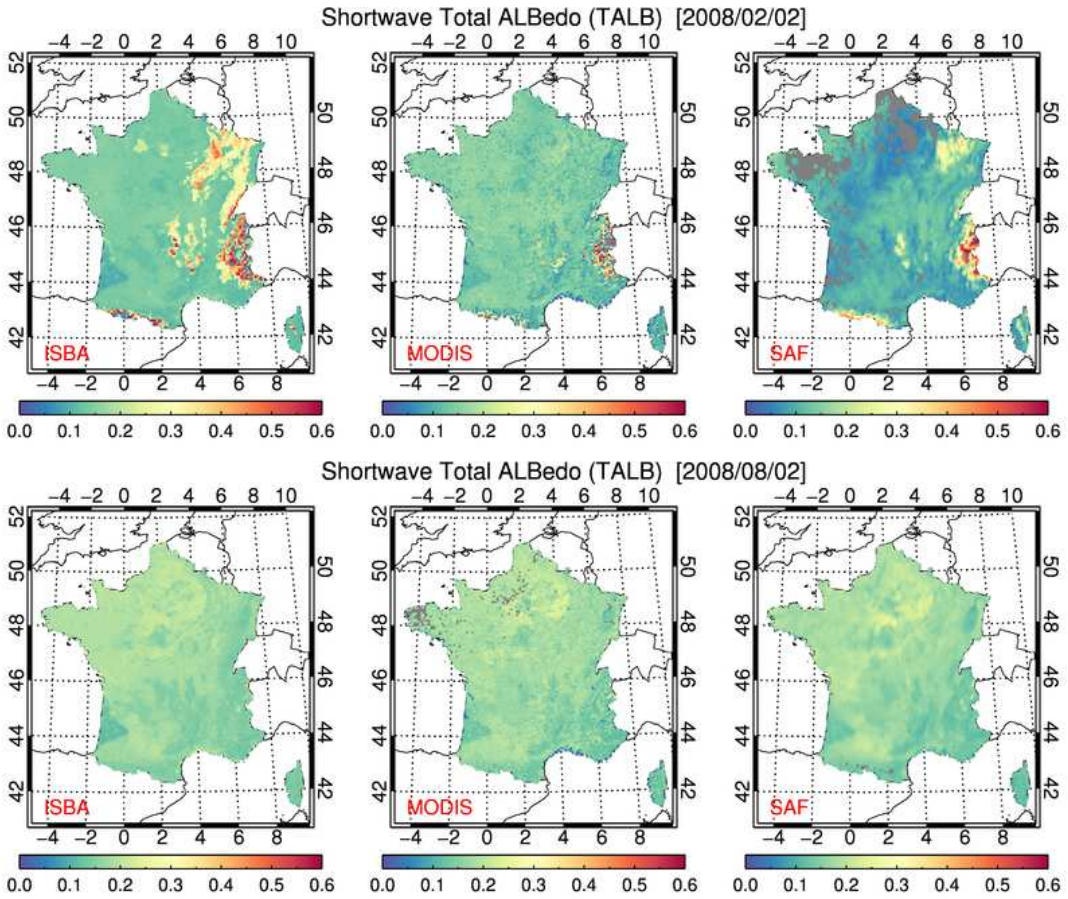

FIGURE 2.16 – Comparison of three types of albedo : (a) ISBA model simulation, (b) MODIS MCD43B3, and (c) SAF L2 1-D albedo on two selected days : 2008/02/03 and 2008/08/03.

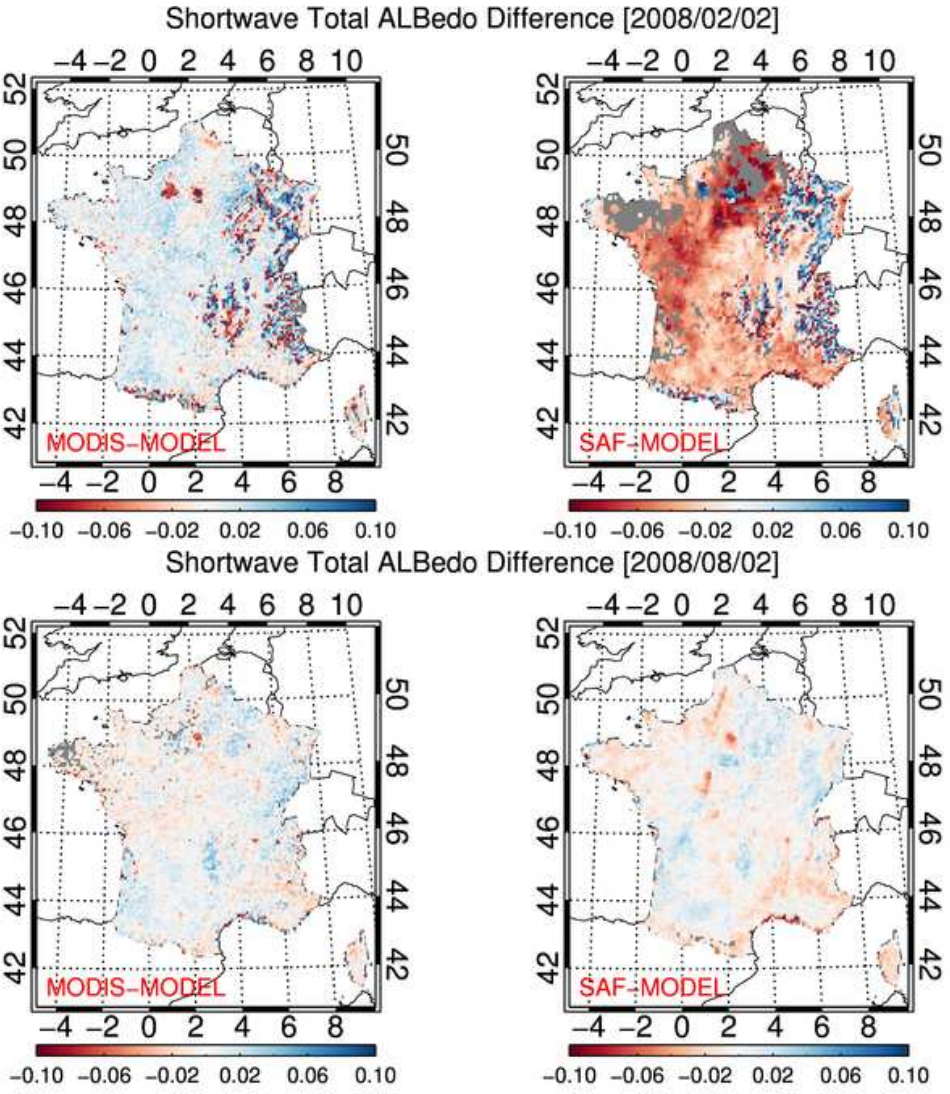

Figure 2.17 – Difference of albedo : (a) MODIS-MODEL, and (b) SAF-MODEL on two selected days : 2008/02/03 and 2008/08/03.

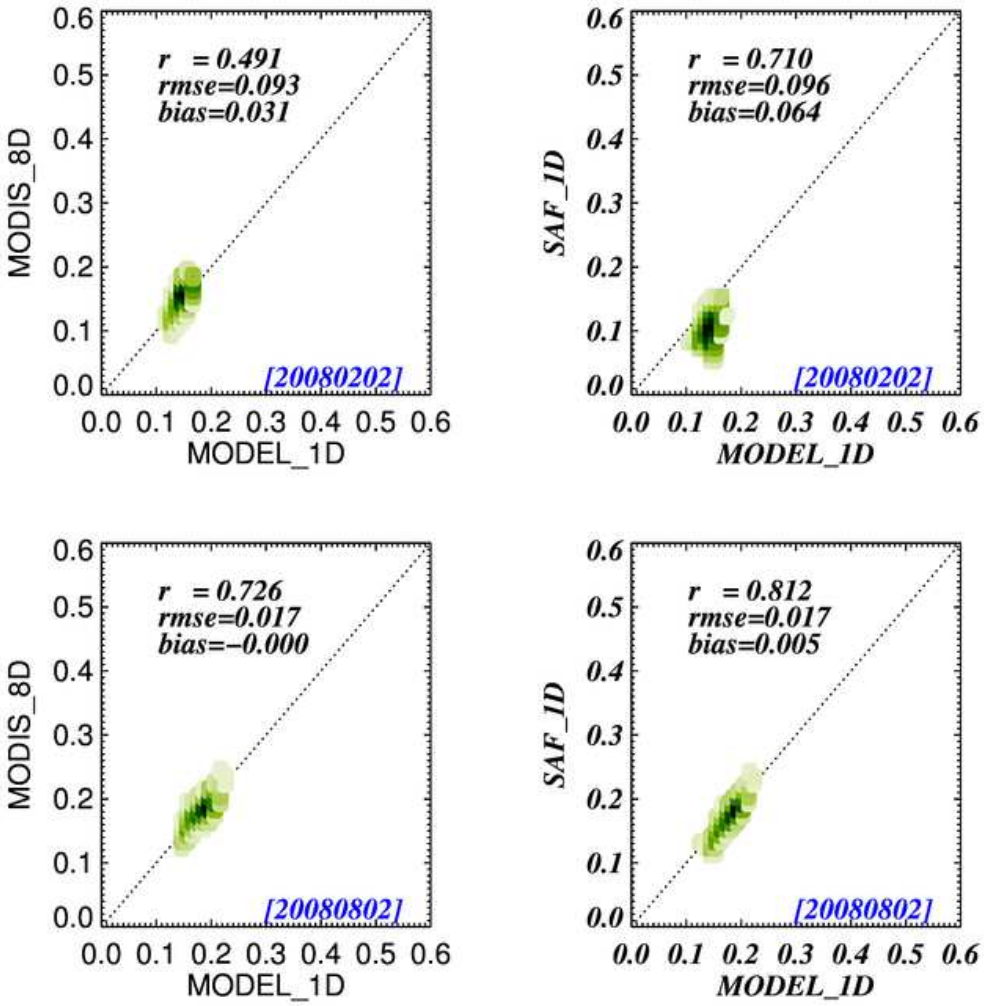

FIGURE 2.18 – Scatter plots of albedo on two selected days 2008/02/03 and 2008/08/03 : (a) MODIS-MODEL, and (b) SAF-MODEL.

2.7 Conclusion

Daily SEVIRI albedo is a product covering MSG disk over Europe, Africa, and eastern part of South America. It is a daily product, while a 10-day composite product is also disseminated. The required specification for LSA-SAF albedo has been fixed to 0.03 for albedo less than 0.15, and 20% for albedo greater than 0.15. Results of comparison show that the SEVIRI visible albedo is comparing well, while slightly overestimated compared to MODIS.

Daily MODIS albedo is generated from MODIS 8 day BRDF/Albedo standard product and daily directional reflectance after a series of processing. The BRDF shape is assumed to be stationary during 8 day period, while the magnitude can be adjusted each day, which is constrained by the directional observation. Both generated BSA and WSA MODIS albedo products show a dependable comparison with SEVIRI equivalent products, as well as original 8 day product over a four year period 2007-2010. The inter-comparison shows good consistency indeed. Finally, the generated daily albedo is validated against 13 FLUXNET stations over France.

Surface albedo parameterization of ISBA-A-gs was presented at Section 2.4. Two versions of ECOCLIMAP databases comprising ecosystem cover and associated parameters are used as geophysical field for ISBA-A-gs model. Albedo climatology used by ISBA-A-gs land surface model is a combination of vegetation and soil albedo weighted by the fraction of vegetation. This latter is a fraction of vegetation as an exponential function of LAI. While the soil and vegetation albedo are reference values for each PFT types, the temporal variation of this albedo is mainly driven by LAI.

The comparison of modeled and observed albedo datasets (SEVIRI and MODIS) are intercompared at 8km spatial resolution. Daily temporal scale reveals that : (1) daily MODIS is comparing favorably with SEVIRI product although it is sometimes higher at winter and early spring period, (2) albedo climatology used by ISBA-A-gs model has distinct difference with both MODIS and SEVIRI daily albedo products. This conclusion fosters the improvement of albedo parameterization to generate a prognostic albedo in ISBA-A-gs.

Chapitre 3

Separation between Soil and Vegetation Albedo

Contents

3.1 Introduction

For modelling purpose, snow-free land surface albedo is commonly depicted from combined patches of vegetation and soil. The so called 'tile' approach facilitates the representation of spatial heterogeneity caused by mixture of soil, vegetation. The total surface albedo is formulated as the sum of soil and vegetation compounds weighted by the vegetation fraction cover. Soil albedo would more likely vary on an hourly-daily basis, as its main perturbing field is soil moisture. Amenable short-term variations of soil albedo connect to rainfall events, which must be accounted for in the energy budget closure.

In vegetated areas, radiation interactions exist between the soil background and the bottom of canopy, which adds to the difficulty to yield a clear separation between the respective soil and vegetation attributes. Moreover, soil and vegetation are also coupled in hydrology processes. For

instance, fully developped vegetation canopies will intercept rainfall, which acts as a regulation of the influence of moisture on the value of soil albedo. At the time of the growing and peak season for vegetation, plant albedo will dominate the surface albedo. During the decay, litter fall will still contaminate the measure of bare soil albedo.

Efforts have been devoted to separate soil and vegetation albedo through regression or inversion of radiative transfer model. The former category is represented by a series of recent studies (Houldcroft et al., 2009; Kaptué Tchuenté et al., 2011; Rechid et al., 2008), to list a few. In these studies, fraction of vegetation or FPAR is treated as the indicator of vegetation albedo contribution, and used to separate vegetation and soil albedo from total albedo. Later category is represented by the study of (Alton et al., 2007), a non-linear two-stream model is used instead of a linear weighted function of soil and vegetation albedo. Soil albedo and leaf absorption are retrieved as time-invariant variables, which shows a good performance for capturing the variation of total White Sky Albedo (WSA).

However, the basic assumption of these static retrieval methods is that soil and vegetation albedo is time-invariant, which might not hold true in reality, especially for semi-arid and fire-porn area. However, incorporating a temporal-variant soil and vegetation properties would make the problem ill-posed. In order to solve this, a priori information is added into the retrieval process, and a dynamic separation is achieved by (Pinty et al., 2011a,b) using their (Joint Reserch Center) JRC 2-stream model. Soil albedo is retrieved as well as vegetation properties as leaf single reflectance, asymmetry factor, employing a priori probability density functions with presumed Gaussian distributions.

3.2 Physical justification of soil and vegetation separation

After the successful application of radiative transfer principles into turbid mediums as planetary atmosphere (Chandrasekhar, 1960), various schemes have been proposed to simulate the photon interaction within canopy (Myneni and Ross, 1991). After the pioneering work of biologist, ecologist, physicist, quantitative relationships are derived from physical principles and field measurements (Ross, 1981). These models are trying to link TOC (Top-of-Canopy) Reflectance with canopy biophysical (e.g. LAI) and biochemical parameters (e.g. leaf water content) (Asner and Wessman, 1998; Huemmrich, 2001; Verhoef, 1984).

Due to the complexity of real scenario, the physical models are always established with various assumptions. According to the complexity, these schemes can be divided into several categories :

(1) *simple analytical models*, as 2-stream (Meador and Weaver, 1980), considering only vertical flux integration, or 4-stream (Liou et al., 1988), adding two extra angles on the basis of 2-stream.

(2) *sophisticated 3D models*, as FLIGHT (North, 1996), DART (Gastellu-Etchegorry et al., 1995).

(3) *stochastic models*, based on the simulation of the trajectory of single photon, as Monte Carlo, RAYTRAN (Govaerts and Verstraete, 1998).

These physical models have acquired long-term popularity by the remote sensing community to retrieve surface parameters from satellite or airborne observations. However, the radiative transfer in terrestrial surface models is not so well represented. This impedes the process of assimilating directly remote sensing observations into land surface models.

In order to incorporate such state-of-art radiative transfer schemes into LSMs, it is beneficial to compare these models with different computational efficiency, physical assumption,numerical precision. How are these models performing under unified parameterization with constrain referring to standard scenarios ? To answer this question, an inter-comparison numerical experiment RAMI has been conducting since 2001. Models are compared within different reference numerical scenarios, with aspect to their energy closure, performance efficiency, precision (Pinty, 2004; Pinty et al., 2001; Widlowski et al., 2011, 2007).

Recently, the 2-stream strategy is revisited and adopted for climate models (Pinty et al., 2006). This model is successfully inverted from MODIS white sky albedo to provide surface datasets (Pinty et al., 2011a,b). For spherical bush canopy, an analytic model is proposed, which serves as a proceeding step towards 3D canopy characterization (Dickinson et al., 2008). A radiative transfer scheme based on Geometric Model (GO) is introduced and implemented for dynamic vegetation model Dynamic Global Vegetation Model (DGVM) (Ni-Meister et al., 2010; Yang et al., 2010). Foliage vertical density function is digested as input accompanying other dynamic structure parameters.

In our study, we choose 2-stream scheme due to its simplicity, popularity and ease to implement. The physical framework of SAIL model is adopted, particularly a little addition is made to simulate BSA, WSA and transmittance besides directional reflectance. Background reflectance is assumed as isotropic, hitherto, equal to albedo. Canopy absorption is derived from energy conservation, which is imposed to our model.

3.2.1 A simple 2-stream model

2-stream scheme is a popular approximation for radiative transfer, who shows a pretty performance for turbid homogeneous media (Chandrasekhar, 1960). A complete review can be referred from (Meador and Weaver, 1980). The obstacle to apply this strategy into canopy modeling has been removed through efforts representing foliage interception, benchmarked by Suit's model. The singular problem of Suit's model is resolved at SAIL model through a description of leaf inclination angle instead of vertical and horizontal projection (Verhoef, 1984). Recently, these schemes are revisited to construct a 2-stream model for climate modeling (Pinty et al., 2007).

Various schemes have been proposed to solve the complex radiative transfer equations. The principle of 2-stream scheme is to express explicitly the flux through integrating radiance at upward and downward bi-hemispheres. Adding solar and observation angles as extra constrain leads

Table 3.1 – The input variables of the 2-stream model.

Acronyms	Variable Meaning
rho	Single Leaf Reflectance
tau	Single Leaf Transmittance
angl	Leaf Incline Angle
lai	Leaf Area Index
Rsoil	Soil Background Reflectance (anisotropic)
tts	Solar Zenith Angle

to more precise directional depiction. In this study, we consider both direct and diffuse incoming radiation, while only diffuse outgoing radiation. This yields four combinations of incoming and outgoing radiance (fig. 3.1).

A 2-stream radiative transfer scheme is employed as observation operator to build the bridge. Both Black Sky Albedo (BSA) and White Sky Albedo (WSA) can be simulated at VIS and NIR spectral range. They depend on (1) canopy structure parameter : Leaf Area Index (LAI), average leaf inclination angle (ALA) ; (2) leaf optical property : leaf reflectance (ρ_l), leaf transmittance (τ_l) ; (3) soil albedo (ρ_s) ; (4) solar zenith angle (SZA) (only for BSA).

The program of the model consists of three functions for calculating Aveg (ALBEDO_VEG), WSA and BSA as listed hereafter :
(1) ALBEDO_VEG(rho, tau, angl)
(2) WSA(rho, tau, angl, lai, Rsoil)
(3) BSA(rho, tau, angl, lai, tts, Rsoil)

The anonymous and the corresponding meaning of inputs are listed in table 3.1 :

The WSA and BSA can be decomposed into six configurations, namely rdd, tdd, rsd, tsd, rdo, tdo.

Limitation of the simplified 2-stream model :

(1) Turbid media, homogenous. Canopy is described as turbid medium without considering the effects of vegetation structure and shadowing effects. The model is more proper for homogenous canopy, such as dense forest or dense crops. However, for sparse vegetation area, canopy structure and shadow effects should be considered, thus Geometric Optical (GO) models would be more proper.

(2) Isotropic assumption for background. Background is assumed to be anisotropic, which is made to easy calculate the interaction with bottom boundary of the canopy. Through in reality, due to different components as well as roughness, there would be anisotropic effects.

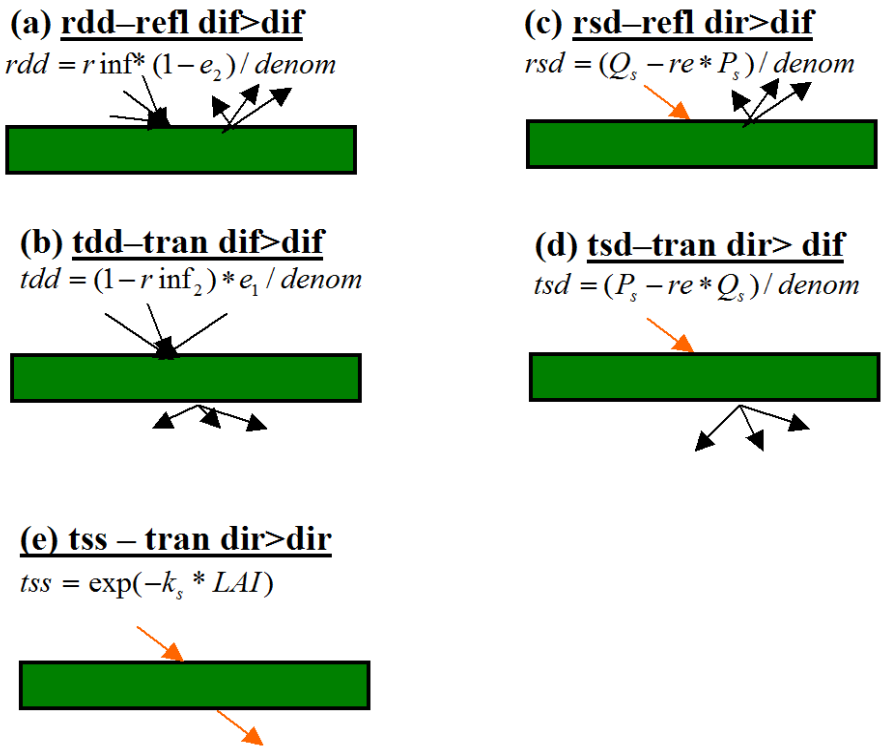

FIGURE 3.1 – Five components of radiation in our 2-stream model (a) rdd-reflectance : diffuse incoming->diffuse outgoing ; (b) tdd-transmittance : diffuse incoming->diffuse outgoing ; (c) rsd-reflectance : solar direction incoming->diffuse outgoing ; (d) tsd-transmittance : solar direction incoming-> diffuse outgoing ; (e) tss-transmittance : solar direction incoming-> solar direction outgoing.

(3) 2-stream approximation. The model based on 2-stream theory, which is the approximation solution integrating upper and lower hemisphere flux. Also solar incoming radiation direction is added in the model. The diffuse part solution would depend on the approximation precision.

3.2.1.1 Physical Basis of Two-stream Scheme

rddt is defined as 'white sky albedo', rsdt is equal to 'black sky albedo'. Explicit expressions can be derived from solving the radiative transfer equations, which are :

$$rddt = rdd + \frac{tdd * \rho_s * tdd}{1 - \rho_s * rdd} \tag{3.1}$$

$$rsdt = rsd + \frac{(tsd + tss) * \rho_s * tdd}{1 - \rho_s * rdd} \tag{3.2}$$

Where, ρ_s is soil albedo, assumed to be isotropic. rdd, tdd, rsd, tsd, tss are five basic components illustrated in 3.1 :

$$rdd = rinf * \frac{1 - e_2}{denom} \tag{3.3}$$

$$tdd = \frac{(1 - rinf_2) * e_1}{denom} \tag{3.4}$$

$$rsd = \frac{(Q_s - re * P_s)}{denom} \tag{3.5}$$

$$tsd = \frac{(P_s - re * Q_s)}{denom} \tag{3.6}$$

$$tss = exp(-k_s * LAI) \tag{3.7}$$

Theses symbols ($rinf$,$rinf_2$,e_1,e_2,re,P_s,Q_s,$denom$,k_s) are calculated as basic quantities as follows :

J_1, J_2 are the source functions. ddb, ddf, sdb, sdf are the interception fraction calculated by integrating diffuse or direct incident angle with leaf angle.

3.2.1.2 Fraction of vegetation cover

Worth to mention that comparing to the form of linear combination of vegetation albedo and soil albedo, which is :

$$A_{tot} = f_{veg}A_{veg} + (1 - f_{veg})A_{soil} \tag{3.8}$$

In our 2-stream model, WSA can also be expanded at a similar linear form as above :

$$WSA = \frac{(1 - e_1^2)}{1 - A_{veg}e_1^2}A_{veg} + \frac{tdd \cdot tdd}{1 - A_{veg}rdd}A_{soil} \tag{3.9}$$

$$BSA = rsd + \frac{(tdd + tss) \cdot A_{soil} \cdot tdd}{1 - A_{soil}rdd}A_{soil} \tag{3.10}$$

Here, A_{veg} is semi-infinite vegetation albedo (LAI$\rightarrow\infty$), which is independent of LAI and defined as :

$$A_{veg} = rinf = (att - m)/sigb \tag{3.11}$$

A_{soil} is soil albedo, thus equal to ρ_s.

Verification (1) : Does WSA converge to A_{veg} when vegetation is dense ?

-From Eq. 3.9, when LAI$\rightarrow\infty$, e_1, tdd$\rightarrow 0, then WSA \rightarrow$A$_{veg}$. This confirms the semi-infinite assumption.

Verification (2) : Interaction of soil and vegetation bottom can be omitted if vegetation is dense or soil is dark ?

-In Eq. 3.9, the term $rdd\cdot A_{soil}$ is in the division. This is due to the interaction between soil and bottom layer of canopy. If it is small enough, such like in case of dense canopy or dark soil, it can be omitted. This yields :

$$WSA \approx \frac{(1-e_1^2)}{1-A_{veg}e^2}A_{veg} + tdd\cdot tdd\cdot A_{soil} \tag{3.12}$$

Verification (3) : Can these two fractions (f_{veg} and f_{soil}) be approximated by exponential functions ?
-Yes, simulations are conducted to plot f_{veg} vs. LAI.

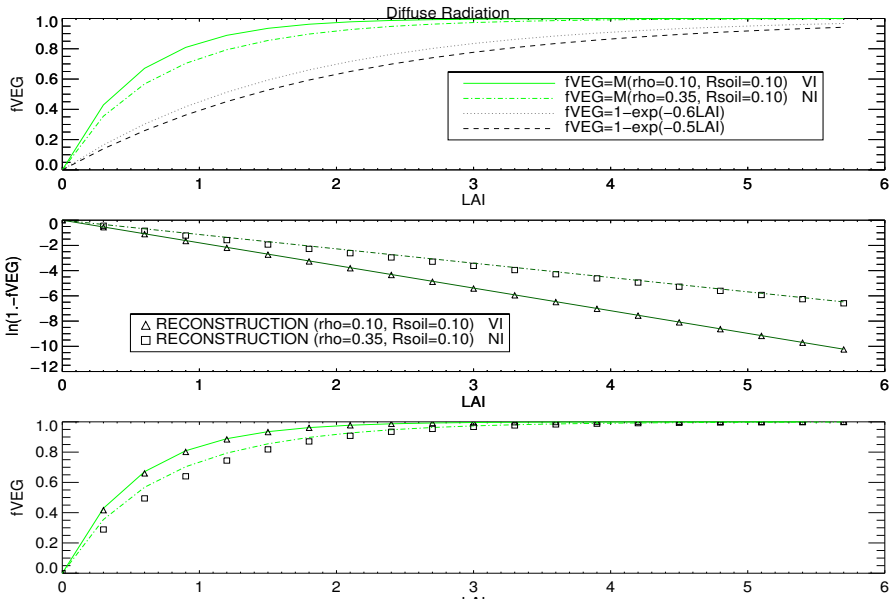

FIGURE 3.2 – Fraction of vegetation cover expressed as exponential function of LAI.

Verification (4) : Are the sum of these two fractions, A_{veg}, A_{soil} equal to one ?
-Yes, these two fractions are defined as :

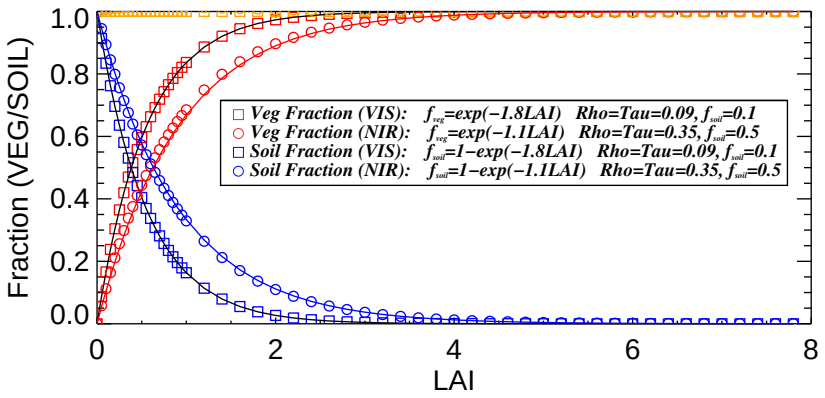

Figure 3.3 – Fraction of vegetation (f_{veg}, red color), fraction of soil (f_{soil}, blue color) and their sum (orange color). Two cases are tested for VIS and NIR taking leaf single scatter reflectance as 0.09 and 0.35, respectively.

$$f_{veg} = \frac{(1 - e_1^2)}{1 - A_{veg}e^2} \tag{3.13}$$

$$f_{soil} = \frac{tdd \cdot tdd}{1 - A_{soil} \cdot rdd} \tag{3.14}$$

Both in VIS and NIR domain, $f_{veg} + f_{soil}$ is approaching to 1 (fig.3.3). This can be proven by simulation with different configuration of ρ_l , τ_l, ρ_s.

Verification (5) : clarification fraction of vegetation cover definition. They might be used improperly.
-In the literature, fraction of vegetation cover is calculated as exponential function of LAI :

$$f_{veg} = 1 - exp(-0.5LAI) \tag{3.15}$$

$$f_{veg} = 1 - exp(-0.6LAI) \tag{3.16}$$

$$f_{veg} = 1 - exp(-\frac{G(\theta)LAI}{cos\theta}) \tag{3.17}$$

Fractional vegetation cover is commonly defined as the gap function at nadir direction. The three functions above are commonly used in remote sensing community and canopy modeling

domain. In Eq. 3.17, if $G(\theta)$ is taken as 0.5 (random distribution case of leaf angle) and as zero (nadir view), Eq. 3.17 becomes Eq 3.15. Similarly, if $G(\theta)$ is taken as 0.5 (random distribution case of leaf angle) while θ as 60°(diffuse or approximation for mid-latitute solar zenith angle), Eq. 3.17 becomes Eq. 3.16. Here, we compare these fraction of vegetation with the one calculated with our 2-stream model. Results are shown in fig. 3.4

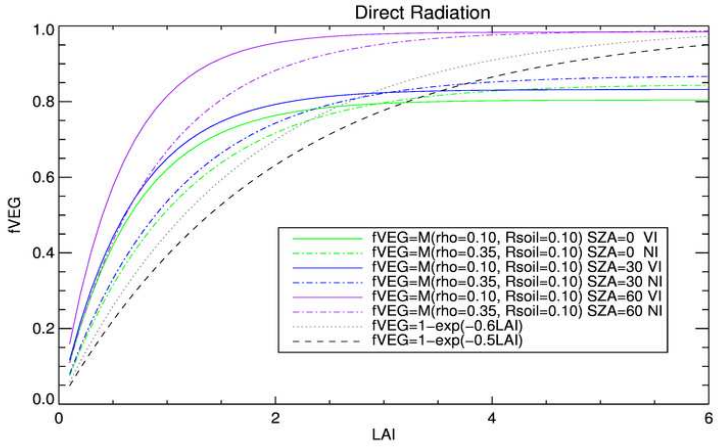

FIGURE 3.4 – The fveg comparison : (1) fVEG from 2-stream model of SZA=0, (2) fVEG from 2-stream model of SZA=30, (3) fVEG from 2-stream model of SZA=60, (4) fVEG=1-exp(-0.6LAI), (5) fVEG=1-exp(-0.5LAI).

3.2.2 Sensitivity test

The objective of this section is to retrieve Rsoil and Rho/Tau simutaneously. Priori to the retrieval, it is worthy to examine the model sensitivity to these two variables. In reality, the similar albedo of vegetation and soil would both contribute to the total albedo. For instance, dense vegetation on bright surface or sparse vegetation on dark surface would make a strong contract of the two components, thus easier to solve the problem. For scenarios like sparse vegetation on bright surface or dense vegetation on dark surface, it is more complicated to achieve the disentangling. The spectral response of MODIS and SEVIRI on soil and green leaves is illustrated in fig. 3.5 .

A sensitivity simulation is illustrated in for both VIS and NIR domain. Rho is varied from 0.05 to 0.30 at the step of 0.05 in VIS domain, while 0.30 to 0.48 at the step of 0.05 in NIR domain. Three types of soil are pre-defined with Rsoil at 0.05, 0.10 and 0.30, representing dark, medium and bright scenarios, respectively.

In VIS domain, as LAI larger than 3, albedo is approaching a stable value. That indicates : (1) total albedo is completely controlled by vegetation, there is nearly no contribution from soil background ; (2) albedo is saturated with LAI, higher LAI have ignorable marginal increase effect on total albedo. When LAI is less than 3, both vegetation and soil contribute to the total albedo. While it is increasing or decreasing with LAI depends on the contrast of vegetation and soil. In

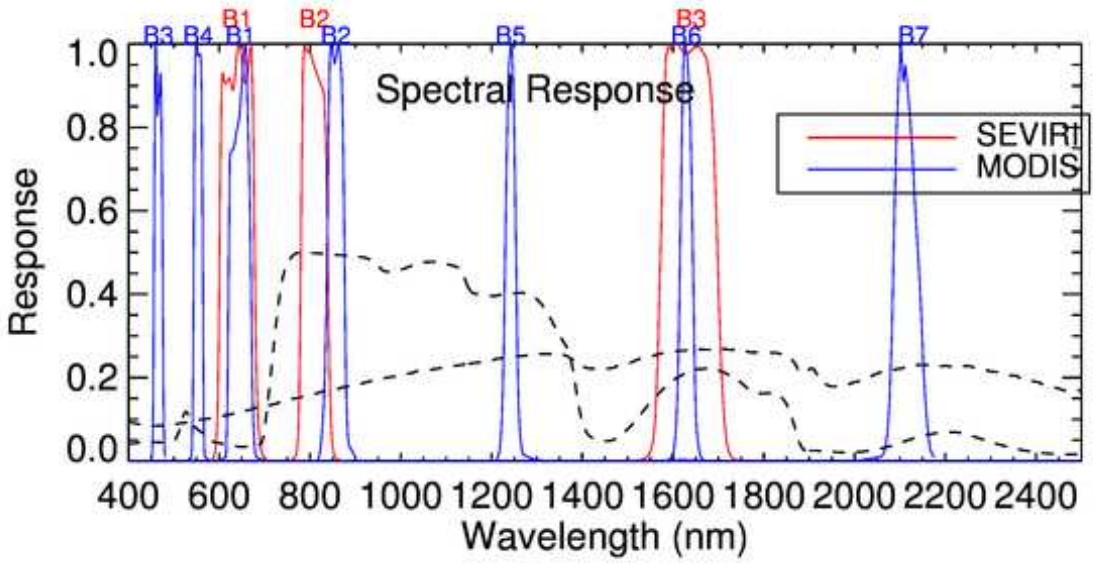

Figure 3.5 – Spectral response functions of MODIS and SEVIRI sensors. Typical spectral curves of soil and green leaves are imposed as slash curves.

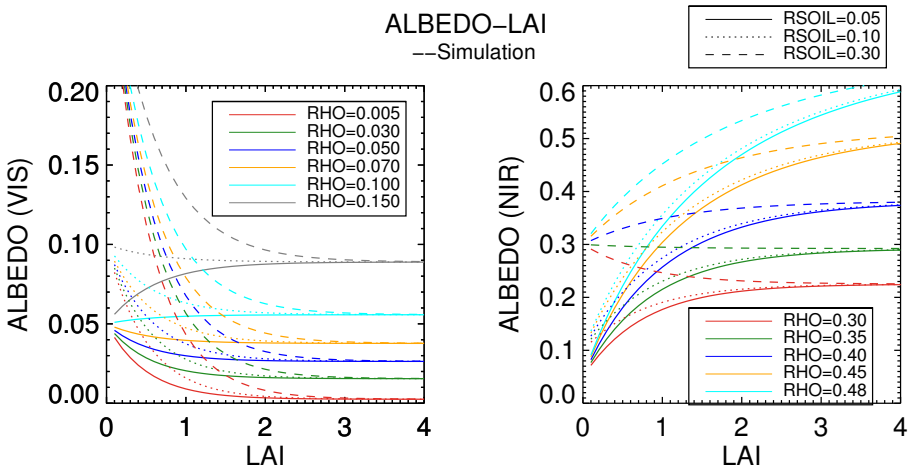

Figure 3.6 – Sensitivity simulation of VIS and NIR albedo with rho and Rsoil.

NIR domain, the same conclusion of sensitivity is achieved as in VIS domain.

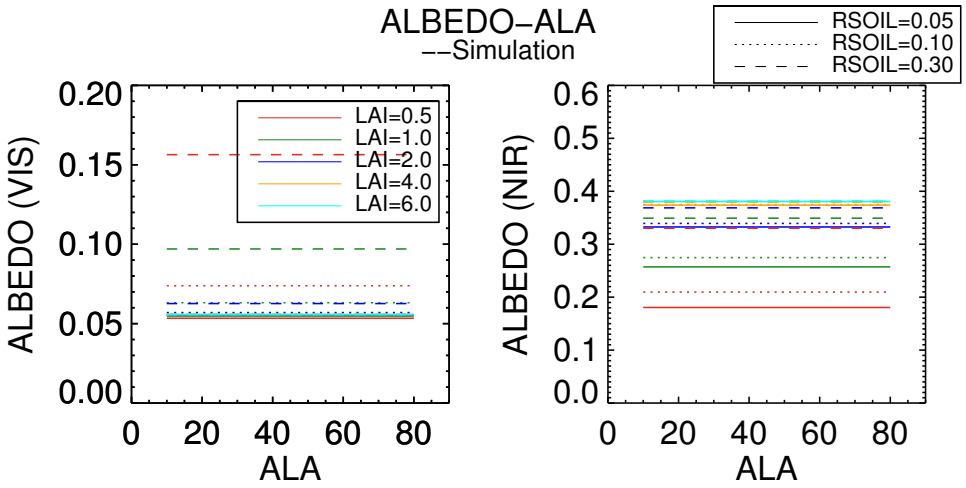

FIGURE 3.7 – Sensitivity test of VIS and NIR WSA with ALA under different configurations of LAI and soil albedo.

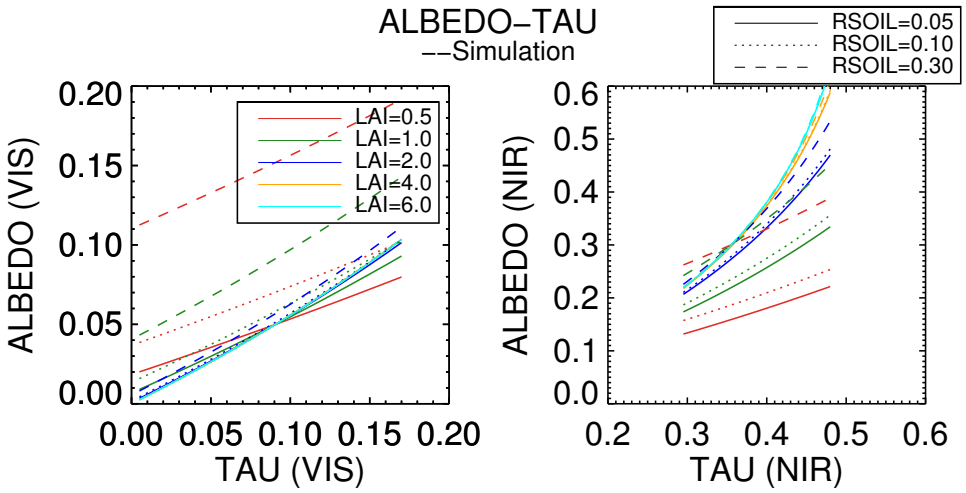

FIGURE 3.8 – Sensitivity test of VIS and NIR WSA with TAU under different configurations of LAI and soil albedo.

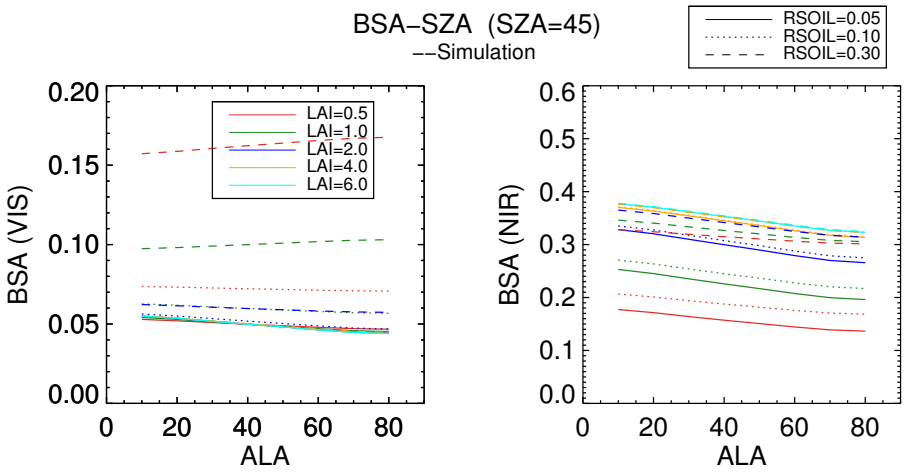

Figure 3.9 – Sensitivity test of VIS and NIR BSA with ALA under different configurations of LAI and soil albedo. SZA is fixed as 45 degree.

3.3 Static Soil and Vegetation Albedo Separation

3.3.1 Existing Global Static Soil Maps

Soil background albedo is measurable from satellite observations, which is an adding information as traditional products as LAI, Fraction of Photosynthetically Active Radiation (FPAR), fCover. A short summary of recent advance of extracting soil background albedo from MODIS standard products is given in section 3.1. Worth to mention is the advance of applying observations from multi-angle sensors to retrieve under-canopy reflectance using geometric model (Canisius and Chen, 2007; Pisek et al., 2010). This method explores the advantage of geo-optical (GO) model to decompose scenario directional reflectance into illuminated vegetation and soil components.

In this section, two global soil albedos datasets are compared at 0.05 ° resolution in VIS (0.30-0.70μm), NIR (0.70-3.0μm) : (1) SWANSEA soil background albedo, (2) CNRM soil background albedo. These two datasets are both using MODIS observations, while developed independently using different methods.

3.3.1.1 SWANSEA soil background albedo

A new vegetation and soil background albedo parameterization is proposed for JULES. For short, we name it 'SWANSEA' soil background albedo. This dataset is developed in an alternative way comparing CNRM albedo dataset. First, a 'NDVI' is constructed through VIS and NIR spectral albedo as follow :

$$NDVI = \frac{\alpha_{nir} - \alpha_{red}}{\alpha_{nir} + \alpha_{red}} \tag{3.18}$$

where α_{red} and α_{nir} are the albedo values for red (channel 1) and nir (channel 2), respectively. This NDVI is used as an indicator for vegetation amount, since publications have shown a near-linear relationship between FAPAR-NDVI. For cells with partially covered vegetation, albedo is linearly related with NDVI. Then, total albedo is regressed against NDVI for both VIS and NIR broadband range. The interception of this regression, corresponding to NDVI equal zero, can be interpreted as soil background albedo.

3.3.1.2 CNRM soil background albedo

Static soil and vegetation albedos are derived as a part of ECOCLIMAP-II physiographic database, which forms a module of the SURFEX platform (REF). This offers a surface initial parameterization to drive SVAT (Soil-Vegetation-Atmosphere Transfer) model considered for meteorological and climatic applications. The maps of soil albedo are generated at the resolution of 1km and encompass African and Europe for time being (Faroux et al., 2013; Kaptué Tchuenté et al., 2011). In this study, we expand the continental soil background albedo dataset to global coverage while at the climate model resolution of 0.05 degree.

This global soil background albedo is generated using 4 years MODIS albedo (MCD43C3) and LAI (MCD15A2) datasets. In this study, Collection 5 of MODIS data records as well as the quality indicators are handled for the period from 2007 to 2010. MCD43C3 is distributed at 0.05°spatial resolution and 16-days interval. MCD15A2 is distributed at 1km spatial resolution and 8 day interval. Both datasets are reprojected from ISIN to Plate Carrrojection and then mosaiced using MRT tool. Note that MCD15A2 is resampled to 0.05°before this process.

Total albedo α_{total} can be formulated as soil albedo α_{soil} and vegetation albedo α_{veg} weighted by the fraction of vegetation f_{veg}, as shown in Eq. 3.19.

$$\alpha_{total} = \alpha_{soil}(1 - f_{veg}) + \alpha_{veg} \cdot f_{veg} \tag{3.19}$$

To separate total albedo into soil and vegetation components, fraction of vegetation is serving as a weighting indicator. It is calculated from LAI using an exponential function (Eq. 3.20).

$$f_{veg} = 1 - e^{-0.6LAI} \tag{3.20}$$

Detailed descriptions of the method can be found in (Kaptué Tchuenté et al., 2010).The wet and dry soil scenarios are mixed together in the analysis. Therefore, retrieved bare soil albedo products would rather depict an average situation although statistically dry situation is more occurent in general, which of course depends on the pixel location.

3.3.1.3 Intercomparison of two Global Soil Albedo Maps

After pre-processing steps, the two datasets are made consistent in both spatial resolution and geographic projection. The comparison with the Swansea static albedo product is conducted at pixel by pixel basis at 0.05 degree resolution. The spatial comparison is displayed in fig. 3.10 for White Sky Albedo (WSA), both at VIS (0.4-0.7μm) and NIR (0.7-3.0μm) ranges.

It can be noticed that both in VIS and NIR domain, gaps exist for both VIS and NIR. This is caused by low confidence in dense vegetation area, such as Amazon and Congo basin, or long-duration of snow coverage, as Siberia for NIR SWANSEA soil albedo product (fig. 3.10). Generally, CNRM albedo is more spatially more complete than SWANSEA albedo.

These two albedo datasets are similar in spatial patterns. In the VIS domain, CNRM albedo is generally lower than SWANSEA albedo all over the world except regions as Southwestern China, Chili. In the NIR domain, these two are very comparative. The areas with slightly higher albedo are : central America, eastern coastal area of South America, eastern part of Africa, central India, eastern part of Australia. The areas with slightly lower albedo are : south Africa, central and western Australia, central Asia, western part of North America.

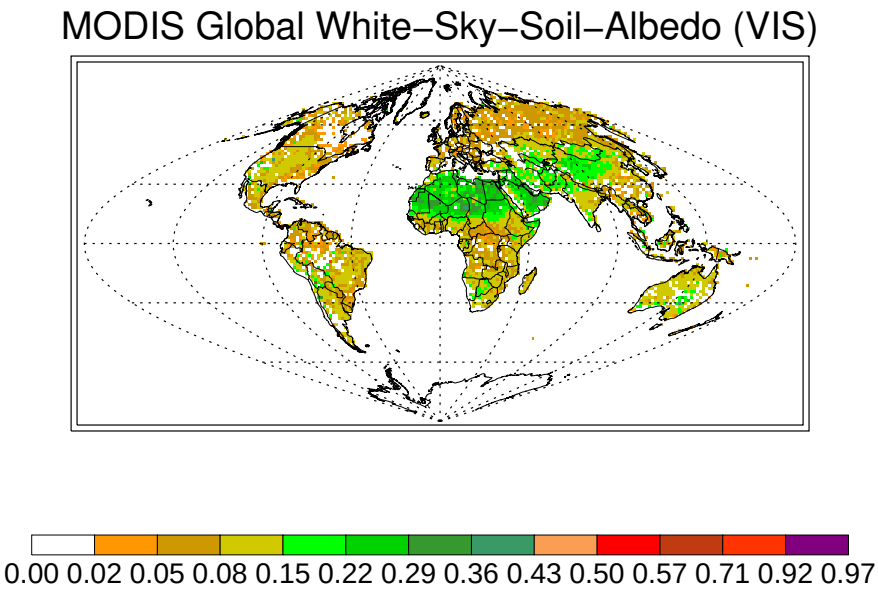

– (a)

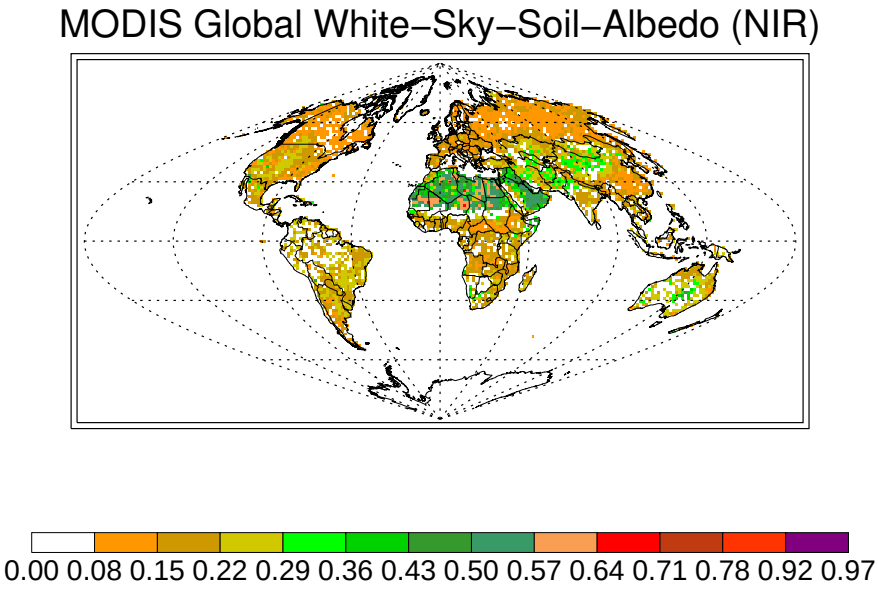

– (b)

FIGURE 3.10 – Comparison of CNRM and SWANSEA global soil background albedo. Noted, the VIS and NIR are using different legends.

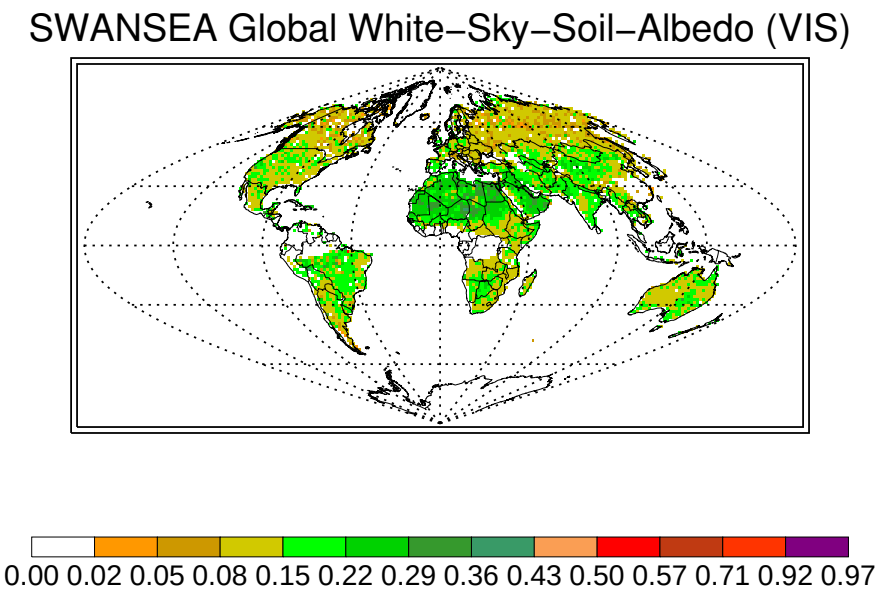

– (c)

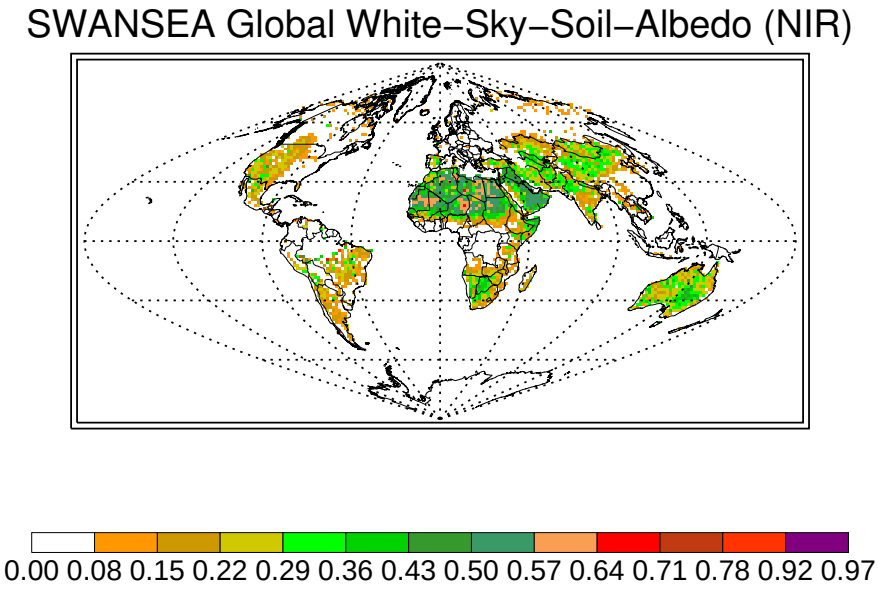

– (d)

Comparison of CNRM and SWANSEA global soil background albedo. Noted, the VIS and NIR are using different legends.

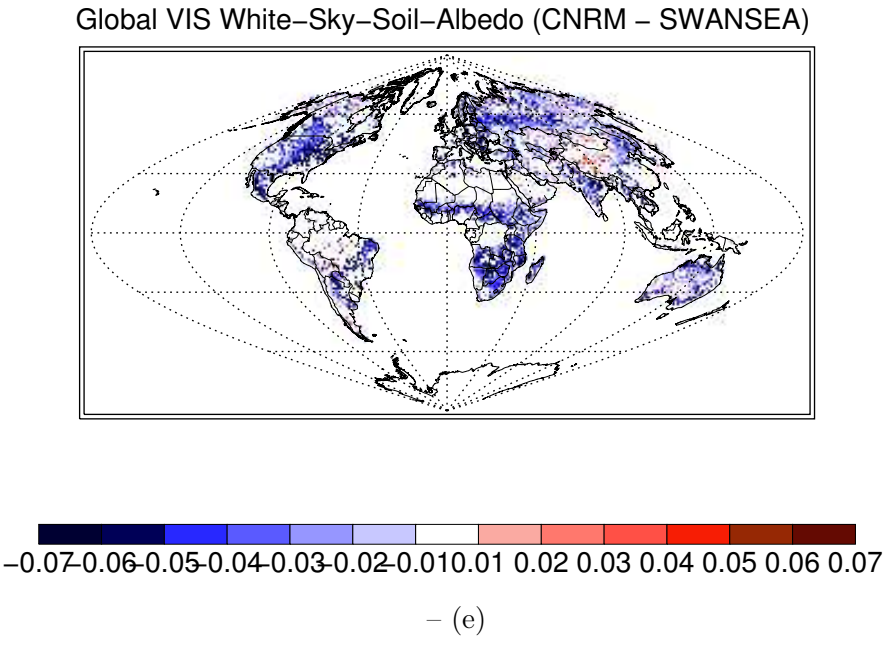

– (e)

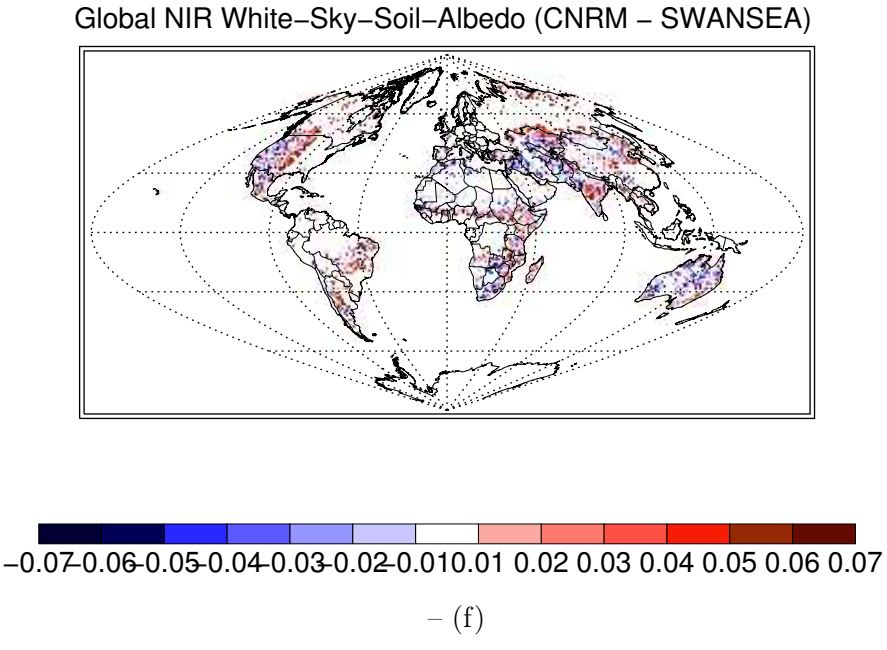

– (f)

Comparison of CNRM and SWANSEA global soil background albedo : (a)global soil background albedo in VIS range using CNRM method, (b)global soil background albedo in NIR range using CNRM method, (c)global soil background albedo in VIS range produced by Univ. SWANSEA, (d)global soil background albedo in NIR range produced by Univ. SWANSEA, (e)global soil background albedo difference in VIS range, (f)global soil background albedo difference in NIR range. Noted : the VIS and NIR are using different legends.

Scatter plots of CNRM soil background albedo vs. SWANSEA soil background albedo are illustrated in fig. 3.11. Snow contaminated areas are excluded from plotting based on MODIS snow flags indicated in MCD43A2. CNRM albedo estimates tend to display lower values than the Swansea product, with a negative mean bias of -0.036 in the visible band and a Root Mean Square Error (RMSE) equals to 0.055. In the near infrared, the agreement is improved and the bias is estimated to 0.029 even with the inclusion of outliers of the University of Swansea products. RMSE is 0.076.

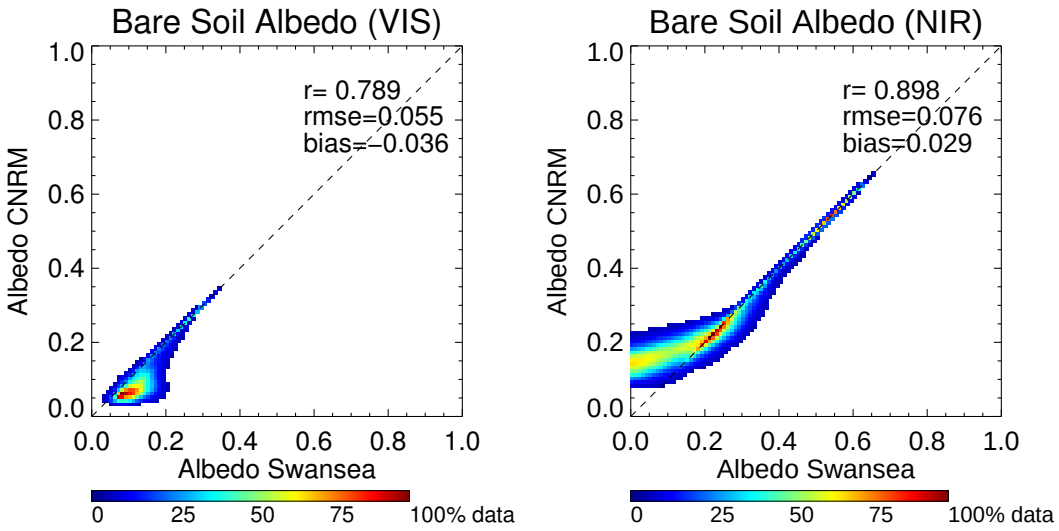

Figure 3.11 – Scatter plots of CNRM vs. SWANSEA global soil background albedo in VIS and NIR ranges.

The high correlation of this two datasets and the consistency of spatial patterns verify indirectly the trustworthy of our CNRM soil background albedo dataset. Bias in both VIS and NIR could be attributed to different elements : the method applied to derive soil background albedo, the different periods of MODIS products involved in the regression and finally the implied vegetation and soil contribution fraction.

3.3.2 2-Stream method based on SAIL

3.3.2.1 Retrieval of Soil Albedo and Leaf Single Reflectance over France

In this chapter, MODIS broadband VIS and NIR WSA albedo (MCD43A3) is considered as observations. It is distributed at 500m spatial resolution each 8 day. 4-year data (2007-2010) is used for this retrieval. The original MODIS WSA albedo products are distributed at integerized sinusoidal (ISIN) projection and 'tile' extent. After reprojection and mosaic, 184 slots over the box [40.01°N, 5.5°W, 51.50°N, 9.91°E] containing France is available for applying our retrieval methods

TABLE 3.2 – The variation range of input variables to generate LUT.

Acronyms	Range	Step
LAI	0.1-8.0	0.1
SZA	5-70°	5°
WSA(VIS)	0.005-0.160	0.005
WSA(NIR)	0.295-0.480	0.005
Rsoil	0.01-0.50	0.01

For retrieving soil background albedo and single scattering albedo simultaneously, a Look-Up-Table (LUT) method is adopted to search the best solution globally. First, a LUT is constructed through simulations varying input variables : rho/tau, angl, lai, Rsoil, tts. The variation range and intervals for different variations are listed in table 3.2. Then, the couple of Rsoil and Rho/Tau minimizing the cost function is taken as the best match to minimize the difference of LUT simulation and observations.

MODIS original 8-D albedo and modelled albedo are compared during the period of 2007-2010 in 12 SMOSMANIA stations (fig. 3.13). Retrieved Wveg and Rsoil are also marked in the figures. For instance, at the station Condom (CDM) next statistics are obtained : in VIS domain, r^2=0.0318, rmse=0.0090 ; in NIR domain, r^2=0.8058, rmse=0.0212. At station Urgons (URG) : in VIS domain, r^2=0.4895, rmse=0.0134 ; in NIR domain, r^2=0.6427, rmse=0.0246. For the whole 12 stations, retrieval results and statistical scores are listed in table 3.3. Generally, the variation of NIR total albedo is well captured by the model with two stable variables Wveg and Rsoil. For VIS total albedo, things are complicated, at URG, SBR, MNT, the correlation is not bad, while for the other stations, the correlation is low.

The dispersion of the original MODIS albedo may due to several factors : (1) the imperfact of the model ; (2) Assumptions of fixed leaf angle, isotropic soil background, etc ; (3) stable variables of Wveg and Rsoil, not considering the dynamic effects of these two.

Soil albedo and Leaf Single Reflectance are retrieved simultaneously over the France, the spatial distribution of these two variables in VIS and NIR domain are mapped in fig. 3.14 . The pattern of Rsoil is simular in VIS and NIR domain, while the quantity of NIR is much higher than VIS. This is consistent with the well-recognized 'soil law'.

The goodness of fit (r^2) is calculated comparing reconstructed albedo with MODIS original product. It is taken to evaluate the performance of the retrieval. For most part of France, r^2 ranges from 0.4-0.8, or even higher. For north-eastern France, it drops to less than 0.2. For VIS WSA, the r^2 is very low for most regions except Massif-central, Corse and Alpes.

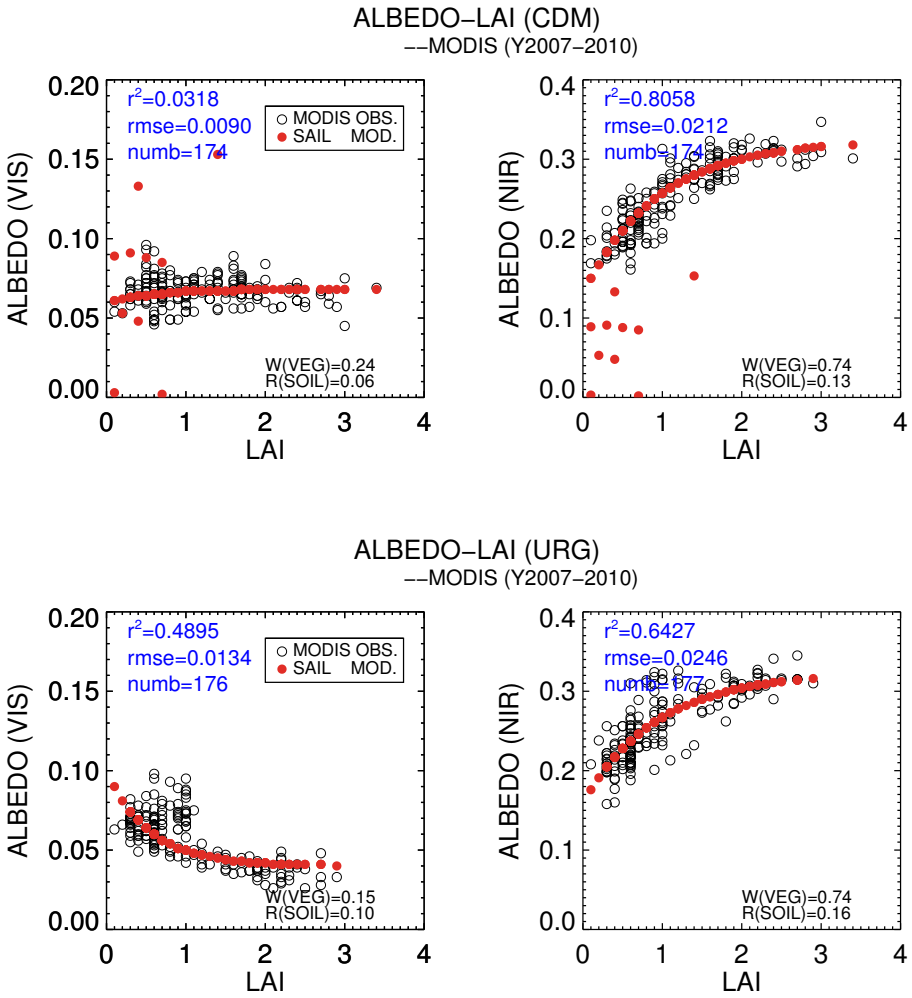

Figure 3.12 – Rsoil and Wveg retrieval in two stations : CDM and URG.

3.3.2.2 Analysis of the results

This part is an attempt for further analysis of the results of Wveg and Rsoil in response to the following questions :
(1) Whether the Wveg is clustered in main PFTs or there is a large inter-PFT variation ?
(2) Whether the Wveg is clustered in ecosystems, and better clustered than in main PFTs ?
(3) Whether Rsoil corresponds to FAO soil classes ?

Fig. 3.15 shows 12 Patches used in ISBA over the box containing the whole France : bare soil (NO), bare rock (ROCK), permanent snow (SNOW), deciduous broadleaved (TREE), needleleaved (CONI), evergreen broadleaved (EVER), C3 crops (C3), C4 crops (C4), irrigated crops (IRR), temperate grassland (GRAS), tropical grassland (TROG), wetlands, parks and gardens

TABLE 3.3 – 2-stream retrieval Wveg, Rsoil and statistical scores for SMOSMANIA stations

Station	Wveg(VIS)	Rsoil(VIS)	r_2(VIS)	rmse(VIS)	Wveg(NIR)	Rsoil(NIR)	r_2(NIR)	rmse(NIR)
CDM	0.24	0.06	0.0318	0.0090	0.74	0.13	0.8058	0.0212
CRD	0.17	0.07	0.0636	0.0129	0.60	0.18	0.0897	0.0298
LHS	0.26	0.08	0.0181	0.0104	0.80	0.16	0.7181	0.0234
LZC	-	-	-	-	-	-	-	-
MNT	0.22	0.09	0.2037	0.0104	0.80	0.16	0.7181	0.0234
MTM	0.17	0.06	0.0374	0.0079	0.66	0.11	0.5759	0.0159
NBN	0.24	0.04	0.1947	0.0063	0.62	0.15	0.3650	0.0108
PRG	0.22	0.06	0.0461	0.0085	0.78	0.14	0.7555	0.0201
SBR	0.16	0.08	0.3385	0.0109	0.65	0.14	0.7111	0.0184
SFL	0.28	0.08	0.0018	0.0113	0.85	0.16	0.8197	0.0251
SVN	0.26	0.09	0.0761	0.0104	0.85	0.18	0.6713	0.0232
URG	0.15	0.10	0.4895	0.0134	0.74	0.16	0.6427	0.0246

Note : There is no retrieval results for LZC since MODIS LAI is identified as fill value over this station.

(PARK). As indicated in the Figure, in France, dominant PFTs are bare soil, irrigated crops, conifer tree, C3 and C4 crops, grassland, as well as a fraction of rocks and tropical grass.

The Wveg and Rsoil products derived from pixel level from the MODIS observations. It corresponds to the combination of patches. Pure pixels are chosen by presuming a dominant patch with fraction larger than 70%.

With these pure PFT pixels, vegetation single scattering reflectance is explored to be linked with PFT types. Mean and standard deviation are calculated within each type of 'pure' PFT pixels. The same process is conducted for dominant ecosystem types.

As illustrated in fig. 3.16, 4 patches are chosen as dominated ones in France, they are : conifer tree, irrigated crops, C4 crop and grassland. It can be observed that using VIS and NIR Wveg, Conifer Trees can be easily separated from the others, grassland can be also separated from Irrigated Crops and C4 crop, though some co-covered regions with C4 crop and irrigated crops. The later two are quite similar, thus difficult to be separated through Wveg VIS/NIR.

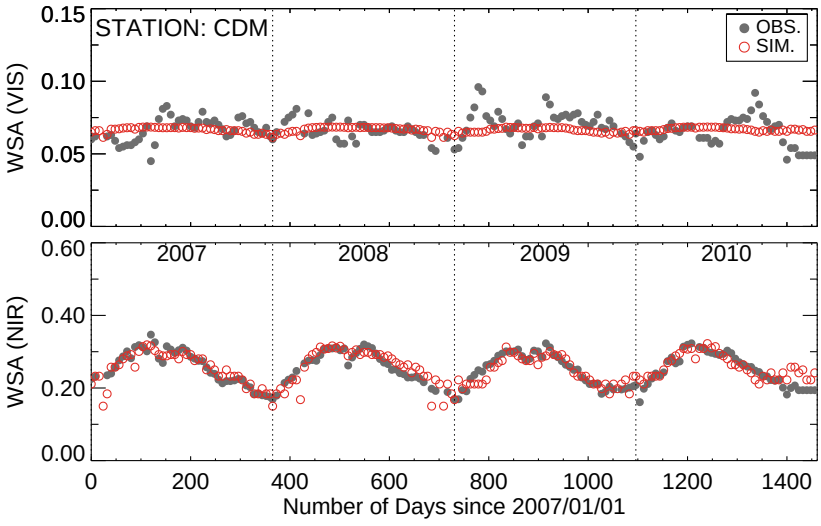

– (a)

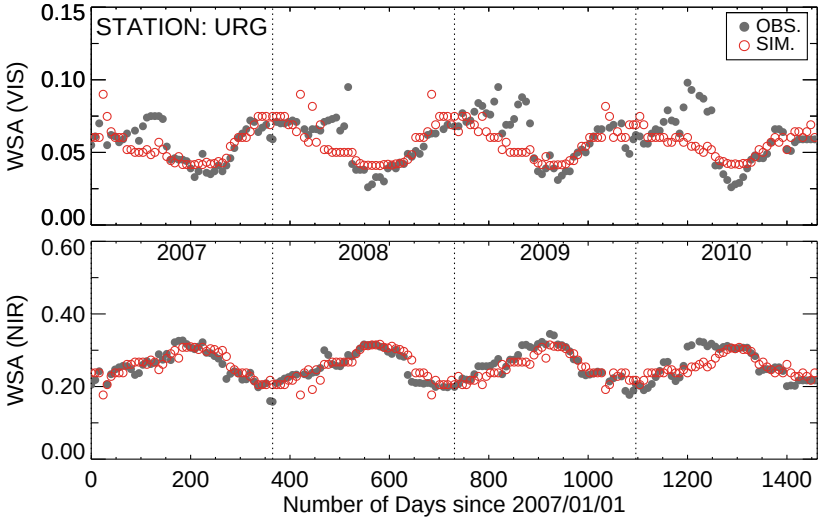

– (b)

Figure 3.13 – Time series of MODIS total albedo is compared with the reconstructed total albedo in two stations during a 4-year period of 2007-2010 : CDM and URG. In the upper panel, MODIS orginal 8-D time series (ORI) are plotted in orange color, reconstructed total albedo (REC) is shown in grey. In the middle panel, the residual of (ORI-REC) is shown. In the lowest panel, in-situ soil moisture recorded from Theta-probe is plotted.

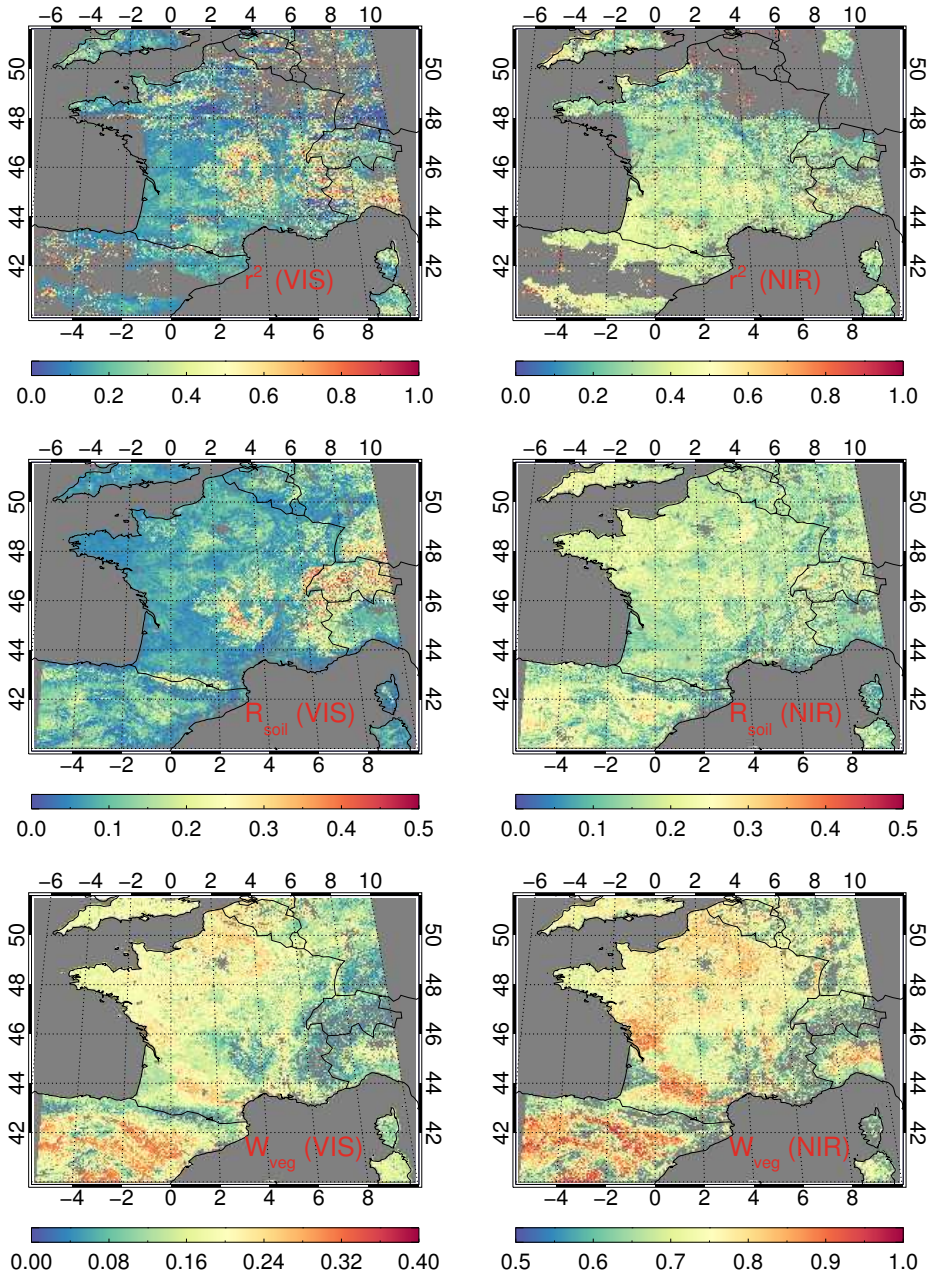

FIGURE 3.14 – Rsoil and Wveg retrieval and associated goodness of fit in the box over the France.

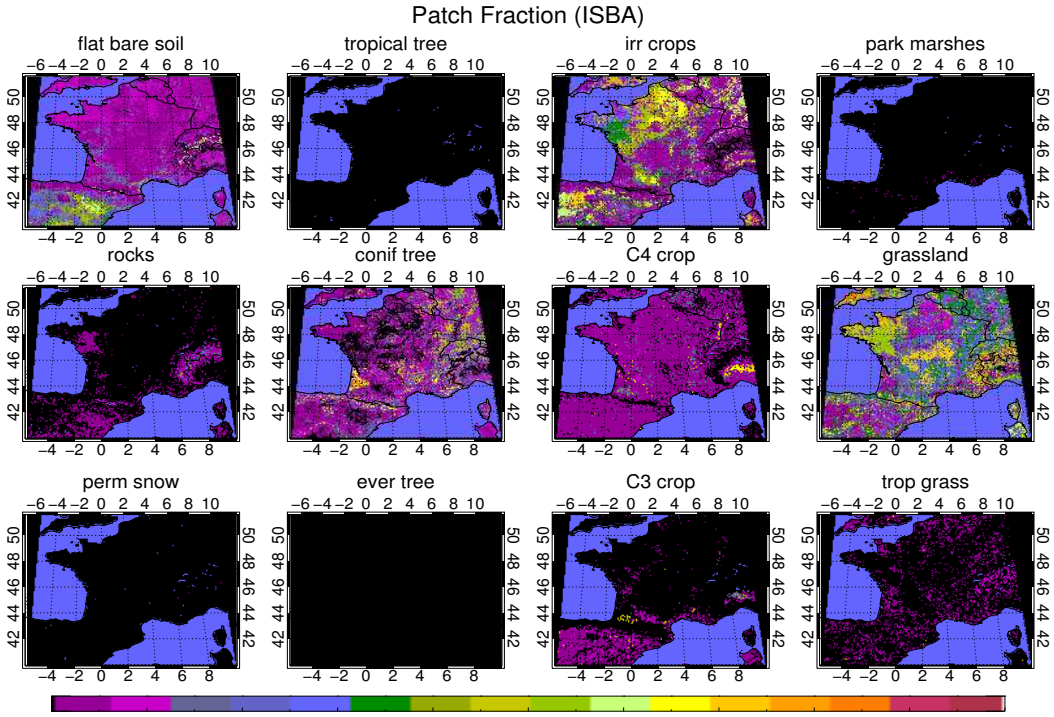

Figure 3.15 – Patches of ISBA over the box containing the France.

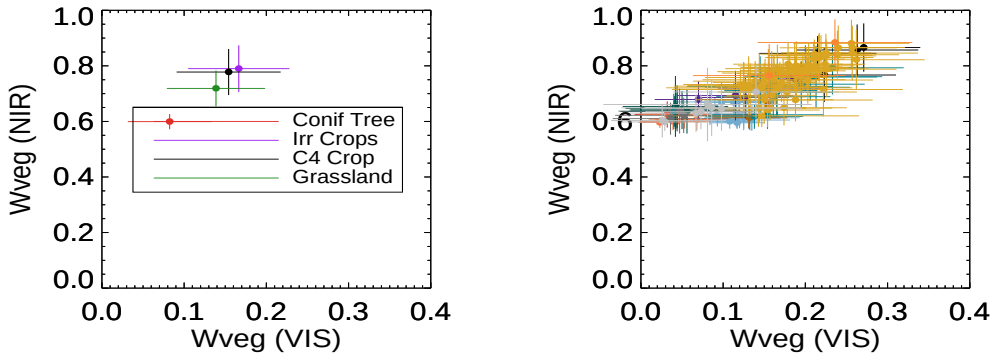

– (a) – (b)

Figure 3.16 – Leaf Single Scattering Reflectance (Wveg) analysis over (a) dominant PFTs and (b) ecosystem in France.

3.4 Dynamic Soil and Vegetation Albedo Separation

In section 3.3, both soil and vegetation albedo are assumed to be temporal stationary. This assumption largely simplifies the required variables for parameterization, thereby favoring the inversion and turns an ill-posed retrieval problem into well-posed one. The regression method is reasonably chosen for such kind of well-constrained problem if a linear model is constructed (as the method of CNRM and University of Swansea presented in section). Otherwise, if the model is non-linear as taken in section , a global searching for best parameter sets to minimize cost function can be achieved by various methods as LUT used.

However, in reality, soil albedo may vary responding to soil moisture, roughness, deposition of litter, etc. Vegetation albedo may present the fluctuation due to chlorophyll, leaf water, etc. These effects would challenge the time-invariant Wveg and Rsoil assumption. If Wveg and Rsoil are both considered as temporal variable, without constrain, the retrieval is an ill-posed problem. To solve this problem, a knowledge-based priori information would be helpful (Li and Strahler, 1996).

3.4.1 A Priori Information

3.4.1.1 A priori Information

Priori information is proven to be helpful and adding information for retrieval process. It is usually represented as probability density function (PDF) for the distribution of each variable and the covariance matrix. In our study, the distribution of a priori ρ_{vis} (τ_{vis}) and ρ_{nir} (τ_{nir}) are assumed to be Gaussian with a centre at Xprior and sigma value of sprior. The distribution parameters used in our study are listed in table 3.4.

3.4.1.2 A priori information constrained within PFT, ecosystem, soil unit

By comparing to applying a general background constrain of a priori information, making use of existing ecosystem or soil classes would add in the knowledge, and thus might add a better constrain for the sake of the retrieval process. In order to check this statement, retrieval results over the France from section 3.3.2.4 are clustered within different PFT types, ecosystem classes and soil mapping units.

TABLE 3.4 – A priori information used for describing leaf single reflectance ρ and soil albedo r Gaussian probability distribution function.

Variables	X_{priori}	σ_{priori}
ρ_{vis}/τ_{vis}	0.12	0.02-0.06
r_{vis}	0.06	0.10
ρ_{nir}/τ_{nir}	0.35	0.02-0.10
r_{nir}	0.20	0.20

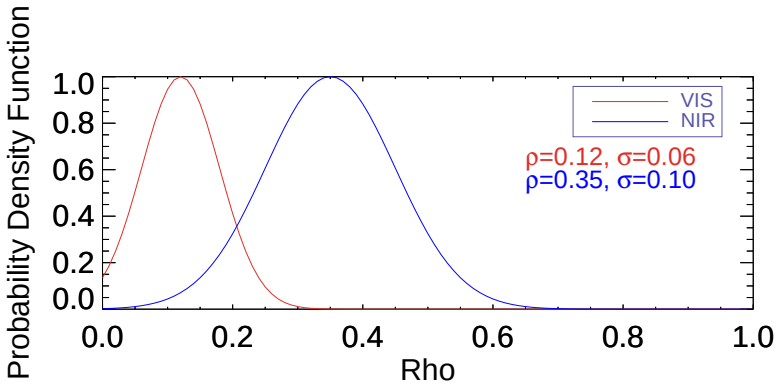

– (a)

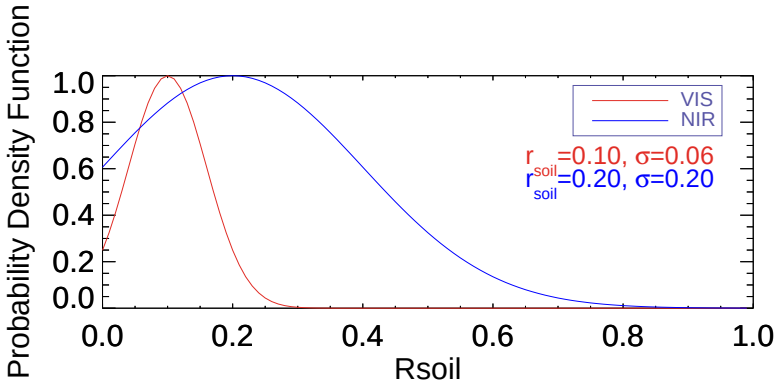

– (b)

Figure 3.17 – Probability density functions for (a) ρ_{vis} (τ_{vis}) and (b) ρ_{nir} (τ_{nir}) as a priori information.

The histograms of the Wveg are presented in 4 'pure' PFTs : Irrigated Crops, Grassland, Conifer Trees, C4 crops (fig. 3.18). It is further approximated by a gaussian function for simplification. It is encouraging to find that most distributions can be well reproduced by Gaussian fit. This conclusion still hold true for ecosystem classes (fig. 3.19). Several soil mapping units are selected to present the statistics results of Rsoil shown in fig. 3.20. For most units, the distribution of Rsoil is presenting the mode of Gaussian.

3.4.2 Radiative Transfer Model for Dynamic Retrieval

A simplified 2-Stream model is used for simulating radiative transfer and canopy albedo considering leaf optical properties, canopy structure, and background albedo. Detailed descriptions can be referred to Section . This model is serving as observation operator for TOC albedo in our retrieval system.

The objective is to find a solution of state variables to fit a cost function considering both observation and background information. Here, model is treated as perfect since albedo is relatively well modelled in two-stream comparing to reflectance and it is difficult to determine model error. Thus the retrieval is quite similar to well-constrained assimilation. This cost function can be represented as :

$$J(X) = \frac{1}{2}[(M(X) - d)^T C_d^{-1}(M(X) - d) + (X - X_{priori})^T C_{Xprior}^{-1}(X - X_{priori})] \tag{3.21}$$

At the right hand side, the former part is the contribution of observation, while the later part is the contribution of a priori information.

The cost function is minimized through a gradient algorithm with constrain. If convergence is achieved, a best solution X is found to minimize $J(X)$.

3.4.3 Application over SMOSMANIA stations

One SMOSMANIA station 'CDM' is chosen to present our retrieval results (fig. 3.21), absolute value and uncertainty information are both presented. The variation of Wveg is spurious in VIS domain, while corresponding well the seasonal cycle in NIR domain. This would be explained by higher signal noise in VIS domain for MODIS 8 day albedo product. Higher sensitivity to LAI also plays a role in this sense, since LAI is considered perfect input for the 2-stream model. Rsoil shows little variation in VIS domain, while high frequent change in NIR. This should be further validated, such as confirmed through comparing with potential causes as soil moisture.

Generally, in winter, Wveg has a higher uncertainty and Rsoil shows a lower uncertainty during the year. In summer, the inverse pattern can be found. This is consistent with mid-latitude northern-hemisphere vegetation amount seasonal cycle. When there is more vegetation amount, it is more difficult to see the underground surface.

Reconstructed albedo is compared with original observations, the temporal trajectory is well captured by the reconstruction results of our Gradient method. Comparing to a priori information and climatology, the dynamic soil albedo and vegetation single reflectance achieve high correspondence with observation (fig. 3.22). Scatter plots show a high correlation and small bias : r^2=0.79 and bias=-0.000000011 for VIS, and r^2=0.95 and bias=-0.00000021 for NIR (fig. 3.23).

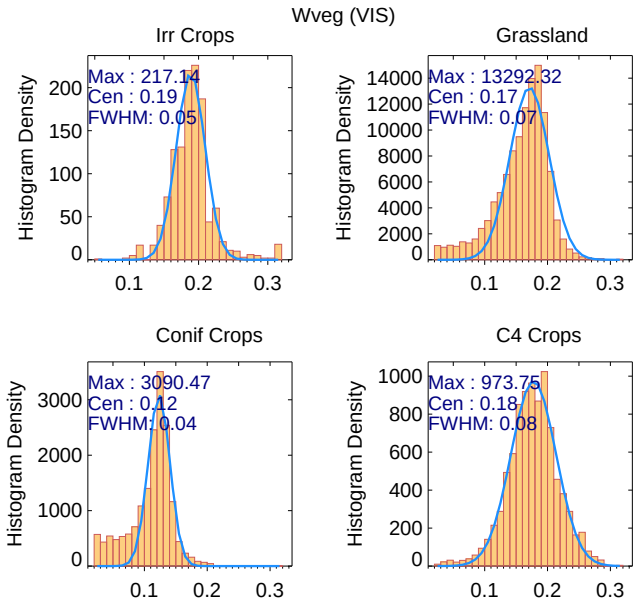

– (a)

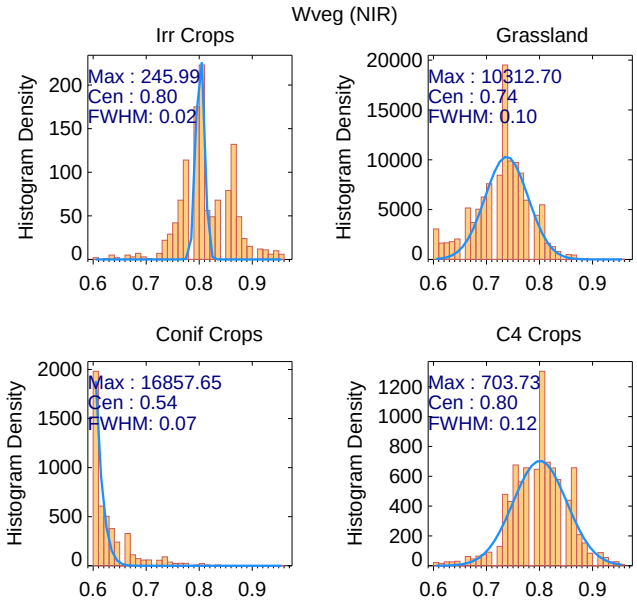

– (b)

Figure 3.18 – Histogram of Wveg (Leaf Single Reflectance) within 4 'pure' PFTs for (a) VIS and (b) NIR.

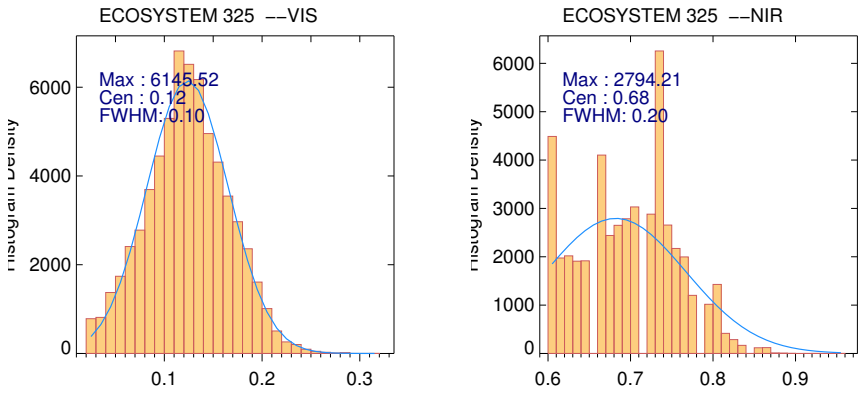

– (a)

– (b)

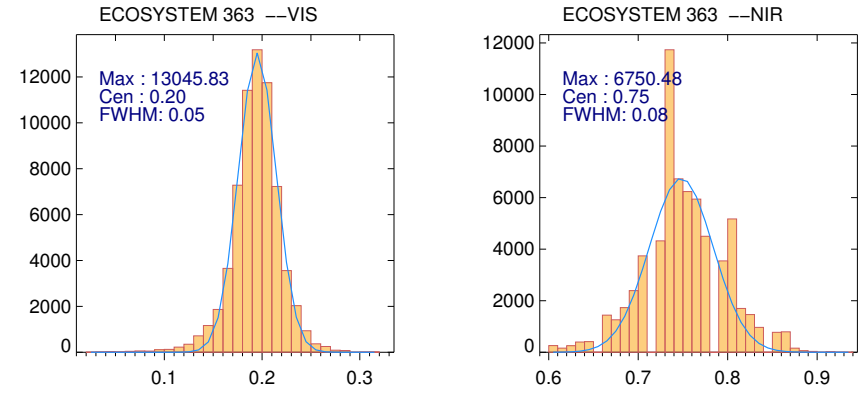

– (c)

– (d)

FIGURE 3.19 – Histogram of Wveg (Leaf Single Reflectance) for ecosystem 325, 363.

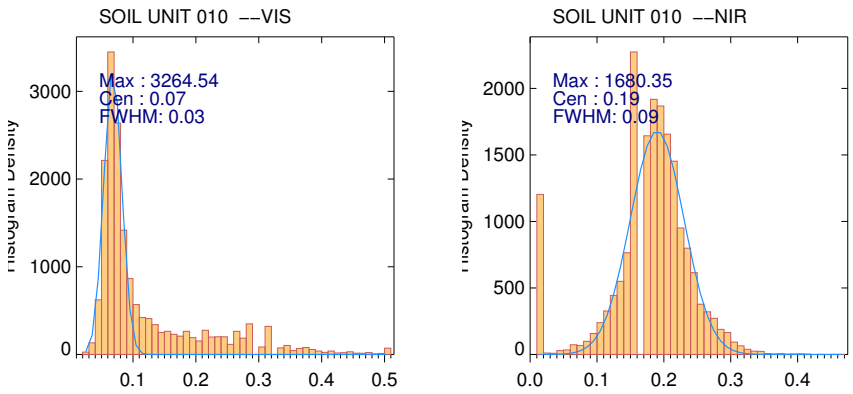

– (a) – (b)

Figure 3.20 – Histogram of Rsoil (Soil Albedo) within soil units for (a) VIS and (b) NIR.

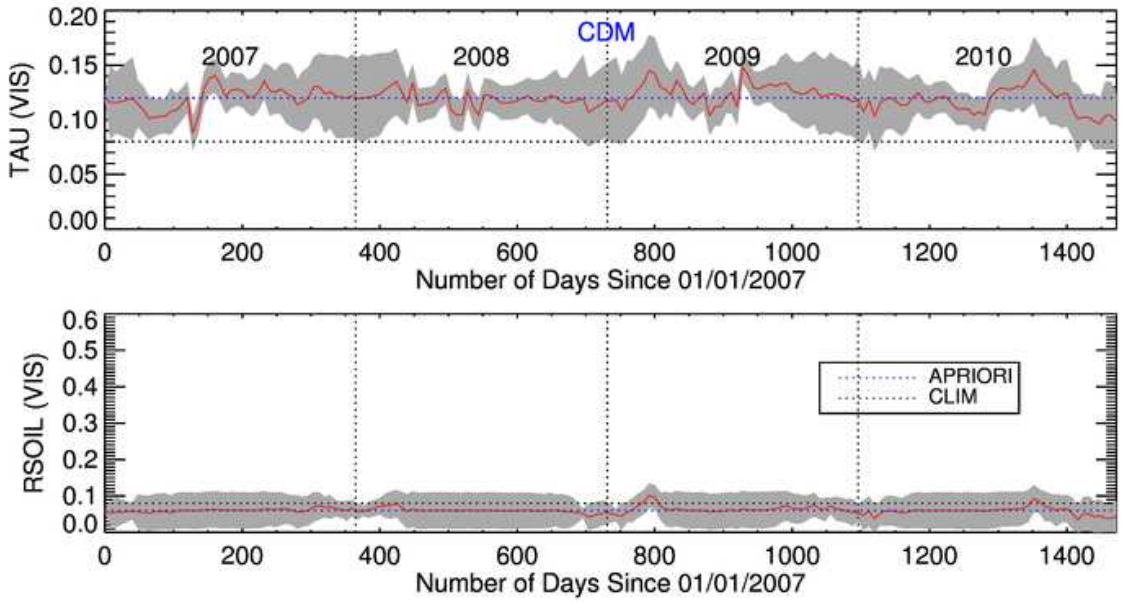

– (a)

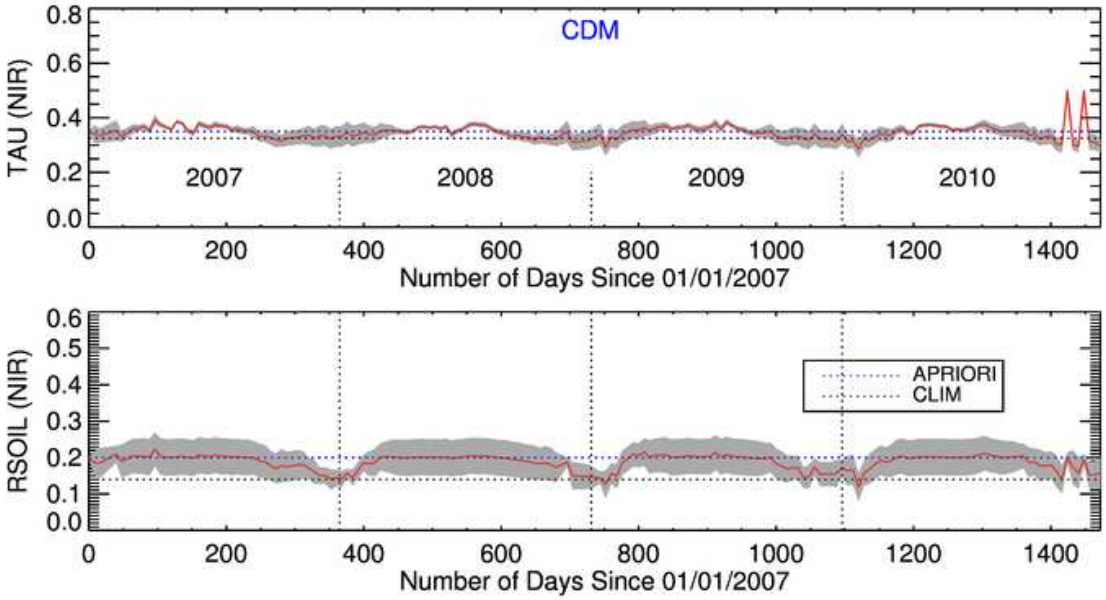

– (b)

FIGURE 3.21 – Leaf reflectance ρ and background albedo R assimilation for Condom station in (a) VIS broadband, and (b) NIR broadband. A priori and climatology information are marked as dashed straight lines in blue and black color, respectively.

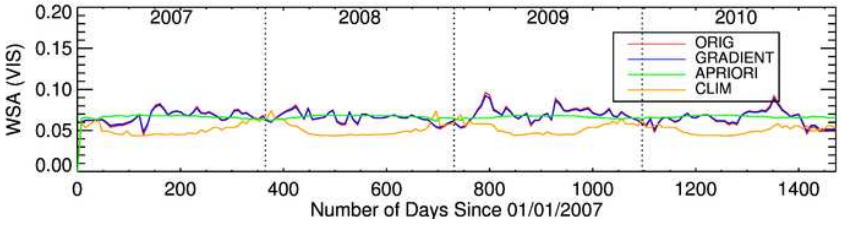

– (a)

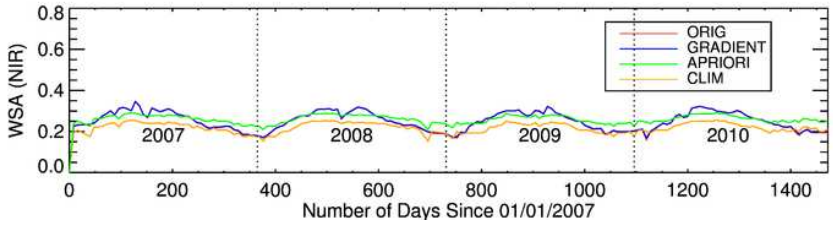

– (a)

Figure 3.22 – Reconstructed WSA for (a) VIS and (b) NIR in Condom station. Original MCD43A3, reconstruction from (1) Gradient method, (2) A priori information and (3) Climatology are also plotted for comparison.

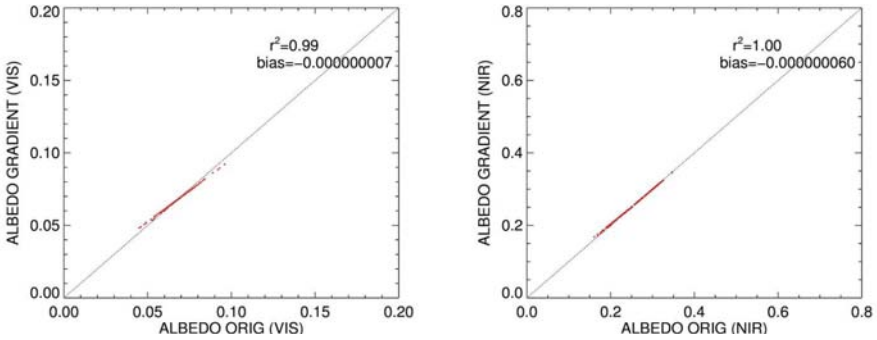

– (a) – (b)

Figure 3.23 – Scatter plot of reconstructed albedo from Gradient method comparing with original MODIS albedo for (a) VIS and (b) NIR range.

3.5 Conclusion

Two global soil background albedo datasets generated using the former method are compared : CNRM and SWANSEA. Spatial patterns are found to be consistent. CNRM albedo estimates tend to display lower values than the Swansea product, with a negative mean bias of 0.036 in the visible band and a Root Mean Square Error (RMSE) equals to 0.055. In the near infrared, the agreement is improved and the bias is estimated to 0.029 even with the inclusion of outliers of the University of Swansea products. RMSE is 0.076.

A canopy radiative transfer model is then proposed based on 2-stream approach, which can relate TOC WSA and BSA. It is simplified from SAIL model considering vegetation structure factor (as LAI, ALA), phyto-elements (leaf reflectance and transmittance), and soil background albedo. Sensitivity test shows the good relation between WSA/BSA with LAI, soil albedo, leaf reflectance, etc. Sensitivity experiment shows that WSA depends on LAI and leaf single reflectance in VIS domain. To separate vegetation and soil, two types of methods are explored to generate soil background albedo and vegetation albedo from satellite products : static method and dynamic method.

(1) Static retrieval is applied to obtain leaf single reflectance and soil reflectance using Look-up table method. These two are considered as temporal invariant. 4 years MODIS albedo and LAI products are used as input for the inversion. Reconstructed WSA and BSA are favorablely comparing with original inputs. For instance, at the station of Condom (CDM) next statistics are obtained : in VIS domain, r^2=0.0318, rmse=0.0090 ; in NIR domain, r^2=0.8058, rmse=0.0212. At station Urgons (URG) : in VIS domain, r^2=0.4895, rmse=0.0134 ; in NIR domain, r^2=0.6427, rmse=0.0246.

(2) A dynamic retrieval method is proposed. The idea is to adjust soil background albedo and leaf single scattering reflectance to match observed WSA and BSA. The difference between observed and simulated albedo is minimized through a Gradient method similar to well-constrained assimilation. Reconstructed albedo is compared with original observations, the temporal trajectory is well captured by the reconstruction results of our Gradient method. Comparing to a priori information and climatology, the dynamic soil albedo and vegetation single reflectance achieve high correspondence with observation.

Chapitre 4

Construction of prognostic albedo

Contents

4.1 Introduction

After the pioneering work on the relationship between bare soil albedo and soil moisture by (Idso et al., 1975), numerous studies have been devoted to investigate a relationship between bare soil albedo and soil moisture (Duke and Guérif, 1998; Liu et al., 2002; Lobell and Asner, 2002; Roxy et al., 2010). A thorough examination underlines the consensus on a non-linear exponential relationship. In the current generation of LSM, bare soil albedo is either assumed stationary or weighted by and empirical factor (usually 0.5) in case of noticed moisture (Dickinson, 1986; Knorr, 1997; Noilhan and Planton, 1989; Oleson et al., 2010; P.J. Sellers and Y. Mintz, 1986). In the Joint UK Land Environment Simulator (JULES), which is based on the Meteorological Office Surface Exchange (MOSES) (Cox et al., 1999), soil albedo is taken from a soil atlas (Wilson, M.F. and Henderson-sellers, 1985). In the Common Land Model (CLM), the moisture influences the soil albedo in a linear fashion with set of parameters borrowed from the literature (Dai et al.,

2003). The interactions between surface and atmosphere in the Soil Biosphere and Atmosphere (ISBA) model are specified using a bare soil albedo based on a number of in-situ measurements (Noilhan and Planton, 1989). All these LSM will undoubtedly benefit from a strategy to combine measurements of land surface albedo with soil moisture information rather than using static bare soil albedo. In this regard, Cedilnik et al. (2012) initiated such projection in considering an analysed surface albedo based on satellite observations in substitution to the climatology.

Vegetation albedo is usually parameterized in LSMs as reference values for PFTs or land cover types because of the necessity to enhance the consistency between the same landscape units. The surface albedo is derived per vegetation type from compilation of records in literature or field experiments. It is a static value along the year. However, in reality, vegetation albedo would change in response to leaf biochemical elements as leaf chlorophyll content, leaf water content, brown pigment, as well as the geometry of the canopy which in fact may echo to stress factors. Moreover, in the 2-stream scheme proposed by Dickinson (1983); Sellers (1985), leaf single reflectance and canopy vegetation albedo are both setted as fixed reference value, while the dependence of these two are not presented in the model, this would makes inconstancy. The feedback effects of canopy albedo and nitrogen content are recently revealed and confirmed by site-level statistics, which implies the benefits to incorporate such relationship in LSMs (Fisher, 2009; Hollinger et al., 2010; Ollinger et al., 2008). Actually, nitrogen is the main component for chlorophyll and protein, and the former plays a direct and main role in light absorption of PAR regime. To our knowledge, high correlation has been shown between leaf total nitrogen content and leaf chlorophyll content for specific species, while it is still uncertain at ecosystem level. Leaf water is shown to have a strong absorbing effect at shortwave infra-red range, which justifies the value to digest SWIR observations to monitoring processes like water stress.

The objective of this chapter is to construct a prognostic total albedo based on surface soil moisture and leaf chlorophyll content. Section 4.2 presents the calibration efforts devoted for establishing the soil moisture effects on soil surface albedo. Section 4.3 introduces how the canopy vegetation albedo is linked with leaf chlorophyll content. Section 4.4 summaries both effects, and conducts a total surface albedo simulation, which is compared with observations at landscape scale.

4.2 Calibration of Soil Surface Albedo with Soil Moisture

4.2.1 Theoretical rationale

A theory explains the darkening of the soil due to wetness by a reduction of the inner material reflection in presence of films of water coating soil particles (Ångström, 1925). Somewhat as a paradox, the multiple bouncing between a light ray and soil attributes leads to an increase probability of light absorption by water component. According to Twomey et al. (1986), such phenomenon could be even enhanced by having a weaker relative index of refraction between soil and water (compared to air), thereby having a less deviated light ray to the advantage of increased soil absorption. Above elements of physics seems to support a better coherent response

to water content for visible wavelengths compared to infrared range. In fact, water absorption is more significant in the near infrared, which could create noise on the results when its characteristics cannot be thoroughly prescribed at coarse scale. Being treated as pure extinction feature of light trapping by any medium, the modeling by an exponential formula seems to find here some justification. The influence of the texture is expected to be significant in theory since the composition in pebbles, stones and relative proportion of sand and clay will shape the dependence of wetness on soil albedo. In this respect, it connects to the degree of porosity while it remains that apparent soil color changes lightly when soils darken.

Despite a panorama of different textures between stations, it could not make clear its influence on the calibration between soil moisture and reflectance at the satellite moderate resolution. Even it is not certain that the collection of ground-based measurements would support a transposition to satellite applications due to the complexity of soil landscape in general. Another key issue that cannot be ignored is the chemistry composition of the water, which encompasses air particles deposition and soil organic matter composition. Knowing how dissolved organic material plays on the deviation from an absorption spectrum of pure water is certainly matter of concern and the role of microbial activity is also probably worth to know. Considering all these sources of uncertainties, it is likely that there exists a physical frontier in terms of appropriate information such like explaining 30% of the variance of the soil reflectance by wetness may be perceived as a reasonable targeted objective. The mixing of different soils at the scale of a satellite pixel justifies the effort for performing directly a calibration at a resolution to be consistent with foremost studies such like meteorological purpose.

Linear or exponential empirical function is found to well approximate the dependence of this dependence, which is confirmed by numerous field and laboratory measurements (Guan et al., 2009; Roxy et al., 2010). A new finding of Liu et al. (2002) shows that after a critical water content value, soil reflectance increases with soil moisture. Recently, surface soil albedo dependence on soil moisture is investigated using in-situ data from the moraine of an Andean glacier (Bolivia), and a good approximation to the exponential function is achieved (Gascoin et al., 2009b). This parameterization is incorporated into ORCHIDEE model, and it is found that an increase in the net radiation and a change of turbulent fluxes at annual and monthly time scales (Gascoin et al., 2009a).

The non-linear exponential relationship between these two quantities seems to be consensual. The relationship between the bare soil albedo and SSM is generally in the form (e.g. Guan et al., 2009 for recent results) :

$$A_{soil} = a_0 + a_1 e^{a_2 SSM} \tag{4.1}$$

This relationship is valid from visible to shortwave infrared as the soil darkening effect is known to be spectrally bland with a rather low spectral dependence of water absorption. Since no in situ observation of albedo is routinely acquired over SMOSMANIA stations, we will only consider satellite-based albedo products to perform the calibration. The three unknown parameters of Eq. **??** are optimized to obtain the best fit between observations of albedo and SMOSMA-

NIA in situ SSM for the year 2008. To mitigate vegetation impact on background soil beneath canopy, only observations during sparse vegetation periods are selected. A threshold of 1 on LAI is arbitrarily imposed as a separator between sparse-vegetated and dense-vegetated period.

4.2.2 Validation over SMOSMANIA stations

4.2.2.1 Description of filed measurement sites and equipements

Stations of SMOSMANIA (Soil Moisture Observing System-Meteorological Automatic Network Integrated Application) are chosen for the field measurements. The full name and locations can be referenced from table 4.1. These stations are originally designed for meteorological measurements founded by Météo-France. It also measures the soil moisture with ThetaProbe automatically for 4 layers : -5, -10, -20, -30cm.

TABLE 4.1 – Soil composition and vegetation types for SMOSMANIA stations.

SITE	SAND(%)	CLAY(%)	SILT(%)	FAO Soil Type	ECOCLIMAP VEG TYPE
CDM	24	40	36	Chromic Cambisols	Estremadura agro-forestry 3
CRD	72	8	20	Cambic Podzols	Western Europe mosaic forest/herbaceous
LHS	23	41	36	Chromic Cambisols	North Mediterranean mosaic crops/other vegetation
LZC	51	17	32	Calcaric Fluvisols	North Mediterranean sparse Shrubs
MTM	42	22	36	Humic Cambisols	European mean altitude mosaic forest/herbaceous
MNT	36	22	42	Dystric Podzoluvisols	Estremadura agro-forestry 3
NBN	25	45	30	Gelic Leptosols	North Mediterranean mosaic forest/herbaceous
PRG	23	41	36	Chromic Cambisols	North Mediterranean dense crops
SBR	87	4	9	Cambic Podzols	Landes Needleleaved Forest
SFL	24	40	36	Chromic Cambisols	North Mediterranean mosaic crops/other vegetation
SVN	36	22	42	Dystric Podzoluvisols	North Mediterranean dense C3 crops
URG	37	19	44	Dystric Podzoluvisols	North Mediterranean C4 irrigated crops

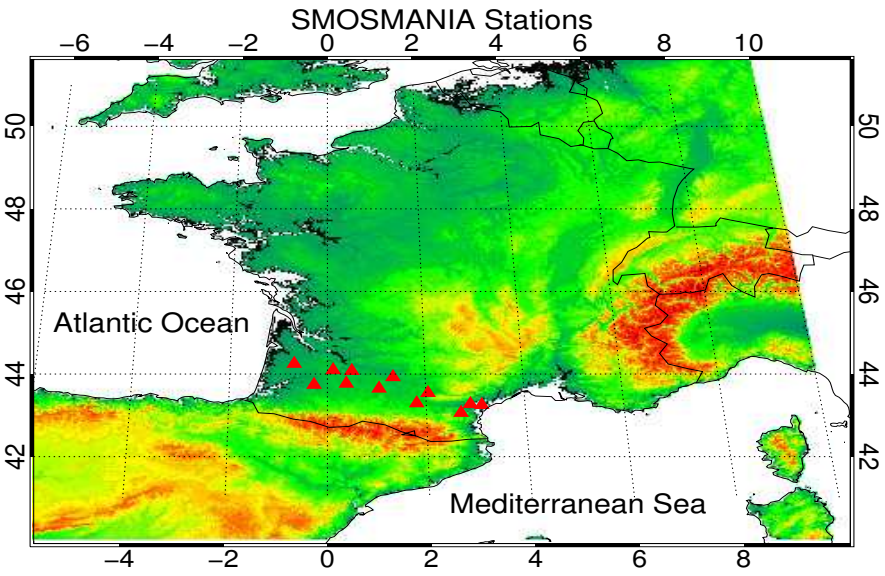

Figure 4.1 – The spatial distribution of SMOSMANIA stations.

The stations were set up on different surface of soil types and covered by different dominant vegetation species. The extracted soil and vegetation information are listed in table 4.1. Sand, clay and silt percentages and soil types are extracted from HWSD (Harmonized World Soil Database) consistent with FAO90 soil map, while the vegetation types are extracted from ECOCLIMAP II database.

SVC HR-1024 albedometer is used for field measurements of albedo due to its fitness of portability. The introduction for this product can be found in website : `http://www.spectravista.com/HR1024.html`. It records the spectral from 350nm-2500nm, and spectral resolution of 3nm. It can be configured with a lens with option of 4°, 8°or a head for hemisphere diffuse integration.

In the field campaign during September 2012, the SVC (Spectra Vista Corporation) Spectroradiometer is used to sample the spectral response of soil targets as well as the 'reference' (sky incoming radiation). Also, a Spectralon (BaSO4) reference panel (99.9% reflectance) was used for calibration purposes. It served as a reference target for the spectroradiometric measurements in order to calculate the target reflectance values (see fig.4.2).

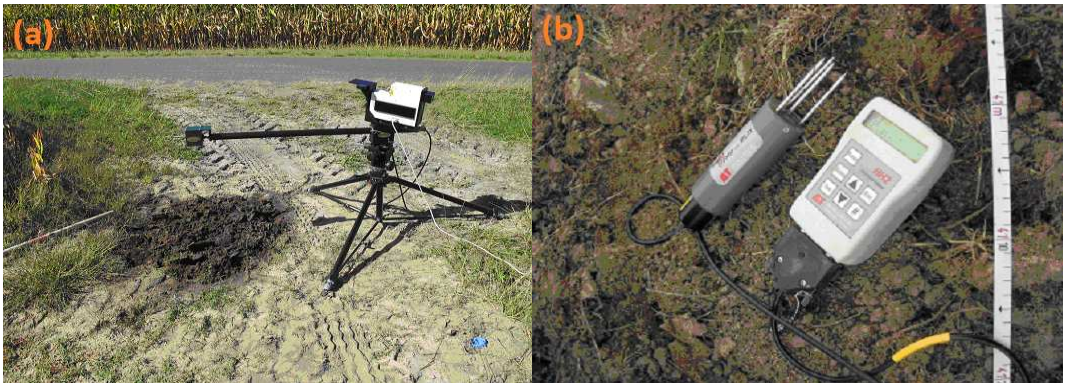

FIGURE 4.2 – (a) SVC Spectroradiometer for bare soil spectral sampling (b) ML3 Theta-Probe for soil moisture measurements.

ML3 Theta-Probe of delta-t company is used for soil moisture measurement, whose description can be found from : `http://www.delta-t.co.uk/`. The SM300 Soil Moisture Sensoroffers convenience and cost saving by combining soil moisture and temperature measurement. It can be used in all soil types, including saline soils. The SM300 Soil Moisture Sensoris a dual purpose soil moisture probe - it can be used both with the HH2 Meter for instant readings, or left in-situ for continuous monitoring with a data logger.

The in-situ surface soil moisture is measured and saved through an automatic logger. The quantity can be conveyed through volume or weight fraction.

4.2.2.2 Measurement method

French SMOSMANIA network is chosen for the calibration due to its accessibility of continuous in-situ soil moisture measurements. 8 stations among 12 of SMOSMANIA network are chosen for the field measurements, namely : CDM, CRD, LHS, LZC, MNT, SBR, SFL, SVN, URG. These sites are covered by different vegetation and characterized with different soil types, ranging from sand-dominated as CRD, to clay-loam dominated as SFL (fig.4.3).

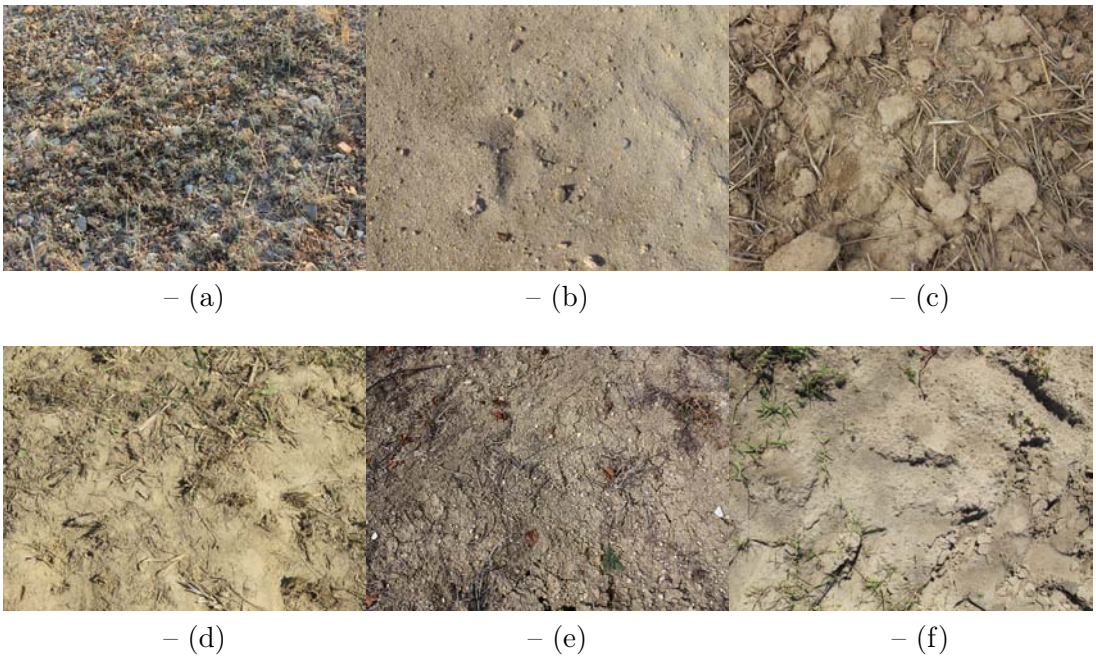

– (a) – (b) – (c)

– (d) – (e) – (f)

Figure 4.3 – Different types of bare soil within 6 SMOSMANIA stations : (a)LZC, (b)SBR, (c)SFL, (d)URG, (e)CDM, (f)CRD.

Two steps are conducted to derive soil albedo : (1) Mesurements of naturally dry and wetted soil spectral at different moisture level ; (2) Spectral integration from nearly continuous spectral to broadband. Soil moisture is logged accompanying spectral measurements synchronously at different moisture level. Details are described as follows :

Dry and wet soil spectral. Measurements are done for dry bare soil with two radiance curves : Reference and Target, as marked with Red and purple in fig.4.3. As noted, the reference of clear blue sky is really approaching to zero during spectral ranges like : 1350-1425mm, and 2400-2500mm. This is mainly due to atmosphere water vapor absorption. Bare soil spectral reflectance is calclulated as the ratio of Reference and Target radiances. The spurious noisy comes from the water vapor absorption bands. It can be noted that bare soil spectral reflectance curves are similar in the shape form with identical absorption ranges.

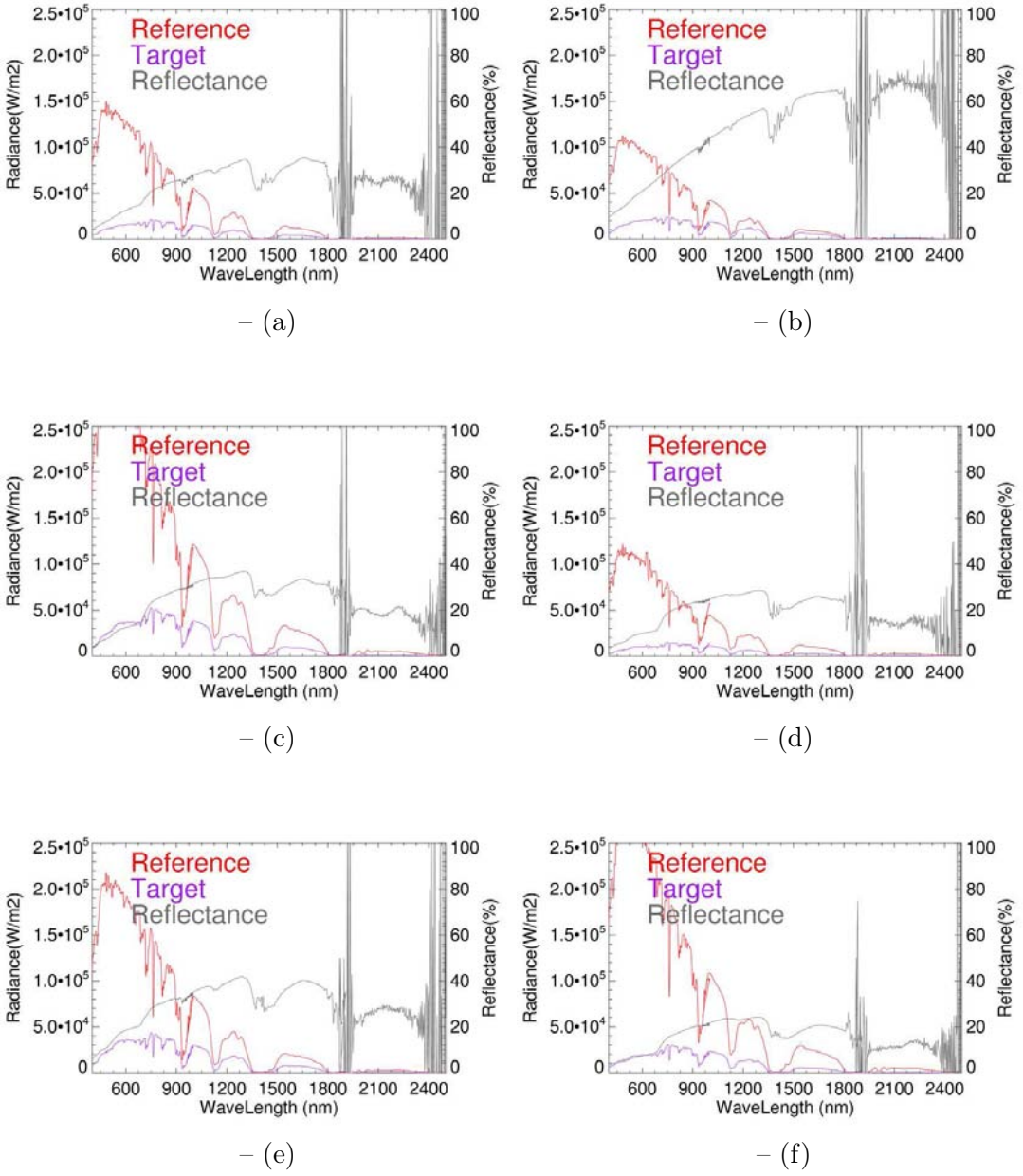

– (a) – (b)

– (c) – (d)

– (e) – (f)

FIGURE 4.4 – Bare soil spectral measured using SVC over 6 SMOSMANIA stations : (a)LZC, (b)SBR, (c)SFL, (d)URG, (e)CDM, (f)CRD.

Spectral to albedo conversion. Broad-band albedo (VIS : 400-700nm, NIR : 700-2500nm) can be calculated through spectral integration. One method is to integrate the original spectrum directly, which needs to know the spectral composition of input radiance, which further depends on the atmosphere status for gas absorption and aerosol scattering. The alternative way is two stepwise : (1) spectral integration is conducted from original spectrum to generate narrow band albedos using spectral response functions of a specific sensor ; (2) the narrow-to-broad (NN-BB) band conversion is performed considering the medium situation of atmosphere status (Liang, 2001). Three sensors SEVIRI, MODIS, VEGETATIONS are considered in step (1) of the second method. Their spectral response functions are plotted in fig. 4.5 to illustrate the differences. Due to the advantage of MODIS in band width and band numbers, it is chosen for our NN-BB conversion.

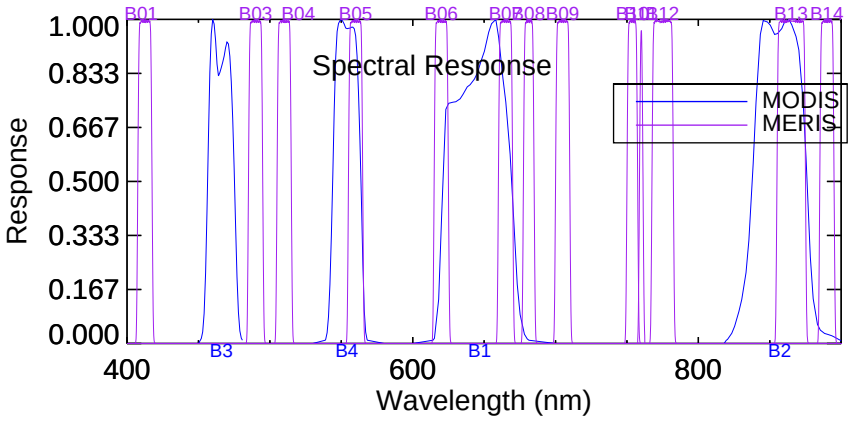

– (a)

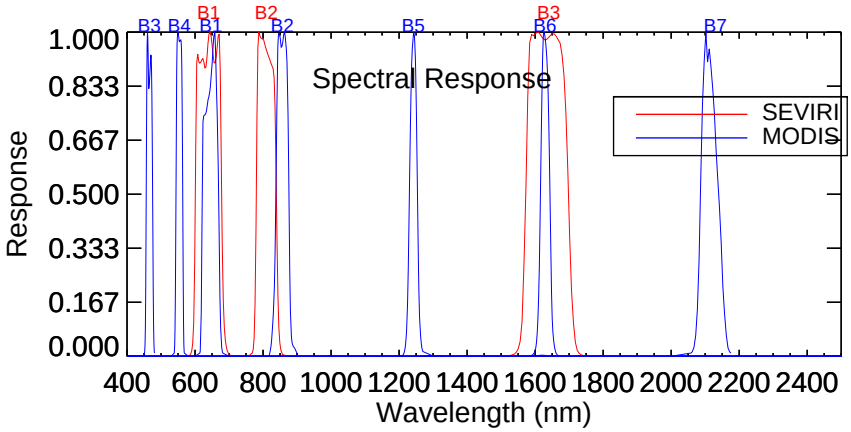

– (b)

Figure 4.5 – Spectral Response Function of four sensors : SEVIRI, MODIS, VEGETATION and MERIS.

Soil Moisture measurements. The surface around the measurement centre with a circle diameter around 2m is completely saturated artificially. Commonly, after several minutes, water penetrates into the deeper soil layer without staking as small 'pool's in the surface. After that, the skin of bare soil is drying gradually with sun ray, temperature and wind. The moisture is measured and logged through Theta-Probe each 5-15 minutes to obtain a soil moisture decreasing profile. At the same time, surface soil reflectance is preserved, this spectral file is associated with corresponding soil moisture measurement.

4.2.2.3 Results

A theory explains the darkening of the soil due to wetness by a reduction of the inner material reflection in presence of films of water coating soil particles (Ångström, 1925). Somewhat as a paradox, the multiple bouncing between a light ray and soil attributes leads to an increase probability of light absorption by water component. According to (Twomey et al., 1986), such phenomenon could be even enhanced by having a weaker relative index of refraction between soil and water (compared to air), thereby having a less deviated light ray to the advantage of increased soil absorption.

The so called 'soil law' can be represented by a constant spectral ratio from surface albedo at VIS and NIR domain. fig. 4.6 shows the soil line for 7 SMOSMANIA stations, within which each point represents one single synchronized measurement of surface albedo and surface moisture. It is found that these stations can be divided into two categories according the spectral ratio : C1 (Category 1), a ratio around 2.7 for CDM, LHS ; and C2 (Category 2), a ratio around 2.0 for CRD, LZC, MNT, SFL, URG.

This relationship of soil surface albedo and soil moisture is valid from visible to shortwave infrared as the soil darkening effect is known to be spectrally bland with a rather low spectral dependence of water absorption. A robust regression is achieved at site LHS (fig. 4.7) for both VIS and NIR domain. The projected dry albedo and wet soil albedo are 0.4, 0.15 at NIR domain, and 0.18, 0.80 at VIS domain. The ratio of NIR/VIS albedo is obeying the ratio derived from 'soil law' (fig. 4.6).

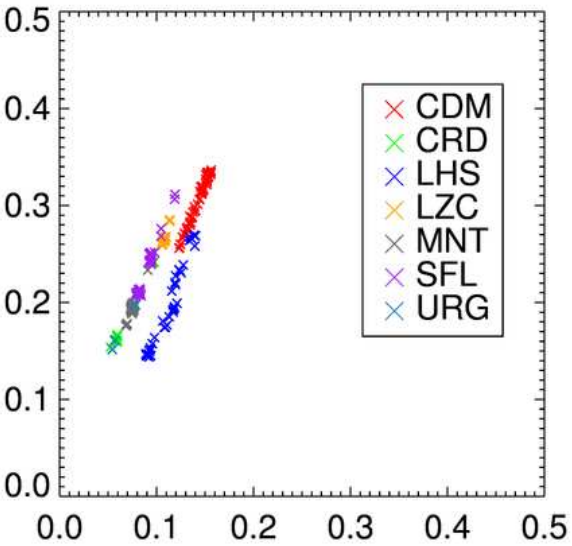

Figure 4.6 – Soil line of bare soil albedo within 7 SMOSMANIA stations.

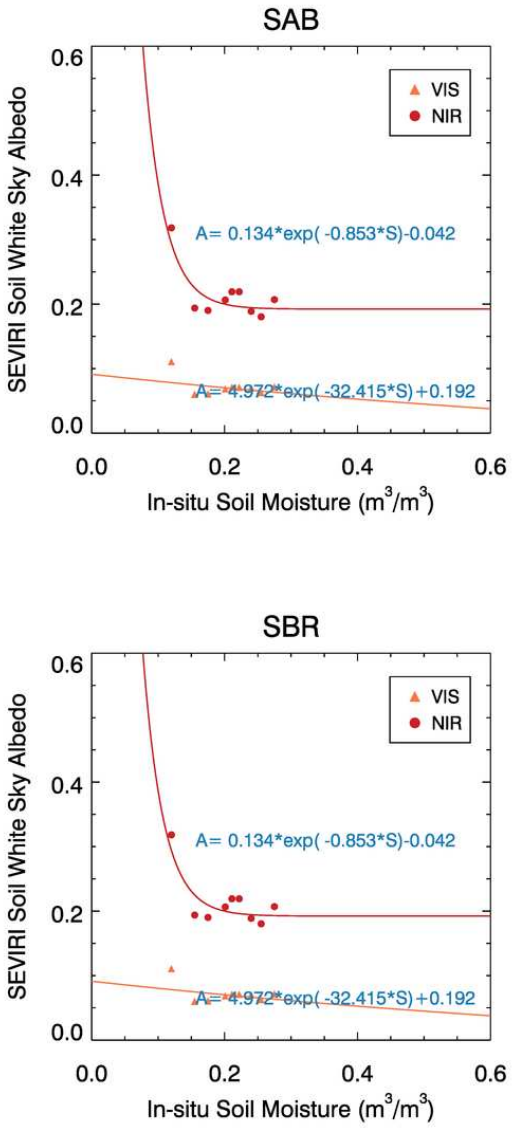

FIGURE 4.7 – The dependence of surface soil albedo on moisture, calibrated at three stations : (a)LHS (b)SBR and (c)URG.

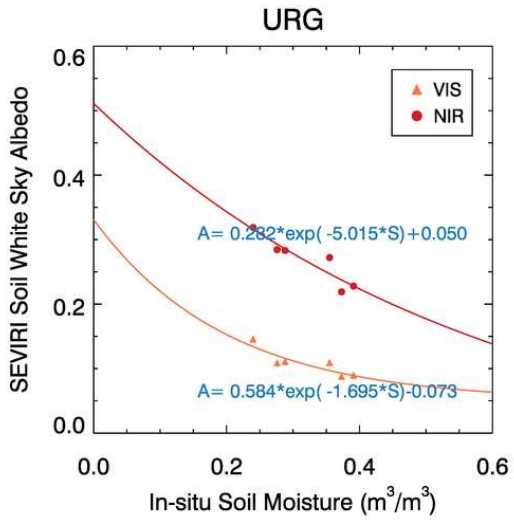

The dependence of surface soil albedo on moisture, calibrated at three stations : (a)LHS (b)SBR and (c)URG.

4.3 Calibration of Vegetation Albedo with Foliage Chlorophyll Content

4.3.1 Introduction

In most Land Surface Models (LSMs), canopy vegetation albedo is parameterized as reference values of Plant Function Types (PFTs). These values are the same for different types of vegetation in one PFT and temporal invariant. Canopy radiative transfer modelling attributes this canopy vegetation albedo into leaf single scattering reflectance, leaf angle distribution. In reality, leaf single scattering reflectance is changing in response to leaf biochemical elements like leaf chlorophyll content (Cab), as proven by leaf color monitoring. Through representing these dynamic effects in LSMs, it is supposed to improve the ability of temporal simulation and spatial representation within one PFT.

Several advances have been conducted to represent these dynamic effects through different schemes. A greenness factor is introduced into semi-statistic surface albedo model, linking to LAI scaled by the maximum value within one PFT (LAI/LAImax), which is proven to improve the performance substantially (Liang, 2005). The relationship of foliage nitrogen content and canopy vegetation albedo is built up at AmeriFlux sites including various vegetation species (Hollinger et al., 2010; Ollinger et al., 2008).

In our study, a scheme is proposed to incorporate Cab to parameterize canopy vegetation albedo. Cab is explicitly parameterized to canopy vegetation albedo through PROSAIL-a combined leaf+canopy model. This canopy vegetation albedo-leaf chlorophyll content relationship considering different configurations could be mimicked by a simple function depending on LAI. The parameterization strategy is tested at a semi-arid site in Spain, and show a primary satisfactory result.

4.3.2 PROSAIL model and sensitivity experiment

In order to establish the relationship of canopy vegetation albedo with biochemical parameters, especially leaf chlorophyll content, a simulation is conducted by PROSAIL model. PROSAIL is a combined radiative transfer model from leaf model (PROSPECT) and canopy model (SAIL). The former is capable to simulate leaf reflectance and transmittance from biochemical element content and mesosphyll structure parameter. The later is constructed to simulate directional reflectance from canopy structural parameters, leaf reflectance/transmittance and background reflectance. This coupled model has been used for more than 30 years extensively for application in agriculture, remote sensing.

Canopy VIS albedo is mainly determined by which parameter ? What is the most sensitive spectral range for leaf chlorophyll content ? Is an observation at this spectral range has enough signal to noise ratio to ensure capture of the perturbation of chlorophyll ? To answer these two questions, a sensitivity experiment is conducted using PROSAIL.

The sensitivity of VIS albedo is tested against each parameter while keep the others fixed. It is found that VIS albedo is mainly determined by two parameters : leaf chlorophyll content and leaf area index (fig. 4.7 fig. 4.8), and the other parameters have minor or no effects. This is consistent with the statements in literatures. This founding offers a possibility to simplify the albedo parameterization in VIS domain.

It can be noticed from fig. 4.7 that Chlorophyll causes variation mostly at the range of 500-700nm (>700nm omitted in the figure). The maximum absorption is achieved around spectral length of 560nm, hitherto, 560nm is considered as the most sensitive spectral range for chlorophyll.

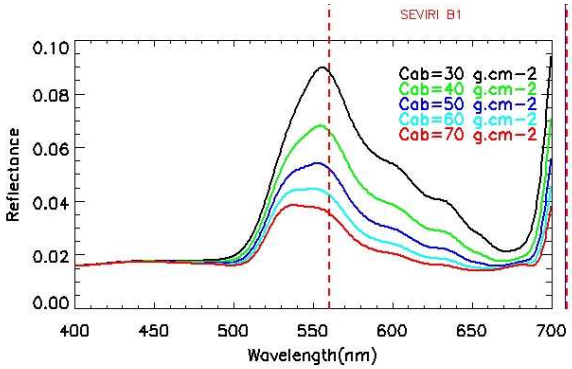

Figure 4.7 – Sensitivity test of reflectance and foliage chlorophyll content.

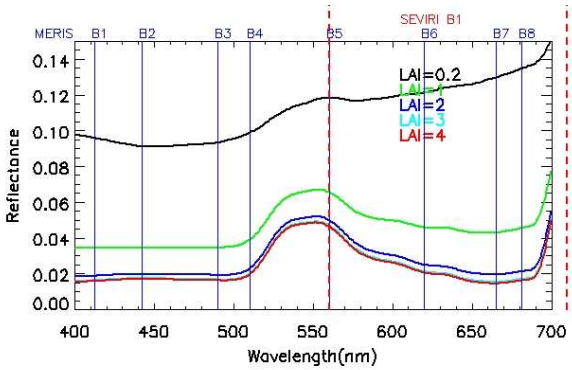

Figure 4.8 – Sensitivity test of reflectance and leaf area index.

To test whether the spectral reflectance has enough signal to noise ratio to ensure capture of the perturbation of chlorophyll, a differential ratio is calculated. This quantity can be understood as the coefficient of elastic recovery : the higher it is, the more Cab signal can be detected from reflectance. A test is conducted using the SEVIRI band 1 (0.6μm) reflectance. It can be noticed that the smaller LAI is, the higher the reflectance is (fig. 4.8). For example, when LAI equal to 1,

TABLE 4.2 – Parameters and its variation range for PROSAIL model.

Parameters	NAME	VALUE	UNIT
Cab	Chlorophyll content	40	36
Car	Carotenoid content	8	20
Cw	Equivalent water thickness	41	36
Cm	Dry matter content	17	32
N	structure coefficient	22	36
LAI	leaf are index	22	42
LIDF	average leaf angle	45	30
RSOIL	soil reflectance	41	36
Skyl	diffuse/direct radiation	4	9

if we take the absolute variation of reflectance as 0.002, a variation of 0.5-2.2 unit of Chlorophyll Content can be detected at the Cab range of 20-40 unit, and 2.2-5.0 unit can be detected for the Cab range of 40-60 unit. This offers a reference of the ability to detect Cab variation from reflectance.

4.3.3 Calibration of reflectance with chlorophyll content

The first step is to construct a dataset with varying Cab in different configuration of other parameters through simulation. Parameters of PROSAIL model and its variation range for simulation are listed in table 4.2.

After stratified by LAI, an inverse function is found suitable to describe the relationship between reflectance at 560nm (R560) and foliage total chlorophyll content (Cab), using the database simulated by the PROSAIL model. Coefficients are related to LAI, which shows a promising precision.

The relationship of R560 and Cab can be approximated through an explicit inverse function (depending on LAI) as follows :

$$R560 = A * \frac{1}{\sqrt{LAI}} \frac{1}{\sqrt{Cab}} + B \tag{4.2}$$

Where, R560 represents the reflectance at wavelength of 560nm, Cab denotes the foliage chlorophyll content, LAI is leaf area index, and A, B are the coefficients to be calibrated (Eq. 4.2). Actually, a value A=0.5 is well-suited, whereas B less than 1% could be neglected.

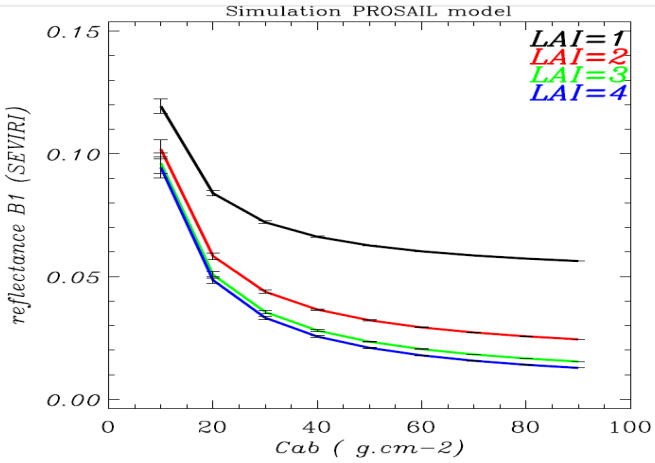

Figure 4.9 – The relationship between reflectance SEVIRI B1 (0.6μm) and Cab calibrated using PROSAIL, stratified by LAI. The variation range is caused by different configurations of other parameters are represented by black vertical bars, while the average dependence is marked by the straight curves.

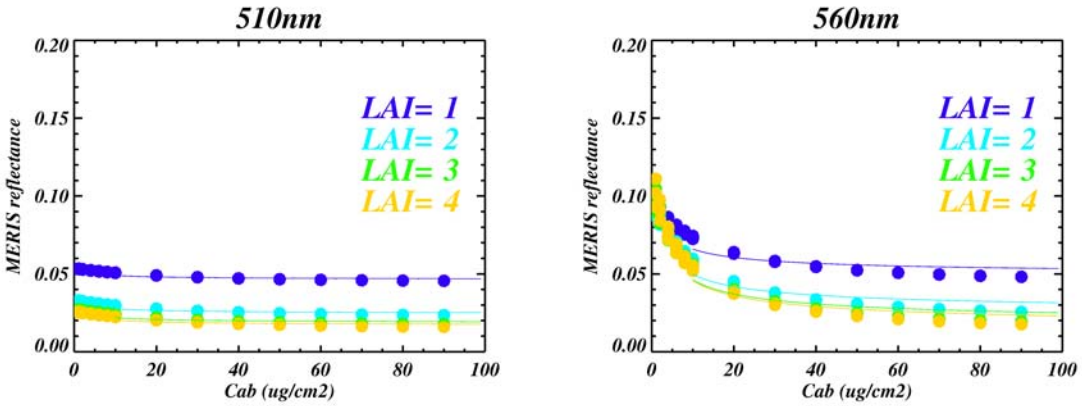

Figure 4.10 – Graph the relationship between TOC reflectance MERIS Band 5 (0.56μm) and Cab calibrated using PROSAIL model and various LAI values. The same relationship at 510nm is shown for the sake of comparison.

4.4 In-situ Validation at Majadas

4.4.1 Site information

Majadas is a site located in the Province of Caceres in Spain, where CEAM is operating a flux tower since May 2003. The natural vegetation type corresponds to the Pyro bourgeaneae Querceto rotundifoliae quercetum mesomediterranean series (Rivas-Martz, 1987), which has been transformed into a wooded (Holm oak) grassland (herbaceous species) containing some shrub species (Cistus ladanifer, Lavandula pedunculata and Ulex europaeus). Natural regrowth

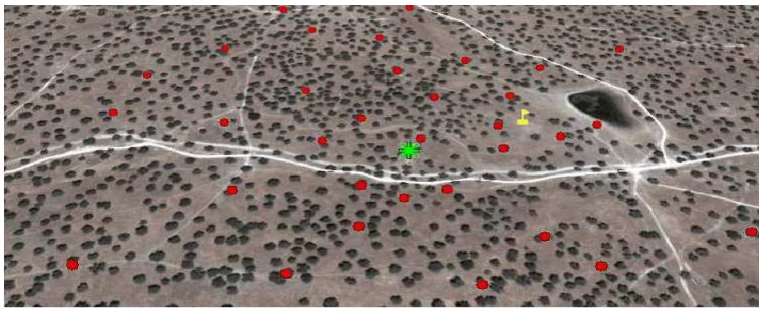

FIGURE 4.11 – Site map of Majadas extracted from GOOGLE MAP.

is good and land management is focused on grazing. Lixisols (non-limestone Miocene substrates) are predominant and soil depth is over 80 cm. Tree density is of about 20 per hectare, with an average height of 8m and an average DBH of 400mm.

Majadas site is a rather sparse vegetation canopy (Dehesa ecosystem), which is in favor to investigate how short-term swath-like variabilities of total albedo could be justified by SM changes.

4.4.2 Separation of Aveg and Asoil

Fraction of vegetation cover can be expressed as an exponential function of LAI, as formulated follow :

$$f_{veg} = e^{-0.6LAI} \tag{4.3}$$

Fig.4.12 shows the seasonal variation of fraction of vegetation at the pixel containing Majadas during one year 2010.

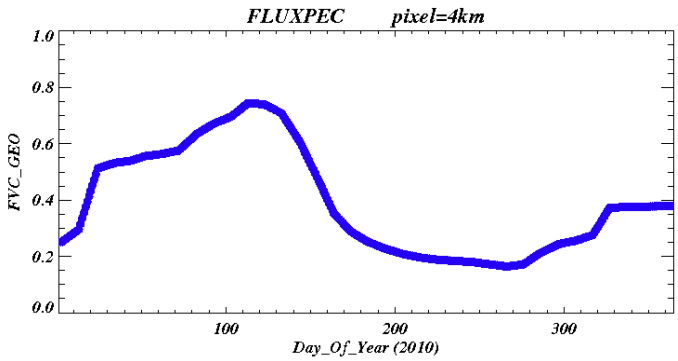

FIGURE 4.12 – Seasonal variation of fraction of vegetation cover.

Total albedo can be expressed as the weighted fraction of vegetation albedo (A_{veg}) and bare soil albedo (A_{soil}) :

$$A_{tot} = f_{veg} \cdot A_{veg} + (1 - f_{veg} \cdot A_{soil}) = (A_{veg} - A_{soil}) \cdot f_{veg} + A_{soil} \tag{4.4}$$

Through linear regression of A_{tot} with f_{veg}, A_{veg} and A_{soil} can be derived from interception and slope.

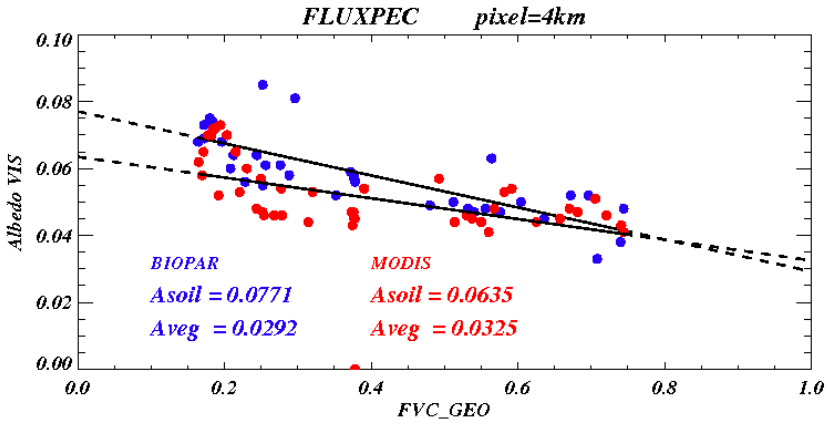

Figure 4.13 – VIS albedo regressed against fraction of vegetation cover to separate soil albedo and vegetation albedo. Two types of products are serving as inputs, namely MODIS (red circles) and BIOPAR(blue circles).

Fig.4.13 illustrates the separation using two types of products as input : MODIS and BIOPAR. MODIS is an 8 day product while BIOPAR is distributed each 10 day. Regressed A_{soil} and A_{tot} are 0.0771 and 0.0292 for BIOPAR inputs ; 0.0635 and 0.0325 for MODIS inputs. The results are a little different, while we put more confidence at BIOPAR products.

4.4.3 Variation of albedo with soil moisture

The time series of albedo are compared with in-situ soil moisture measurement during 2010 (fig.4.13). Daily variation of albedo is argued to be mainly attributed to moisture effect. It can be observed that these albedos are showing opposite trend as soil moisture at -4cm. Usually, after the rainfall, soil moisture at any layer rises up rapidly following by a graduate decrease, with a more reactivity at the skin surface at -4cm and less for the other depths (-8cm, -10cm and -20cm). For this favorable situation, the best calibration is established between soil moisture at -4cm and VIS albedo from SEVIRI.

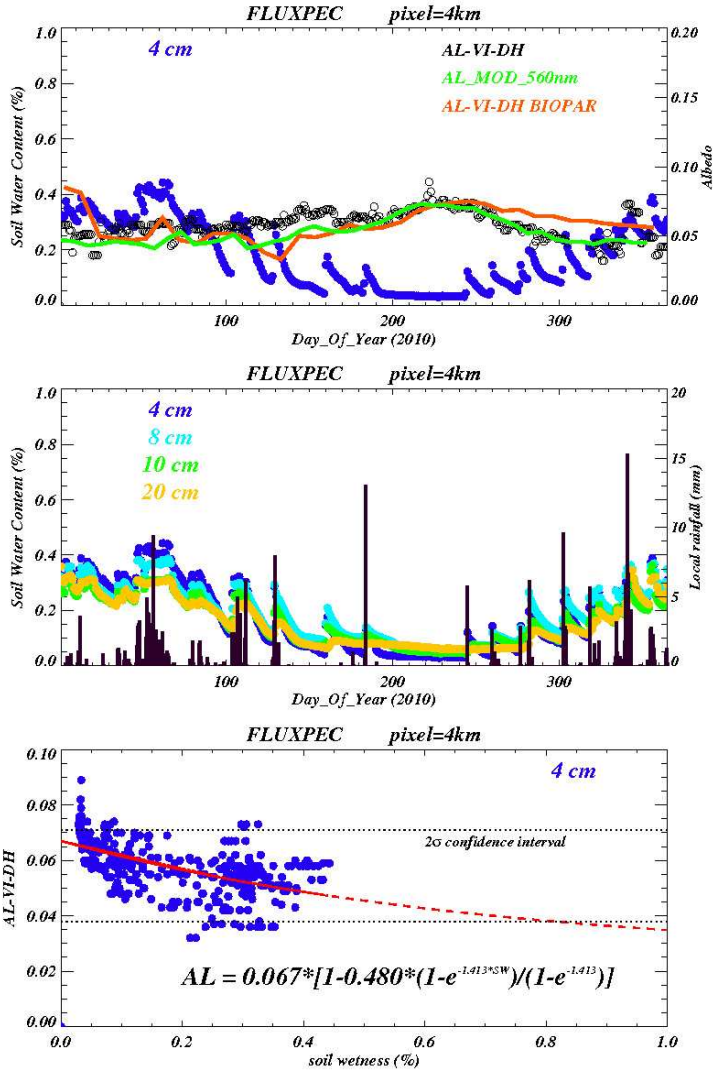

FIGURE 4.14 – (a) Time series of various albedo products at 4km resolution : broadband VIS black sky albedo of SEVIRI(black circles), BIOPAR(brown curves), spectral albedo at 560nm of MODIS(green curve). The in-situ surface soil moisture at -4cm is imposed (dark blue curve). (b) In-situ soil moisture measurements at 4 layers : -4cm, -8cm, -10cm, -20cm, in reaction with local rainfall. (c) albedo calibrated with surface soil moisture (-4cm) using an exponential-like function.

4.4.4 Calibration of Aveg with Cab

In situ measurement of *Cab* is used to derive the vegetation albedo at 560nm from the theoretical relationship presented in Eq. 4.1 based on PROSAIL simulations. fig. 4.15 demonstrates that the temporal evolution of vegetation albedo once corrected for LAI is well correlated with the inverse of the chlorophyll content as predicted by the theory. Incidentally, it could be verified that in this case the chlorophyll content is well correlated with nitrogen content.

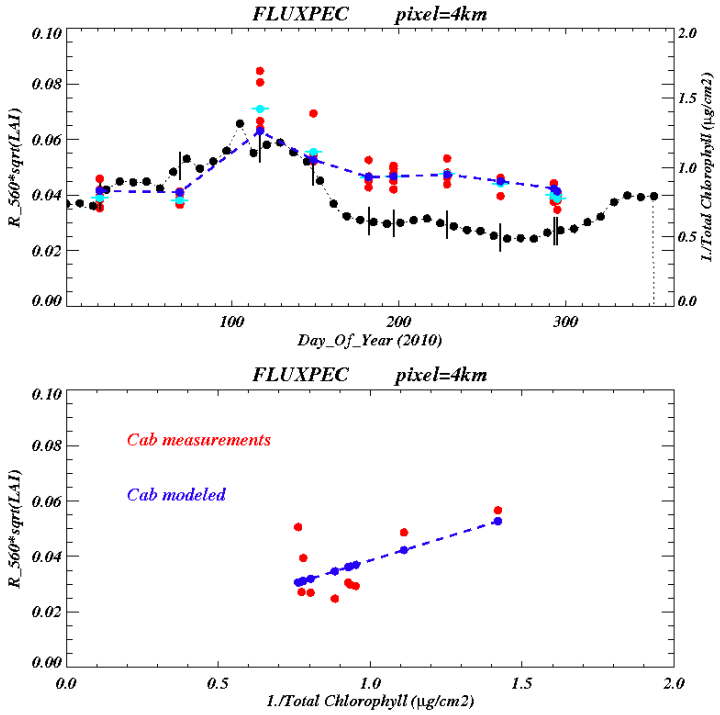

Figure 4.15 – (a) Seasonal variation of measured Cab (red circles), averaged measured Cab (blue circles), and the quantity R560*sqrt(LAI) using MODIS reflectance at 560nm and Biopar LAI (black circles) (b) R560*sqrt(LAI) against 1/Cab, the red points are in-situ measurement of Cab, where the dark blue line shows the regression using Eq. 4.1.

A prognostic soil albedo is first achieved from its climatological value as defined in Chapter 3, updating in time through the relationship between soil albedo and wetness that appears on fig. 4.14. The vegetation albedo at 560nm is converted into VIS albedo to match with SEVIRI observations after being updated based on chlorophyll seasonal variations. Results are shown in fig. 4.17 below.

It comes out that this prognostic albedo is well correlated with local rainfall, as it could be expected, which is less conspicuous for SEVIRI. One reason for that is that we may assume that soil wetness is fairly distributed over a grid mesh of 4 km, representing the size of a SEVIRI pixel, whereas it is probably not the case. Even in the rather flat area of Majadas, runoff and drainage may alter the patterns of soil wetness distribution at landscape scale. In fact, satellite-based surface albedo shows a delay of reaction in time to rainfall episode. This is somewhat

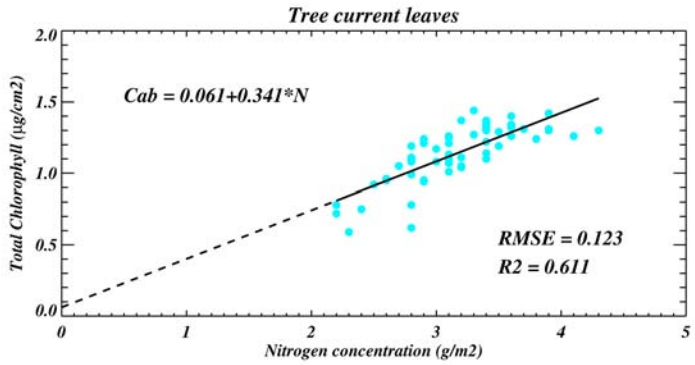

FIGURE 4.16 – Relationship between total chlorophyll and nitrogen at Majadas anchor station for tree leaves.

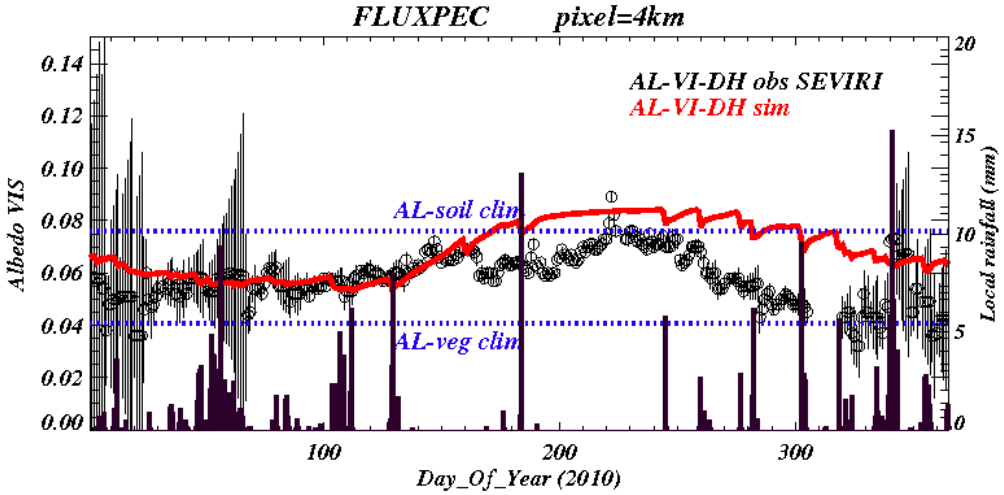

FIGURE 4.17 – Yearly variations of observed and simulated albedo et Majadas station. Chronology of rainfall events is shown for the sake of comparison with albedo products. Error bar represents uncertainty assessment for SEVIRI albedo in link to persistence information.

obvious as rainfall and cloud occurrence, which masks the surface for optical wavelengths, are concomitant events. But satellite-based surface albedo from SEVIRI seems to be more impacted to soil wetness still because of the non evenly distribution over the dehesa ecosystem in Majadas.

Interestingly, the climatologic albedos for soil and vegetation correspond to max and min values of total albedo, respectively.The timing between the BioPAr vegetation fraction FVC_GEO displayed in fig. 4.12 with a peak occuring in April well captures the seasonality of annual grassland (fig. 4.18). But instead all satellite albedo values (see fig. 4.14) show a decrease in the middle of the summerime that cannot well reproduced in terms of intensity by the prognostic albedo, even accounting by a decrease in chlorophylle.Neither the slight change in leaf mass area of the oak trees could not explain such observed depletion of the satellite albedo, whatever the scale is in fact.

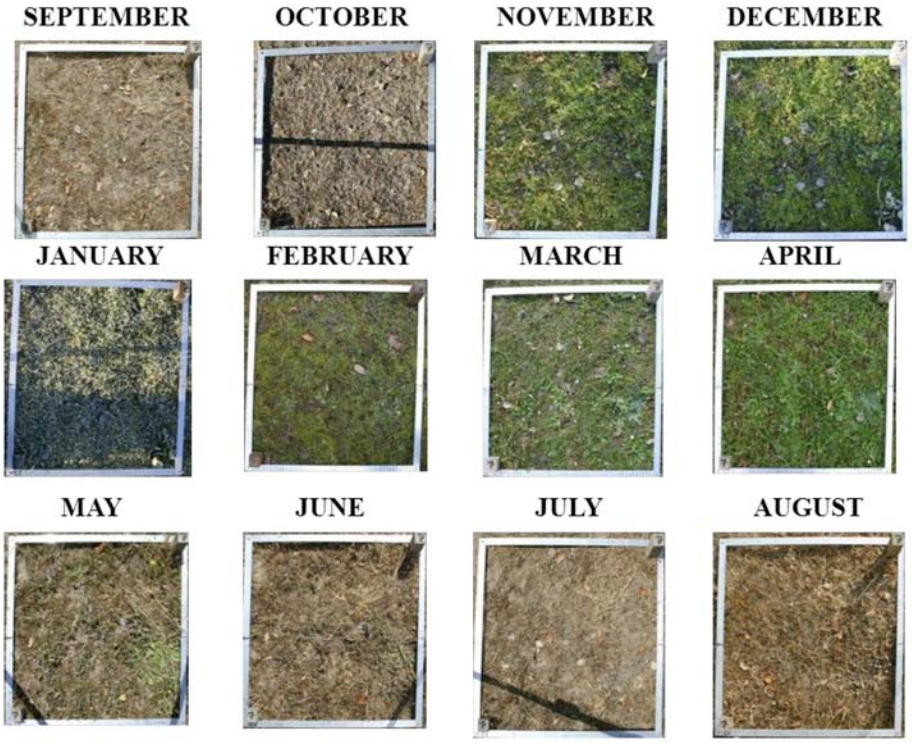

Figure 4.18 – Phenology of the herbaceous layer in Majadas.

4.5 Conclusion

In this chapter, a prognostic albedo parameterization scheme is proposed. Total albedo can be separated into soil and vegetation albedo weighted by vegetation fraction. In this scheme, these two components are parameterized separately. The former is described as an exponential function on soil moisture, while the later as a simple function on leaf chlorophyll content. This scheme is validated using in-situ measurements and satellite products at the Majadas station.

Soil surface albedo dependence with surface soil moisture can be depicted by a non-linear exponential function. It is found that this relationship can be well calibrated using SEVIRI albedo and surface soil moisture within 12 stations over south-western France. Results show the consistency of the calibrated function either with SEVIRI albedo or in-situ measurement.

Vegetation albedo is parameterized as a function of leaf chlorophyll content. PROSAIL simulation reveals that chlorophyll and LAI are two principle ingredients entering the determination of the dynamic VIS albedo. Moreover, 560nm spectral range is found to be the most sensitive to chlorophyll. Following this, an inverse function is proposed for VIS albedo parameterization and performs well approximating simulation results.

Validation of this prognostic total albedo is conducted at Majadas station for both soil and vegetation albedo. These two components can be separated through a linear regression method, and compare well with the climatology, which adds consistence to the entire study. Soil albedo from SEVIRI product presents an exponential relationship with in-situ surface soil moisture measurement, which is prominent. Field measured chlorophyll content is used to calibrate the function we proposed for vegetation albedo parameterization. Good performance is achieved during the first 150 days of year 2010, while discrepancies exist after Julian day 150. This might be due to dead vegetation caused by dry weather during summer time. But likely more insight into this issue remains to be further investigated.

Lire la deuxième partie de la thèse